ON FLOW MASERS WITH SEPARATED EMISSION FIELDS

by

Wilfred H.U. Krause M.Sc.

A thesis

submitted to the University of Keele

for the Degree of Doctor of Philosophy

Department of Physics,
University of Keele,
Staffordshire.

September, 1969.

ACKNOWLEDGEMENTS

The author is indebted to Dr. D.G. Holloway for his supervision, guidance and helpful criticisms. Thanks are also due to Professor D.J.E. Ingram for providing laboratory facilities and to the University of Keele for providing a Research Scholarship which enabled the work to be carried out.

The co-operation of Dr. D.C. Lainé and the members of the Maser Group is gratefully acknowledged.

Especial thanks are due to the technical staff of the Physics Department and also to the staff of the University Workshop for their co-operation and assistance.

Thanks are also due to Miss Kay B. Davies for her care in typing this thesis and to Mr. M. Cheney for his assistance in photographical work.

W.H.U. Krause

SYNOPSIS

In 1954 the invention of the ammonia molecular beam maser oscillator, through Charles Hard TOWNES and co-workers and Nikolaï Gennadievich BASOV and Alexander Mikhaïlovich PROKHOROV, opened a new area of applied physics, the field of quantum electronics. Ten years later the importance of the invention of the new device which consists essentially of a microwave resonator and excited ammonia molecules which pass through the resonator was acknowledged by the award of the 1964 NOBEL Prize in physics to the above workers.

Soon after the invention of the maser principle, an ammonia beam maser utilizing separated emission fields was brought into operation, a device which consists of two separated microwave resonators through which the ammonia beam maser passes in succession. It is now well known that this two-cavity variant has great practical advantages over the original one-cavity ammonia beam maser.

However, not all of the macroscopic effects observed using the two-cavity ammonia beam maser could be explained in a straightforward manner. One of the more obscure effects presents itself as follows: If the frequency of the auto-oscillation in the first resonator is detuned from one side of the possible frequency range in which generation occurs to the other then the intensity of the electromagnetic radiation in the second cavity can go through two maxima, with a gap in the middle.

This effect, the "double-hump detuning phenomenon", which was first observed by the Russian research group of BASOV in 1962, has since then been a challenge to several theoretical and experimental workers. BASOV and co-workers themselves made two different attempts in order to explain this phenomenon. At the Third International Conference on Quantum Electronics, held in Paris in 1963, this team reported that the effect might occur because the transition probability of the molecules passing through the second resonator depends on the degree of excitation of the first cavity. However, in 1967 BASOV and co-workers published a paper where it is suggested that the double-hump detuning phenomenon might well arise because of the interference which occurs between the emissions from molecules which move with different velocities and radiate fields with different phases.

On the other hand, research activities in fields other than microwave spectroscopy have made it possible to devise masers which are similar to the ammonia beam maser in that excited particles pass through a tuned resonant component, but which emit at quite different frequencies, e.g. in the audio-frequency range or in the mm wave range. However, up to now none of these different masers has been furnished with a successive resonator.

It is the purpose of this thesis to report for the first time the successful operation of a tandem maser which is not a two-cavity molecular beam maser. The author devised and investigated a maser where excited protons in water pass successively through two tuned solenoids.

The system is based on a conventional proton magnetometer maser oscillating in the magnetic field of the earth at a frequency near to 2 kHz.

The general result of the investigation is that despite the enormous frequency difference (audio-frequency compared with a microwave frequency) the two coil nuclear maser behaves in much the same way as a two cavity ammonia beam maser. For the two-coil nuclear maser the double-hump detuning phenomenon can be explained in terms of the motion of the macroscopic nuclear magnetization, and an analysis by means of BLOCH's equations is possible. It is shown that the double-hump detuning phenomenon is produced by a fundamental radiation process occurring in the first emission coil and, therefore, that it is not a second-order effect such as could occur because of the non-uniform velocity distribution of the excited particles. It is also shown that for the two-resonator ammonia beam maser the detuning phenomenon can be explained in terms of quantum mechanical probabilities, when a uniform velocity distribution of the ammonia molecules is assumed. Those results agree qualitatively with the results which have been obtained using BLOCH's equations and which have been verified experimentally by means of the two-coil nuclear maser.

A second distinctive feature of the conventional two-cavity ammonia beam maser is that if the first resonator is sufficiently detuned, generation in the second resonator can take place simultaneously

at two different frequencies. The analogous effect has been observed using the two-coil nuclear maser.

The conventional one-coil nuclear maser which is currently used as a magnetometer has the disadvantage that it does not offer a suitable criterion for tuning the oscillation frequency accurately to the LARMOR frequency. For the two-cavity ammonia beam maser it has previously been proposed to modulate mechanically the inter-cavity distance and to use zero phase modulation as a means of tuning the maser frequency accurately to the centre frequency of the molecular transition. It is shown that by modulating mechanically the inter-coil distance of the two-coil nuclear maser, a suitable tuning criterion can be obtained in an analogous manner. A second tuning criterion is offered by the double-hump detuning phenomenon.

In Chapter I the maser principle is discussed using a classical model, and the different maser types which are of interest in the context of this thesis are enumerated. Chapter II contains a review of previous work on two-cavity ammonia beam masers. Chapter III reviews the conventional theory of nuclear masers. In Chapters IV to IX the two-coil nuclear maser is investigated. Chapter X contains a general discussion of the two-resonator maser problem in terms of quantum-mechanical probabilities. Some general remarks concerning practical applications of two-resonator masers are made. The conclusions are summarized in a final section.

CONTENTS

CHAPTER V (continued)

CHAPTER X (continued)

CHAPTER I

INTRODUCTION TO FLOW MASERS

1.1 Introduction

Flow masers with separated emission fields belong to a class of more complicated maser devices which can be derived from some basic maser types. In this introductory chapter first a definition of a flow maser with separated emission fields is given, and thereafter the maser principle is discussed qualitatively with the aid of a macroscopic model. The basic flow masers are enumerated.

1.2 Definitions

The maser, being an acronym for "molecular amplification by stimulated emission of radiation" (TOWNES 1964) is a generator or amplifier of electro-magnetic energy. The essential components of this device are a resonant component and appropriate excited atoms or molecules which are present inside the resonant component. Depending on the operation frequency involved, the resonant component may be a tuned radio-frequency coil (solenoid), a tuned parallel-plate condenser, a microwave cavity or a parallel-plate resonator (FABRY-PEROT resonator). The excited atoms may be part of a solid, gas or liquid. If these atoms are contained in a stationary sample, the system might be called a stationary maser. For example, crystal

masers or gas cell masers belong to this class. If the atoms remain inside the resonant component for a limited time only, the device is hereinafter called a flow maser. Examples of flow masers are liquid flow masers, gas diffusion masers and beam masers. In these latter cases the atoms enter the resonant component in an excited state and leave it in general partly de-excited, i.e. the fraction of atoms in the state of lower energy has increased but has not reached its thermal-equilibrium value. If the partly de-excited atoms emerging from the resonant component are utilized to provoke maser action in a further resonant component, a device results which hereafter is referred to as a flow maser with separated emission fields. Optical masers, or lasers, are excluded from the following, although the realization of a flow maser with separated emission fields is in principle not limited to particular frequency ranges.

1.3 Basic Maser Principle*

It is known that atoms, ions and molecules exist in certain stationary states characterized by discrete energy levels E_1, E_2, ..., and that they are capable of significant interaction with electromagnetic energy of frequency ν, if the BOHR frequency condition $h\nu = E_m - E_n$ is satisfied for some pairs of levels. According to EINSTEIN, the

---

* Introductory treatments of masers are now found in numerous textbooks, e.g. SINGER 1959, TROUP 1959, YARIV 1967.

emission of radiation from atoms is made by two different mechanisms by incoherent spontaneous emission and by coherent induced or stimulated emission. Stimulated emission can be regarded as the inverse of absorption, and hence is sometimes called "negative absorption". Both stimulated emission and absorption are provoked by the presence of radiation in the environment of the atoms, the stimulated emission being proportional to the population of the state of higher energy, the absorption being proportional to the population of the state of lower energy. In a solid, liquid or gas in thermal equilibrium the relative population of atomic energy states is governed by the BOLTZMANN distribution which predicts for any positive absolute temperature a higher population for the state of lower energy. Hence in all substances which are in thermal equilibrium absorption is predominant.

However, there exist a number of techniques (Section 1.5) which upset thermal equilibrium and achieve "population inversion" in certain gases, liquids and solids. If population inversion is achieved, i.e. if the population of the upper energy level is made larger than the population of the lower one, stimulated emission becomes predominant and can be utilized for amplification purposes. In order to obtain generation, one produces positive feedback by some resonant circuit and ensures that the energy gained from the energy state pair via stimulated atomic transitions is greater than the circuit losses (GORDON, ZEIGER and TOWNES 1954).

1.4 Macroscopic Embodiment of the Maser Principle

It is possible to obtain a physical picture of the dynamics of the system 'excited atoms - resonant circuit' by considering a "macroscopic maser" which was recently proposed by DEHMELT (1968). In this mechanical model, see Fig. 1, the resonant circuit is simulated by a rigid pendulum which oscillates in the plane of the drawing. In place of an atom, a loaded gyroscope is chosen whose precession frequency due to the gravitational pull on the load M is equal to the pendulum's frequency of oscillation. In Fig. 1 the "excited" state is shown, i.e. the vector $\vec{A}$ which points from the centre point of the suspension to M is directed upwards. In the equilibrium state $\vec{A}$ would point downwards.

The choice of a gyroscope is justified by two fundamental theorems:

THEOREM 1 : Any two level atomic system, as far as its motion is concerned, is equivalent to a spin $\frac{1}{2}$ precessing in a magnetic field.

THEOREM 2 : In a magnetic field, the motion of a spin $\frac{1}{2}$ is equivalent to the motion of a macroscopic magnetized gyroscope.

The first theorem can be proved quantum-mechanically (FEYNMAN, VERNON and HELLWARTH 1957) and is experimentally well established. It led, for example, to many attempts (MACOMBER 1968) to find the optical analogues of numerous transient phenomena which have previously been observed in the field of nuclear magnetic resonance (NMR) and

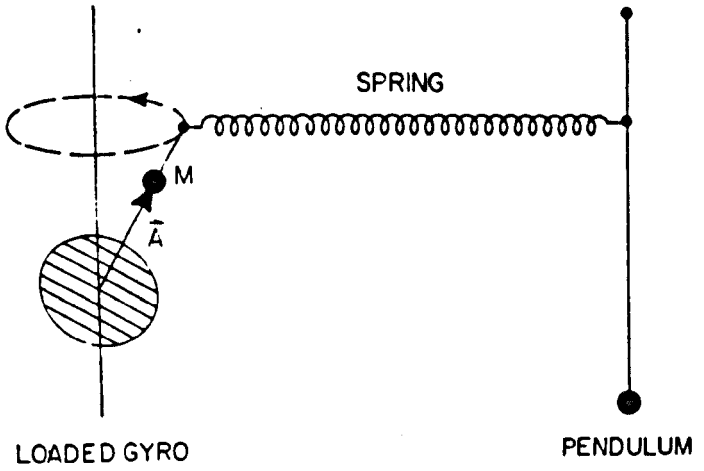

FIG. 1. Macroscopic maser. After H.G. DEHMELT: Am. J. Phys. 36 (1968) 911.

which are there well understood. The most dramatic success has been the observation of photon echoes (KURNIT, ABELLA and HARTMANN 1964), analogous to NMR spin echoes (HAHN 1950), in a laser illuminated ruby crystal, where the precession of the dipole-moment during a stimulated electric-dipole transition can not as in the magnetic case of a spin $\frac{1}{2}$ be visualized as happening in real physical space. The second theorem is also well known (BLOCH 1946).

DEHMELT proposes to couple the two macroscopic systems by means of a light soft spring which carries a point on a rod of the pendulum close to the fulcrum to a point on the axis of the gyroscope. The excitation of the pendulum would then be nearly proportional to the rotating component of the vector $\vec{A}$, and the macroscopic maser would simulate the excitation of a resonant circuit by the fluctuating atomic dipole moment which appears during a stimulated atomic transition.

With $\vec{A}$ pointing initially upwards, energy can flow from the gyroscope to the pendulum, combined with a gradual tilting of $\vec{A}$ towards its equilibrium position of lowest energy. Since this process will be triggered off by some random motion, a transient excitation of the pendulum results. Any excited two-level atomic system coupled to a resonant circuit shows this transient maser action, for example excited protons in a drop of benzene contained in a tuned radio-frequency coil which is located in a magnetic field (SZÖKE and MEIBOOM 1958).

The process of $\vec{A}$ tilting downwards is reversible, i.e. a "π pulse" (HAHN 1950) from an external oscillator would swing the gyroscope from its equilibrium position of lowest energy into its "excited" state. The same result can be achieved by the method of "sudden (here gravitational) field reversal" (PURCELL and POUND 1951) which was first applied to achieve population inversion of the ^{7}Li nuclei in a crystal of lithium fluoride.

Concerning the time in which $\vec{A}$ tilts downwards, it will flip over at a faster rate the lower the friction in the fulcrum of the pendulum. In fact theory (BLOEMBERGEN and POUND 1954) shows that the "radiation damping" time of a system 'excited atoms - tuned circuit' is inversely proportional to the quality factor of the circuit.

In order to achieve continuous maser oscillation, one has to replace continuously the gyroscope. This can be done at a random rate, since the initial phase of the rotating component of $\vec{A}$ is always and only determined by the phase of the oscillating pendulum. Hence any randomly arriving "excited" gyroscope "radiates" its energy into the same phase, i.e. the "atoms" co-operate (DICKE 1954) in the process of establishing a coherent "emission field". Maser generation could be described as "phase-locked stimulated emission of radiation".
One could simulate the random arrival of excited atoms at the resonant component as well by forcing $\vec{A}$ at a random rate into its upright position.

DEHMELT'S macroscopic maser is a fair analogue of a real maser. In fact in a magnetic maser there is also the gyroscope like precession of a vector (magnetic-dipole moment) about the direction of a constant (magnetic) field (Chapter III ff.). There are however also masers which operate on an electric-dipole transition. In the latter case the motion of the electric-dipole moment during a stimulated transition is difficult to visualize. However, according to FEYNMAN, VERNON and HELLWARTH (1957), it is nevertheless possible to understand this motion as a precession about the direction of some "effective" field in an abstract space.

In the masers available the methods applied to achieve population inversion of the two energy levels often differ from each other considerably. This does however not alter the fact that DEHMELT's macroscopic maser is an analogue of each of them. In the following section the basic flow masers are enumerated and the different inversion techniques are briefly mentioned. A detailed description of a magnetic maser will be given in the course of this thesis.

1.5 The Basic Flow Masers

In the first successful maser (GORDON, ZEIGER and TOWNES 1954) population inversion was obtained by spatial separation of ammonia molecules in different energy states. The ammonia molecule has a pair of energy levels which are separated by 23.870 GHz. The electric dipole moment of the molecule has opposite sign in each of the two

states of this pair, which is called an inversion doublet. Like many other molecules, the ammonia molecule exhibits the quadratic STARK splitting of its energy levels, i.e. if the molecule is brought into a an electrostatic field ε then the energy of the upper level increases with ε^2 while the energy of the lower level decreases with ε^2.
In order to achieve spatial separation of the molecules being in different energy states, one can send a beam of molecules through a strongly inhomogeneous electrostatic field in which ε^2 has a large field gradient perpendicular to the flow direction. The molecules in the lower energy state will then be deflected spatially towards field regions of higher ε^2, and the molecules in the higher energy state will be deflected towards field regions of lower ε^2. Hence by passing a beam of ammonia molecules through an electrostatic focuser TOWNES and co-workers were able to remove the ammonia molecules being in the state of lower energy from the molecular beam. The beam of the remaining excited ammonia molecules possessing the negative dipole moment passed through a microwave cavity tuned to the above transition frequency of the inversion doublet. If the power emitted by the molecules was larger than the power losses caused by eddy currents circulating in the cavity walls, microwave amplification could be achieved. If the power emitted by the molecules was larger than the sum of the power dissipated in the cavity walls and the power escaping through the coupling hole of the cavity, stable auto-oscillations were observed.

By utilizing other molecules, e.g. formaldehyde, the principle of the molecular beam maser operating on an electric dipole transition can be applied in the megahertz frequency range (SHIMODA, TAKUMA and SHIMIZU 1960) as well as in the mm-wave range (MARCUSE 1961). While in the former case the spatially separated excited molecules pass through a parallel-plate condenser tuned by a radio-frequency coil, in the latter case the excited molecules pass through a parallel plate resonator (FABRY-PEROT resonator).

As was first demonstrated by STERN and GERLACH (1924) a beam of magnetic particles can be separated spatially in an inhomogeneous magnetic field. This is used in the atomic hydrogen beam maser (GOLDENBERG, KLEPPNER and RAMSEY 1960) where atoms in a higher magnetic state pass into a microwave cavity. This maser operates on a magnetic-dipole transition between "hyperfine" levels of the hydrogen ground state which are produced by the interaction of the electron and proton spins. The operation frequency is 1.420 GHz. A quantum-mechanical formula states that the transition probability per unit time for a magnetic dipole bathed in radiation of the frequency required to cause transitions is proportional to the square of the matrix element of the component of the magnetic-dipole moment parallel to the radiation field. This matrix element of the magnetic-dipole moment of the hydrogen atom is smaller than for electric-dipole transitions of molecules by about two orders of magnitude, and in order to compensate its smallness it is necessary either to increase the beam flux by a factor of about 10^4

or to increase the residence time of the hydrogen atoms in the cavity by a factor of about 100. In the hydrogen maser this problem is solved by greatly increasing the residence time (to 1 sec compared with about 10^{-4} sec in a molecular beam maser) through the use of a storage bulb located inside the microwave cavity. The hydrogen beam enters the storage bulb through an orifice, and after many wall collisions the atoms leave through the same orifice.

In the first magnetic maser to operate on a nuclear magnetic-dipole transition (ABRAGAM, SOLOMON and COMBRISSON 1957) the active material was an aqueous solution of the peroxylamine disulphate ion $(SO_3)_2NO^{--}$, inserted into a tuned solenoid, in a weak magnetic field, e.g. the magnetic field of the earth. The electron spin of this ion experiences a magnetic field from the nitrogen nucleus which is larger than the external field. It gives rise to a pair of energy levels which are separated by 56 MHz. The proton spin of the water in the earth's magnetic field produces a pair of energy levels which are separated by about 2 kHz. If the 56 MHz electron spin resonance is saturated by means of a large radio-frequency magnetic field oscillating at 56 MHz, then the result is a large negative nuclear magnetic polarisation of the substance, i.e. the populations of the levels of the 2 kHz nuclear ZEEMAN transition are not only inverted but also considerably re-distributed with respect to the corresponding thermal-equilibrium populations. This phenomenon which is called the dipolar OVERHAUSER effect is tightly connected with the paramagnetic relaxation

of the ion. In the earth's magnetic field this maser oscillates at a frequency near to 2 kHz. It can be operated both as a stationary maser and as a flow maser (PÉPIN 1968). A similar nuclear maser oscillating in a large magnetic field at a corresponding higher frequency has been described by GANSSEN (1962).

Dynamic polarization by means of the OVERHAUSER effect is not the sole method available to obtain a strong negative nuclear magnetic polarization in a liquid. At high magnetic fields and room temperature uncancelled proton spins are provided in sufficient numbers by such convenient liquids as water and benzene. BENOIT (1958, 1959) devised an efficient flow system where the liquid maser medium, tap water for example, passes first through the pole gap of a strong electromagnet, where the liquid is prepolarized, and then into a tube through which the liquid flows out of the field. At the edge of the magnet an auxiliary coil is wrapped around the tube. The terminals of this coil are connected to an external low frequency oscillator. As the liquid passes through the coil the macroscopic nuclear magnetization inverts by "adiabatic fast passage" in the low frequency field which excites this inversion in the inhomogeneous fringe field of the magnet. The excited protons can then be used to produce maser oscillations in a tuned radio frequency coil located in a weaker direction field some meters away or located between the polefaces of the prepolarizing magnet itself. For the case that the emission coil was placed in a weak field, maser oscillations could still be observed

at a field as small as 0.06 gauss, and the frequency of oscillation was then as low as 250 Hz. In the earth's magnetic field of about 0.5 gauss the frequency of oscillation is near to 2 kHz. In a large field of 7000 gauss the frequency of oscillation is about 30 MHz. This maser type will be discussed in more detail in Chapters IV and V.

A nuclear flow maser utilizing ^{3}He nuclei (spin $\frac{1}{2}$) is also possible. COLGROVE, SCHAERER and WALTERS (1963) found that by transferring angular momentum from circularly polarized "optical pumping" light to helium-3 in a magnetic field, both an enhancement and an inversion of the nuclear magnetic polarization of this gas can be achieved. This is made possible through the phenomenon of "spin exchange", i.e. transfer of orientation from one species of atom to another by collision. ROBINSON and MYINT (1964) utilized this pumping method in order to devise a helium-3 nuclear maser. The helium-3 gas was confined to two glass bulbs, 3.5 cm in diameter, and a thin diffusion pipe connecting the bulbs. In one of the spheres population inversion was achieved by optical pumping, the other bulb was placed inside a radio-frequency coil tuned to the nuclear ZEEMAN transition. This separation of optical orientation and stimulated emission is arranged in order to prevent the pumping inducing frequency shifts. With a magnetic direction field of 32 gauss the frequency of oscillation was 103 kHz.

All masers enumerated here can be applied as stable oscillators and for spectrometric purposes. The hydrogen maser is at present the most accurate frequency standard; its long-term fractional variations are not larger than about 10^{-13}. The nuclear masers find in addition applications as accurate magnetometers and gyrometers, the accuracy being about 10^{-6}.

Stationary masers are not relevant to the following. The two stationary types are BLOEMBERGEN's (1955) three-level solid state maser (low noise microwave amplifier) and the optically pumped rubidium gas cell maser (atomic frequency standard) of DAVIDOVITS (1964).

1.6 Summary

The types of flow masers available at the present time are the beam masers, the liquid flow nuclear masers and the helium-3 diffusion nuclear maser. With the exception of molecular beam masers which operate on an electric-dipole transition, all flow masers enumerated utilize a magnetic-dipole transition. Although in some cases more than two energy levels are utilized in order to achieve population inversion, the actual maser action occurs always between two levels only. Theorem I stresses a certain analogy which exists between all of these masers.

CHAPTER II

PREVIOUS WORK ON FLOW MASERS WITH SEPARATED EMISSION FIELDS

2.1 Introduction

After the advent of the ammonia beam maser in 1954, experimental interest in the characteristics of the flow of ammonia molecules emerging from the cavity of an oscillating ammonia maser led to the construction of the first two-cavity ammonia beam maser. The behaviour of this type of system, which was found to be rather complex, has been investigated by several workers. Practical applications other than in the investigation of general radiation processes were also realized or proposed. However, among the effects observed there is at least one which still needs cogent explanation: the "double-hump detuning phenomena" observed in the second cavity as the first cavity is gradually detuned. The purpose of this chapter is to give a critical review of the previous work on two-cavity ammonia beam masers. In fact as far as literature indicates, up to now only the ammonia beam maser has been operated with tandem resonators.

2.2 HIGA's Experiment

The first to operate an ammonia beam maser with cascaded cavities was HIGA (1957). In this experiment a beam of excited ammonia molecules passed first through the normal maser cavity and then, a few centimeters away, through a second cavity. It was observed that:

a) maser oscillations can occur simultaneously in both resonators;

b) as the first cavity is tuned away from the "centre of gravity" of the molecular resonance line, the frequency of oscillations in the second cavity follows precisely the frequency of oscillation in the first resonator;

c) when the first cavity is detuned sufficiently, two different oscillations can build up in the second cavity, at the frequency at which the first resonator oscillates and at the centre of gravity of the molecular resonance line.

As is usual for ammonia beam masers, cylindrical cavities were used. The above phenomena are, however, not produced by radiation which escapes through the open ends of the first cavity and which is picked up by the second cavity. Such direct electromagnetic coupling can be avoided by the use of close fitting end caps which have only a small orifice for the beam to pass through.

The sole coupling present was via the molecular beam which is obviously in some particular dynamic state after emerging from the first cavity. HIGA was the first to use the expression "ringing" molecules in this context. In fact the dynamic behaviour of the molecules emerging from the first cavity is now generally termed "molecular ringing".

Qualitative explanations of molecular ringing have been given by WELLS (1958), BASOV and ORAEVSKII (1962) and ORAEVSKII (1964, 1967) on the basis of quantum-mechanics. In order to understand this

phenomenon it is necessary to consider the radiation process in the first cavity. The electromagnetic field of radiation in the first cavity is coherent. This indicates that the emissions of the individual molecules do not occur independently from each other, or that the different molecules co-operate in establishing the coherent emission field in this cavity. This co-operation occurs because the different molecules interact indirectly with each other through the electromagnetic field of radiation which they produce as a whole. In other words, the radiation field in the first resonator produces states with definite coherent phase relations between the individual molecules. These phase relations which are impressed on the molecular beam in the first cavity are preserved as the molecules emerge from its exit. The emerging molecules are in a coherent dynamic state, or "superradiant" state (DICKE 1954), and the "ringing" frequency equals the frequency of the auto-oscillation in the first resonator. The second resonator is excited by the beam of ringing molecules, so that the frequency of oscillation in the second resonator equals the frequency of the auto-oscillation in the first resonator.

According to WELLS, a crude explanation of the self-modulation effect which leads to a beat note in the second cavity is as follows. As the first cavity is detuned the molecules enter the second resonator with a probability of being in the excited state considerably larger than $\frac{1}{2}$. Thus, if the second cavity is capable of producing auto-oscillations on its own, it will do so as though

the first cavity had been omitted. Since there will be nevertheless some ringing at the frequency of the auto-oscillation in the first cavity, two oscillations occur simultaneously in the second cavity.

2.3 The Double-Hump Detuning Phenomenon

Since HIGA's (1957) experiment molecular ringing has been a challenge to numerous experimentaland theoretical workers. The main work on ammonia beam masers with two and more successive cavities was performed in the research group of Prof. BASOV at the Lebedev Institute in Moscow. STRAKHOVSKII and TATARENKOV (1962) and BASOV, ORAEVSKII, STRAKHOVSKII and TATARENKOV (1964a,b) investigated the dependence of the radiation power in the second cavity on the focusser voltage and on the detuning of the first cavity. Fig. 2 shows their experimental result including the "double-hump detuning phenomenon". It is seen that as the first cavity is detuned through its full oscillatory range, the intensity of the radiation in the second cavity can go through two maxima, with a gap in the middle. This double-hump detuning phenomenon occurs at a high focusser voltage. At low focusser voltages the dependence of the radiation intensity in the second cavity on the detuning of the first cavity is bell-shaped.

In judging these curves one has to know that the number of spatially separated high-state molecules entering the first cavity increases approximately as the square of the focusser voltage (BARNES 1959). The detuning characteristic of the first coil is always bell-shaped, regardless of the magnitude of the focusser voltage.

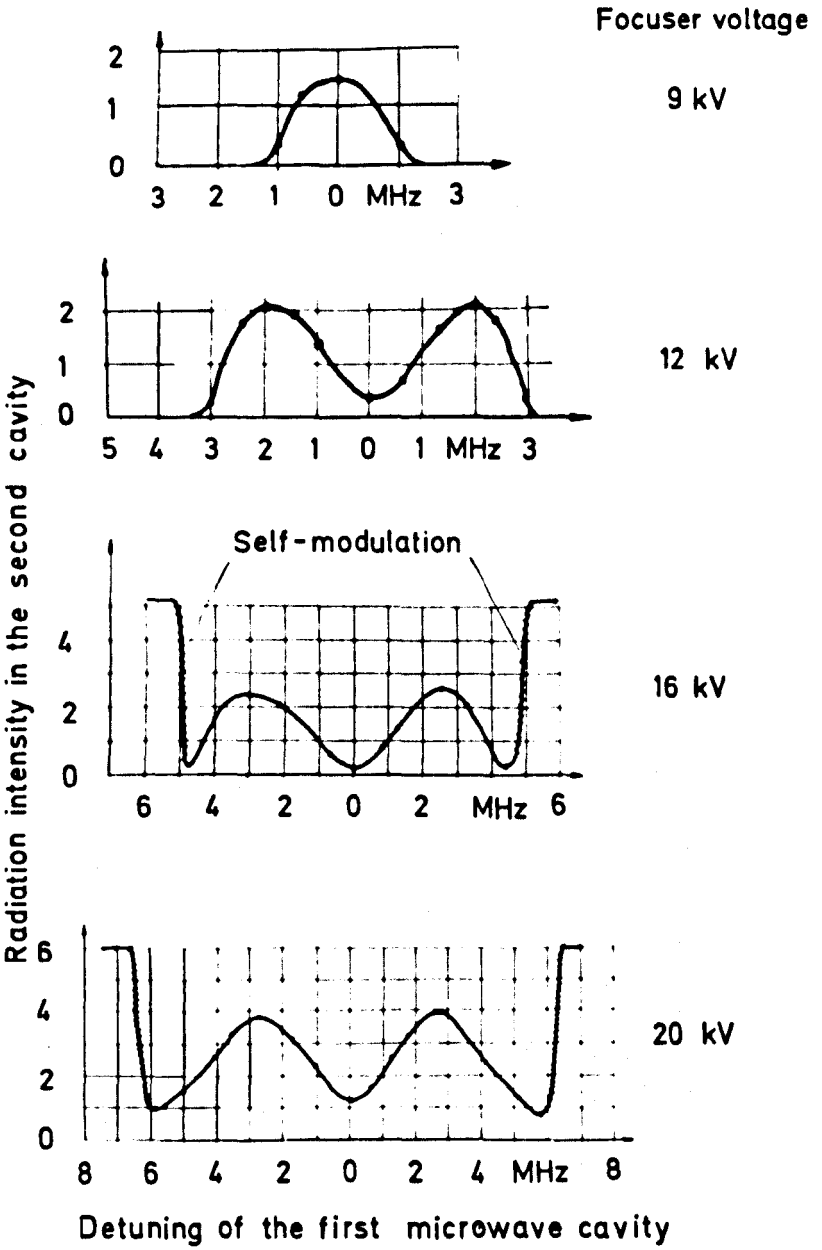

FIG. 2. The double-hump detuning phenomenon of series-cavity ammonia beam masers. After measurements of BASOV and coworkers, 1964.

The bar-crossed tracks of the curves shown in Fig. 2 indicate the region where HIGA's self-modulation effect occurs in the second cavity.

The double-hump detuning phenomenon was observed independently from the above workers by LAINÉ and SRIVASTAVA (1963) and also further investigated by SMITH and LAINÉ (1968). However, SMITH and LAINÉ (1966a,b) found also a double-hump detuning phenomenon for a low focusser voltage, and they suggest that this second gap might eventually arise from a hyperfine splitting of the inversion line.

2.4 Theoretical Investigations of the Double-Hump Detuning Phenomenon

In order to explain the complicated behaviour of two-cavity ammonia beam masers, BASOV and co-workers (1964a,b) attempted first a quantum-mechanical theory. A rough estimate showed that if the first cavity is tuned exactly to the centre of gravity of the molecular resonance line then for a large electric field amplitude in the first cavity, the radiation intensity in the second cavity could eventually become zero, in agreement with experiment,(see Fig. 2). The double-hump detuning phenomenon was, however, not explained, even qualitatively.

While BASOV and co-workers used a classical description for the radiation field, LI TIE-CHENG and FANG LI-ZHI (1964) utilized a theory where the radiation field was quantized. These latter workers predict that if the first cavity is detuned through its full range, there should be certain frequency sectors for which no oscillations are

induced in the second cavity, and other frequency sectors for which oscillations in the second cavity should be allowed. The curves in Fig. 2 show however no discontinuities inside the frequency range of oscillations, and hence this theory could be only correct if the intensity curves represented in Fig. 2 were smeared out by some instrument effect. However, the theory of these workers does not also explain the appearance of a single hump at low focusser voltages (see Fig. 2) and hence does not appear to be satisfactory.

Recently BASOV, ORAEVSKII and USPENSKII (1967) produced a new theory and attempted to explain the double-hump detuning phenomenon by "the interference (which) occurs between the emissions of molecules which move with different velocities and radiate fields with different phases". They predict that for zero detuning of the first cavity the radiation field in the second cavity might for a certain adjustment of all parameters involved become zero because of interference effects. They remark however: "... we are largely unclear up to now as to why a gap appears in the center of the line ("field amplitude in the second resonator as a function of the frequency detuning of the first resonator") at large screen voltages."

It appears that much of this uncertainty about the origin of the double-hump detuning phenomenon is due to the fact that the theories produced for the two-cavity maser are rather difficult to check experimentally, for several reasons. The output power of an ammonia maser is only about 10^{-10} watts and hence not easy to measure absolutely. It is

also difficult to measure the mean velocity of the molecules and hence the residence times the molecules spend inside the cavities. Because of the divergence of the molecular beam, not all molecules are able to reach the second cavity. The two cavities are placed inside a vacuum housing and hence the system is difficult to handle experimentally. Moreover, MUKHAMEDGALIEVA and STRAKHOVSKII (1966) found recently that the vacuum housing acts on the molecules emerging from the first resonator like an "external" multimode resonator.

2.5 Realised and Proposed Applications for Multi-Cavity Beam Masers

Nevertheless, in the practical application as a frequency standard a series-cavity beam maser has great advantages over a one-cavity beam maser.

In any maser the phenomenon of frequency "pulling" occurs, i.e. when the maser is detuned or detunes itself then the maser oscillates neither on the exact molecular transition frequency nor on the natural resonant frequency of the resonator, but in between. If the cavity is detuned, then the actual frequency of oscillation depends both on the degree of the detuning and on the quality factor of the resonant circuit. In order to reduce this frequency pulling BONAMI, HERMANN, DE PRINS and KARTASCHOFF (1957) introduced the use of a parallel-cavity system consisting of two critically coupled cavities side by side, with the beam passing only through one cavity. In this arrangement the flat phase curve characteristic near resonance is used

for the reduction of the cavity pulling. (The same principle can be used to reduce the frequency pulling in a nuclear flow maser, HENNEQUIN 1961. Two critically coupled LC circuits are used in this case.)

However, the quality factor of the system is affected by the load resistance, and there are perturbing influences from varying impedances reflected back into the cavity through the wave guide hole. As pointed out by REDER and BICKART (1960), this is particularly disturbing in a practical maser frequency standard in which the maser drives an electron frequency translator. Here the environmental conditions of shock and vibration tend to de-lock the system, and hence the coupling hole has to be larger than one would like to tolerate. Moreover, the cavity is usually tuned by electro-heating, and the need for an output waveguide sets a further problem to the temperature control.

These problems are completely absent in a beam maser which uses two decoupled cavities in series. Here the tuning of the second resonator does not affect the molecular ringing frequency, and the coupling waveguide can be connected to the second resonator.

BASOV and co-workers observed that the gap in the double-hump detuning phenomenon can reach zero only if the first cavity is exactly tuned to the centre of gravity of the molecular resonance line. Hence the double-hump detuning phenomenon of two-cavity masers can be utilized as a tuning criterion. The conventional tuning methods

(BECKER 1966) for one-cavity masers are rather complicated. VESELAGO, ORAEVSKII, STRAKHOVSKII and TATARENKOV (1965) propose the use of distance modulation of the two cavities as a means of tuning the first cavity exactly to resonance. From theoretical considerations (ORAEVSKII 1965), the phase difference between the oscillations in the two cavities is given by

$$\Delta\psi = (\omega_1 - \omega_{21}) \frac{\Delta\ell}{\bar{v}} \qquad (1)$$

where ω_1 is the frequency of oscillation in the first resonator, ω_{21} is the centre frequency of the molecular transition, $\Delta\ell$ is the inter-cavity distance, and $\bar{v}$ is the velocity of the molecular beam. Assuming $\Delta\ell$ = 10cm, $\bar{v}$ = 5 x 10^4cm/sec, $\omega_1 - \omega_{21} = 10^{-10}\omega_{21}$, then $\Delta\psi \approx 2 \times 10^{-4}$, corresponding to a phase change of about 0.01°. If this small angle could be measured it would be possible to tune the maser frequency with an accuracy of 10^{-10}. However, as far as literature indicates, up to now this latter tuning method has not been verified in practice. Besides the difficulty of measuring a phase angle as small as this, there is also the problem that moving parts in inside the vacuum housing affect slightly the ringing frequency (MUKHAMEDGALIEVA and STRAKHOVSKII 1966).

DE PRINS (1961) found that the stability of a maser frequency standard can be enhanced by the use of two oppositely directed, spatially overlapping beams, and similar experiments have also been carried out with two-cavity masers.

MUKHAMEDGALIEVA, ORAEVSKII and STRAKHOVSKII (1965) devised a "molecular ringing amplifier", a two-cavity system with two oppositely directed ammonia beams. The quality factor of the second cavity was kept low in order to prevent self-excitation in this resonator. The beam of ringing molecules emerging from the first resonator induced oscillations in the second cavity. These oscillations were found to be amplified by the oppositely directed intense beam of molecules. If the second cavity is also capable of auto-oscillations then this system has over a one-cavity maser clock the additional advantage that a condition of mutual synchronisation of the two radiation fields can be established (BELENOV and ORAEVSKII 1966). This should also enhance the frequency stability. An experimental investigation of this type of system was recently reported by KROUPNOV, SKORTSOV and SINEGOUBKO (1968).

SUCHKIN (1966) proposes the "moleculechron", a maser scheme which consists of an arbitrary number of single-beam, two-cavity masers coupled to each other by waveguides containing ferrite isolators, each further stage enhancing the accuracy. However, as far as literature indicates, up to now this proposal has not been verified in practice.

An application of two-cavity masers which is not directly relevant to the following is in the molecular spectrometry (BASOV, ORAEVSKII, STRAKHOVSKII and USPENSKII 1966, KUKOLICH 1967). Here it is found that two-cavity masers can have a larger resolution power than conventional one-cavity maser spectrometers.

2.6 Summary and Conclusion

Flow masers with separated emission fields are remarkable because of the great variety of types of operation that are in principle possible. However, as far as literature indicates, up to now only the ammonia beam maser has been furnished with tandem resonators, and only in this single case have steps been taken to exploit the possible advantages of separated emission fields.

The phenomenon of "molecular ringing" as observed with two-cavity ammonia beam masers has produced some macroscopic effects which still need cogent explanation. On the other hand, Theorem I,(Section 1.4), suggests that the macroscopic phenomena produced by the ammonia molecules which are in a coherent superradiant state, should find their exact analogues in the macroscopic phenomena produced by an assembly of coherently precessing spin $\frac{1}{2}$'s in a magnetic field, if the experimental conditions are analogous.

This suggests investigating the possibility of constructing a two-resonator maser which operates on a magnetic dipole transition. If this system can be realized and the analogy to a two-cavity ammonia beam maser be established, an answer to the open questions might eventually be found by analogous experiments. Moreover, a two-resonator magnetic maser might perhaps find corresponding practical applications.

In order to attack the problem, one could choose either a nuclear flow maser or the hydrogen maser as a starting base. The latter is not only difficult to build, but it also carries with it unnecessary

complications arising from electromagnetic field theory, or microwave theory, which is not essential in the basic operation of a maser. Hence it is preferable to use a nuclear flow maser for this investigation.

CHAPTER III

NUCLEAR MAGNETIC RESONANCE AND MASERS

3.1 Introduction

In Chapter II it was suggested that the investigation of a nuclear maser utilizing separated emission fields should reveal information about the possible existence of analogies to a two-cavity ammonia beam maser.

The purpose of the present chapter is to formulate the conditions under which a conventional one-coil nuclear maser oscillates. The theory presented here is the conventional classical one; it uses BLOCH's phenomenological equations and a coupling equation for the system 'spin-circuit'.

Before the analysis of the one-coil nuclear maser is presented some general aspects of the phenomenon of nuclear magnetic resonance are reviewed.

3.2 Some Aspects of Nuclear Magnetic Resonance*

A nuclear maser utilizes a working substance which contains atomic nuclei of spin $\frac{1}{2}$, e.g. protons, subjected to a constant magnetic field $\vec{H}_o$. A pair of nuclear ZEEMAN energy levels, $m_I = +\frac{1}{2}$, $m_I = -\frac{1}{2}$,

---

* Text books on nuclear magnetic resonance; e.g. ABRAGAM (1961), ANDREW (1958), GRIVET (1955), LÖSCHE (1957).

is thereby produced. The magnetic moment of the nucleus, $\vec{\mu}$, has opposite sign in each of the two states of this pair.

In thermal equilibrium at temperature T the numbers of nuclei per unit volume in the upper and lower states, $N_{-\frac{1}{2}}$ and $N_{+\frac{1}{2}}$, are governed by the BOLTZMANN relation $N_{-\frac{1}{2}}/N_{+\frac{1}{2}} = \exp(-\Delta E/kT)$, where $\Delta E = E_2 - E_1 = h\nu_o$ in the energy separation of the two levels ($E_2 > E_1$), and k is BOLTZMANN's constant. Hence in thermal equilibrium the state of the higher energy E_2 is less populated that the state of the lower energy E_1. The consequence of the surplus in the lower energy state is that the collection of nuclei exhibits a net longitudinal magnetic moment per unit volume $\vec{M}_o = \vec{\mu}(N_{+\frac{1}{2}} - N_{-\frac{1}{2}}) = \chi_o \vec{H}_o$ parallel to the direction of the field $\vec{H}_o$. Here χ_o is the static nuclear magnetic susceptibility.

In Section 3.4 it will be shown that one of the conditions for a nuclear maser to oscillate is that $\vec{M}_o$ be aligned antiparallel to the field $\vec{H}_o$, i.e. population inversion must be achieved. If the populations are inverted then the situation is one of anti-thermal equilibrium, and one can describe this by introducing a "negative" spin temperature (PURCELL and POUND 1951).

In NMR experiments the magnetic nuclei are bathed in a radio-frequency magnetic field $\vec{H}_1$ rotating with an angular velocity $\omega_o = \gamma H_o = 2\pi\Delta E/h$ in a plane perpendicular to the direction of the field $\vec{H}_o$. Thereby transitions ($m_I = +\frac{1}{2}$) $\rightleftarrows$ ($m_I = -\frac{1}{2}$) accompanied by the absorption or emission of a quantum $h\nu_o$ are induced. As a consequence of the resonance effect the thermal equilibrium will be disturbed.

A further consequence of the presence of the radio-frequency magnetic field will be that definite phase relations between the motions of the individual spins are produced. The existence of this phase coherence allows for a classical discussion of the NMR phenomenon in terms of one macroscopic magnet as first introduced by BLOCH (1946) in his theory of nuclear induction.

According to BLOCH, the motion of a macroscopic nuclear magnetization $\vec{M}$ of a collection of nuclei subjected to a magnetic field $\vec{H}$ resembles essentially the motion of the axis of a gyroscope (see Fig. 3).

The equation governing the motion of $\vec{M}$ is essentially NEWTON's law of motion:

Rate of change of angular momentum = torque applied to the system

A magnet with moment $\vec{M}$ in a field $\vec{H}$ experiences a torque $\vec{M} \times \vec{H}$. On the other hand, the intrinsic mechanical angular momentum of a nucleus, $\vec{a}$, contributes to a macroscopic angular momentum per unit volume $\vec{A}$. Since $\vec{\mu}$ and $\vec{a}$ are co-linear one may write NEWTON's law of motion in the form of the equation:

$$\frac{\overrightarrow{dM}}{dt} = \gamma \vec{M} \times \vec{H} \qquad (1)$$

where $\gamma = \frac{M}{A} = \frac{\mu}{a}$ is the magnetogyric ratio, a constant.

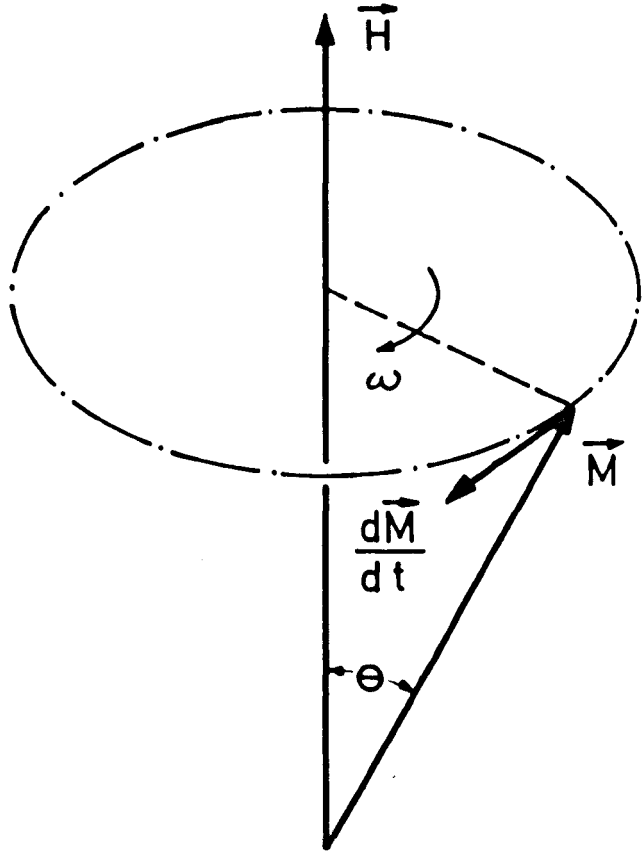

FIG. 3. Precession of a magnetic moment $\vec{M}$ around a magnetic field $\vec{H}$ according to the law $d\vec{M}/dt = \gamma(\vec{M} \times \vec{H})$.

When $\vec{H}$ is a d.c. magnetic field $\vec{H}_o$, the above equation describes a precession of the magnetization vector $\vec{M}$ in a cone about the direction of $\vec{H}_o$, with an angular velocity $\omega_o = \gamma H_o$, and with the cone angle always remaining equal to its initially imposed value θ. This is the phenomenon of the "free" LARMOR precession of $\vec{M}$. It can occur after the external radio-frequency field $\vec{H}_1$, which produces the phase coherence between the individual spins is switched off. The lifetime due to spontaneous emission of a coherently excited system of spins can be many orders of magnitude shorter than for incoherent excitation. Hence it is often said that a coherently excited system of spins is in a coherent "superradiant" state. The radiation from an assembly of spins being in a superradiant state is called "superradiation" (Section 3.3).

In other words, when a magnetic field $\vec{H}_1$ rotating at right angles to the direction of $\vec{H}_o$ is applied to a collection of nuclei, the nuclei are drawn into phase with $\vec{H}_1$, so that they all precess together. However, when the driving field $\vec{H}_1$ is removed, the nuclei will only then continue to precess in phase if they all "see" the precisely identical field $\vec{H}_o$. In practice the field $\vec{H}_o$ is always somewhat inhomogeneous, and because of this spread of magnetic fields over the sample, some nuclei will precess more rapidly than others, and a gradual loss in phase coherence will be the result. If the spread of the magnetic fields is ΔH, then the LARMOR frequencies will be spread over a range $\gamma \Delta H$, and it is convenient to define a spin-spin

interaction time

$$T_2^* \simeq \frac{1}{\gamma \Delta H} \tag{2}$$

This spin-spin interaction time is a "phase memory" time; it is the characteristic time for the precessing spins to lose their phase coherence.

The dynamics of a collection of nuclear spins subjected to combined d.c. and a.c. magnetic fields and to natural relaxation produced by spin-spin interaction and by thermal spin-lattice relaxation can be studied by BLOCH's phenomenological equations

$$\frac{\vec{dM}}{dt} = \gamma(\vec{M} \times \vec{H})_{\perp} - \frac{\vec{M}}{T_2^*} \tag{3}$$

$$\frac{dM_z}{dt} = \gamma(\vec{M} \times \vec{H})_z - \frac{M_z - M_o}{T_1} \tag{4}$$

In discussing the motion of the magnetization vector in a cartesian coordinate system it is a convention to choose the z axis parallel to the direction of the constant field $\vec{H}_o$ so that $H_z = H_o$. The index $\perp$ stands here for the transverse component of the vector in the xOy plane.

BLOCH's phenomenological equations, Eqs. (3) amd (4), consist of the normal equation of motion, Eq. (1), to which phenomenological relaxation terms are added. According to Eq. (3), T_2^* is the time constant characterizing the complete disappearance of the transverse

component of the magnetization in the absence of a.c. fields. The spin-spin interaction time is also called transverse relaxation time.

The parameter T_1 is the spin-lattice relaxation time, or longitudinal relaxation time. According to Eq. (4) it corresponds to the time constant with which the longitudinal component M_z relaxes towards its equilibrium value M_o in the absence of a.c. fields. The spin-lattice relaxation is a consequence of the thermal contact between the spins and the surrounding matter, the "lattice".

By solving BLOCH's equations one can show (e.g. ABRAGAM 1961) that the saturation of the spin system subjected to a rotating field $\vec{H}_1$ operates through the function

$$M_z = \frac{(\omega_o - \omega)^2 T_2^{*2}}{1 + (\omega_o - \omega)^2 T_2^{*2} + \gamma^2 H_1^2 T_1 T_2^*} M_o \qquad (5)$$

This relation is of some importance in the theory of nuclear masers since the spin saturation is the mechanism which limits the growth of the amplitude of the auto-oscillation in a nuclear maser.

In the normal NMR experiments, where no population inversion is used, $N_{+\frac{1}{2}}$ is greater than $N_{-\frac{1}{2}}$, and under the influence of $\vec{H}_1$, therefore, more nuclei are excited from the lower to the upper level than from the upper to the lower level. This results in a net energy absorption, which appears as a line in the nuclear resonance spectrum. One can show that if $\gamma^2 H_1^2 T_1 T_2^* \ll 1$, i.e. if the saturation is

negligible, the power absorbed by the spin system at any angular frequency ω of $\vec{H_1}$ is given by

$$P = H_1^2 \chi_o \omega_o \frac{2T_2^*}{1 + (\omega_o - \omega)^2 T_2^{*2}}$$

The fraction on the right hand side is the normalized line shape function, a LORENTZIAN characteristic of a damped harmonic oscillator with a mean life time T_2^*. It might be seen that the absorption curve is at half its maximum intensity when $(\omega_o - \omega)T_2^* = 1$, i.e. the full "half-power" half width of the resonance line is given by

$$\Delta\omega = \frac{1}{T_2^*} \tag{6}$$

This relation enables one to measure T_2^*, provided the NMR absorption line is also in practice LORENTZIAN and the spin saturation is negligibly small. If expressed in units of the magnetic field, the "half-power" half width of the resonance line is given by $\Delta H = \frac{1}{\gamma T_2^*}$.

If population inversion is achieved then under the influence of $\vec{H_1}$ more nuclei are excited from the upper to the lower state than vice versa. Since stimulated emission is the exact counterpart of absorption, the sign of the NMR line will be inverted.

In a maser the quality factor of the resonance circuit, $Q = \omega_c/\Delta\omega_c$, plays a central role. It is sometimes helpful to compare this with the "quality factor of the resonance line", $Q_n = \omega_o/(2\Delta\omega)$,

or

$$Q_n = \frac{\omega_o T_2^*}{2}$$

For a given sample in a static magnetic field Q_n is the larger the higher the homogeneity of this field.

We shall conclude this section with a remark on the direct practical application of the NMR phenomenon. The relation $\omega_o = \gamma H_o$ links linearly the value of the field H_o to the circular frequency ω_o. If H_o is known the magnetogyric ratio γ can be determined by measuring $\nu_o = \omega_o/(2\pi)$. On the other hand, if γ is known magnetic fields can be determined by measuring ν_o. In fact NMR magnetometers including nuclear masers are widely used for the measurement of weak magnetic fields (GRIVET 1960, GRIVET and MALNAR 1967). Other examples for direct practical applications are the stabilization of magnetic fields (ZHERNOVOI and LATYSHEV 1965) and the stabilization of electric d.c. currents (GRIVET, SAUZADE and LORY 1964).

3.3 Principle of a Nuclear Maser

BLOEMBERGEN and POUND (1954) were the first to study the coupling between a collection of nuclear spins and an LC circuit. According to these workers, if a macroscopic magnetization is brought into the plane perpendicular to the field $\vec{H}_o$, e.g. by means of a $\pi/2$ pulse, then the system is radiation unstable. The latter is the case because the following "fictitious" feedback loop is closed: the macro-

scopic transverse rotating moment induces an e.m.f. in the coil arranged in the xOy plane - the e.m.f. produces an electric current i in the tuned circuit - the current i circulating in the coil produces a linearly polarized magnetic reaction field of amplitude $2H_1$ - the proper rotating component H_1 drives the transverse magnetic moment. (A linearly polarized field can be resolved in two circularly polarized components; the counter-rotating component can be shown to have negligible effect on a spin system.) The subsequent flow of energy from the working substance to the tuned circuit is possible only if the moment $\vec{M}$ turns back into its position of lowest energy parallel to the field $\vec{H_o}$. This process happens in a characteristic "radiation damping" time $\tau_r = (2\pi\gamma M_o Q)^{-1}$, if the individual precessing moments remain in phase. Here η = (volumen of sample/volumen of coil) is the filling factor. In other words, if $T_2^* >> \tau_r$, then the transverse magnetic moment starts to radiate all magnetic energy away. This phenomenon has been called "super-radiation".

A nuclear maser operates very similarly. The difference is that it starts off with $\vec{M}_o$ pointing initially in the direction antiparallel to $\vec{H}_o$. The small transverse magnetic moment necessary to start the feedback cycle is here created by random noise. The possibility that a magnetization - M_o could be radiation unstable was originally overlooked by BLOEMBERGEN and POUND, but VLADIMIRSKY (1957) showed that the oscillation condition for a nuclear maser is $\tau_r < T_2^*$. The situation in an electron spin resonance maser is

analogous (COMBRISSON, HONIG and TOWNES 1956). The condition for a negative macroscopic moment $-M_o$ to be radiation unstable can be expressed by an inequality which is now generally known as TOWNES' condition:

$$Q \geq Q_\ell = (2\pi\eta M_o T_2^*)^{-1}$$

If the quality factor of the circuit is smaller than the limiting value Q_ℓ, then notwithstanding the presence of the tuned circuit, the negative longitudinal moment is stable and decreases exponentially without the appearance of auto-oscillations.

For the case that the circuit be slightly mistuned, a case which concerns us since we are especially interested in detuning phenomena, a more general analysis is necessary.

3.4 Interaction of Nuclear Spins with an Electronic Circuit

Theories of nuclear masers have been published by VLADIMIRSKY (1957), BENOIT (1959), COMBRISSON (1960), SOLOMON (1961), ABRAGAM (1961), FRIC (1961) and ZHERNOVOI and LATHYSHEV (1965). The final formulae derived in the following are well known, though the derivation differs in some points from that of previous authors.

The equivalent circuit of a maser coil is shown in Fig. 4. It will be assumed that the coil axis coincides with the x axis. If the macroscopic magnetization of the sample located inside the solenoid precesses about the constant field $\vec{H}_o$ applied parallel to the

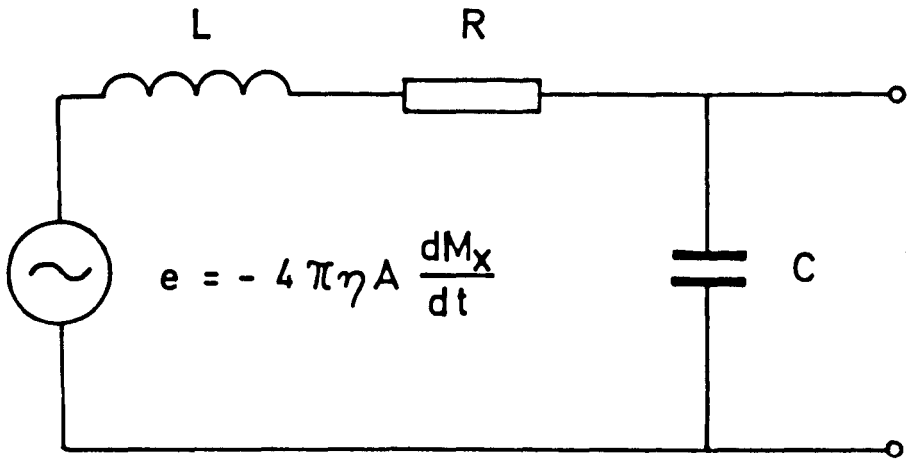

FIG. 4. Equivalent circuit of an emission coil.

z axis, an electromotive force $e = -4\pi\eta A\frac{dM_x}{dt}$ will be induced in the coil. Here $\eta = V/V_c$ is the filling factor, V is the sample volume, V_c is the coil volume, and A is the total turn area of the coil. The e.m.f. produces in the electronic circuit a current i given by

$$L\frac{di}{dt} + Ri + \frac{1}{C}\int idt = e$$

where L and R are the self-inductance and the resistance of the coil respectively, and C is the tuning capacity.

The current i circulating in the coil gives rise to a magnetic reaction field H_x which is, by the definition of the inductance L of the coil, given by $\phi = AH_x = Li$, or

$$\frac{d^2H_x}{dt^2} + \frac{\omega_c}{Q}\frac{dH_x}{dt} + \omega_c{}^2H_x = 4\pi\eta\frac{d^2M_x}{dt^2} \qquad (8)$$

Here use has been made of the relations $LC\omega_c{}^2 = 1$ and $Q = L\omega_c/R$.

The quality factor of the coil can be considered as constant in the environment of the resonant frequency of the circuit, ω_c, such that $Q = L\omega_o/R$. The detuning of the resonant circuit, β, can be defined by $\omega_c = \omega_o(1 + \beta)$. If one introduces this latter relation with Eq. (8) and takes into account that the reaction of the spin system on H_x can be described by BLOCH's equations, with Eqs. (3) and (4), the following set of equations is obtained:

$$Q\frac{d^2H_x}{dt^2} + \omega_o\frac{dH_x}{dt} + Q\omega_o{}^2(1 + \beta)^2H_x = 4\pi\eta\frac{d^2M_x}{dt^2} \qquad (9)$$

$$\frac{dM_x}{dt} = \omega_o M_y - \frac{M_x}{T_2^*} \tag{10}$$

$$\frac{dM_x}{dt} = -\omega_o M_x + \gamma H_x M_z - \frac{M_y}{T_2^*} \tag{11}$$

$$\frac{dM_z}{dt} = -\gamma H_x M_y - \frac{M_z - M_o}{T_1} \tag{12}$$

Here M_x, M_y, M_z are the components of the macroscopic moment $\vec{M}$. For $M_x = M_y = H_x = 0$ one obtains the trivial solution

$$M_z = M_o + (M_{zo} - M_o)\exp(-t/T_1)$$

which describes the ordinary exponential evolution of the longitudinal moment from an initial state M_{zo}.

The set Eqs. (9) - (12) is nonlinear, and the usual technique of investigating the instability of the system is to look for small deviations ∂M_x, ∂M_y, ∂M_z from the ordinary exponential evolution. We shall instead rely on the fact that M_z is a slowly varying parameter and drop Eq. (12). Then the remaining three equations are linear, and the corresponding set of characteristic equations is

$$4\pi\eta Q p^2 M_x + Q_p^2 + \omega_o p + Q\omega_o^2(1+\beta)^2 \; H_x = 0$$

$$(p + \frac{1}{T_2^*})M_x - \omega_o M_y = 0$$

$$\omega_o M_x + (p + \frac{1}{T_2^*})M_y - \gamma M_z = 0$$

By solving the characteristic determinant of this linear set, one obtains the characteristic equation

$$a_o p^4 + a_1 p^3 + a_2 p^2 + a_3 p + a_4 = 0 \qquad (13)$$

where

$$a_o = Q$$

$$a_1 = \omega_o\left(1 + \frac{Q}{Q_n}\right)$$

$$a_2 = \omega_o{}^3\left[\frac{Q}{Q_n}(1+\beta)^2 + 1 + \frac{1}{QQ_n} + \frac{1}{4Q_n{}^2}\right] + \omega_o 4\pi\eta\gamma Q M_z$$

$$a_3 = \omega_o{}^3\left[\frac{Q}{Q_n}(1+\beta)^2 + 1 + \frac{1}{4Q_n{}^2}\right]$$

$$a_4 = \omega_o{}^4 Q(1+\beta)^2\left(1 + \frac{1}{4Q_n{}^2}\right)$$

Here use has been made of Eq. (7). Since $Q, Q_n \gg 1$, the terms $\frac{1}{QQ_n}$ and $\frac{1}{4Q_n{}^2}$ will be neglected.

Oscillation condition

For sinusoidal auto-oscillations, $p = j\omega$, and the real and the imaginary parts of Eq. (13) must become zero independently. The oscillation condition is thus found to be $a_2 = a_o(a_3/a_1) + a_4(a_1/a_3)$. The result is

$$2\pi\eta\gamma Q T_2^* M_z + 1 = -\left[\frac{2Q_n\beta}{2+Q_n}\right]^2 = -a \qquad (14)$$

It may be noted that for this equation to be fulfilled, M_z must have a negative value, i.e. population inversion is a pre-condition for auto-oscillations in the system 'spin-circuit'.

Threshold of oscillations

If the quality factor of the circuit Q is reduced to its threshold value Q_ℓ where the maser ceases to oscillate, then M_2 becomes the static polarization $-M_o$ used in the maser:

$$2\pi\eta\gamma Q_\ell T_2^* M_o - 1 = \left[\frac{2Q_\ell Q_n \beta}{Q_\ell + Q_n}\right]^2 = b \tag{15}$$

Auto-oscillations are obtained for $Q \geq Q_\ell$. For $\beta = 0$, Eq. (15) reduces to TOWNES' condition

$$Q_{\ell o} = (2\pi\eta T_2^* M_o)^{-1} \tag{16}$$

With the aid of Eq. (16), Eq. (15) can be written in the form

$$\frac{Q_\ell}{Q_{\ell o}} = 1 + b \tag{17}$$

Maximal detuning

The maximal detuning β_m is reached if Q_ℓ approaches the fixed Q of the circuit. Eq. (17) then becomes

$$\frac{Q}{Q_{\ell o}} = 1 + \left[\frac{2QQ_n\beta_m}{Q+Q_n}\right]^2 = 1 + c \tag{18}$$

Re-arranging this equation, the maximal detuning is given by

$$\beta_m = \left[\frac{\omega_c - \omega_o}{\omega_o}\right]_{max} = \frac{Q + Q_n}{2QQ_n}\left[\frac{Q}{Q_{\ell o}} - 1\right]^{\frac{1}{2}} \tag{19}$$

If the circuit is mistuned beyond the value β_m then no auto-oscillations can occur in the system 'spin-circuit'. The range of oscillations is maximum for $Q = 2Q_{\ell o}$.

Frequency of emission

The frequency of the auto-oscillations is given by $\omega^2 = a_1/a_3$ or

$$\omega^2 = \frac{\omega_o^2}{Q + Q_n}\left[Q_n + Q(1 + \beta)^2\right]$$

Since $(\omega^2 - \omega_o^2)/\omega_o^2 \approx 2(\omega - \omega_o)\omega_o$, with Eq. (7) this equation can be written in the form

$$(\omega - \omega_o)T_2^* = a^{\frac{1}{2}} \tag{20}$$

or as

$$\omega - \omega_o = \frac{Q}{Q + Q_n}(\omega_c - \omega_o) \tag{21}$$

The latter equation which is known as the "pulling formula" means that if the first maser coil is tuned to ω_c, different from ω_o, the frequency of oscillation ω differs both from ω_o, and ω_c. In order for ω to remain in the direct environment of ω_o the inequality $Q/(Q + Q_n) \ll 1$ must be satisfied.

Although the initial set of four differential equations has been mutilated by dropping the equation containing dM_z/dt, the final results agree with those derived by other authors.

3.5 Detuning Characteristic of a Nuclear Maser

The saturation of the spin system, expressed by Eq. (5), will limit the growth of the amplitude of the maser oscillations, i.e. the field H_x produced by the circulating current in the coil will induce a certain amount of saturation in order for the oscillation condition Eq. (14) to remain valid.

Eliminating M_z and M_o between Eqs. (14), (5) and (2), the amplitude $2H_1$ of the linearly polarized field H_x induced by the circulating current in the coil is given by

$$\gamma^2 H_1^2 T_1 T_2^* = \frac{Q}{Q_\ell}(1 + b) - 1 - a$$

Using Eq. (17) gives

$$\gamma^2 H_1^2 T_1 T_2^* = \frac{Q}{Q_{\ell o}} - 1 - a$$

For $\beta = 0$ one can write

$$\gamma^2 H_{1o}^2 T_1 T_2^* = \frac{Q}{Q_{\ell o}} - 1 = c$$

where $2H_{1o}$ is the amplitude of H_x for zero detuning. Combining these latter equations gives.

$$\frac{H_1^2}{H_{1o}^2} = 1 - \frac{a}{c}$$

Introducing the quantities a and c from Eqs. (14) and (18), the field amplitude $2H_1$ dependent on the detuning is given by

$$\frac{H_1^2}{H_{1o}^2} + \frac{\beta^2}{\beta_m^2} = 1$$

Since the voltage across the solenoid E is proportional to the field H_x, one obtains the relation

$$\frac{E^2}{E_o^2} + \frac{\beta^2}{\beta_m^2} = 1 \qquad (22)$$

where E_o is the voltage across the coil for zero detuning.

According to this calculation, the detuning characteristic of a maser is a semi-ellipse, a result which was also derived by FRIC (1961) in a different way.

3.6 Summary

In this chapter we have essentially re-derived the well known conditions under which a conventional one-coil nuclear maser oscillates. It has been shown that for auto-oscillations to occur the static nuclear magnetization must have a negative sign, i.e. population inversion of the two nuclear ZEEMAN energy levels must be achieved. Even if the populations are inverted, the maser will only oscillate if the quality factor of the resonance circuit, Q, exceeds a certain threshold value Q_ℓ. If the circuit is detuned beyond a certain value β_m then the maser will cease oscillating. The amplitude of the voltage available from the terminals of the maser coil depends monotonically on the frequency detuning.

CHAPTER IV

PREPARATION OF THE NEGATIVE LONGITUDINAL MAGNETIZATION

4.1 Introduction

In Chapter III it was shown that a necessary condition for a nuclear maser to oscillate is that the populations of the nuclear ZEEMAN energy levels of the nuclei be inverted. In thermal equilibrium the magnetization $M_o = \chi_o H_o$ is always parallel to the applied field. By inverting the populations of the energy levels one creates a situation where the magnetization is antiparallel to the field. In reviewing in Chapter I the different nuclear flow masers available, it was seen that different conventional techniques achieve this.

In the present investigation BENOIT's liquid-flow method has been used in order to obtain population inversion. This technique makes use of the prepolarization of the nuclei in a strong field and of the method of adiabatic fast passage. The object of the present chapter is to describe the experimental technique applied to achieve negative longitudinal magnetization and to give the corresponding experimental data.

Once the magnetization is inverted it will decrease in magnitude because of the thermal relaxation of the spin system. A measurement of the longitudinal relaxation time T_1 will also be reported in this Chapter.

First a general outline of the experimental two-coil proton maser devised shall be given.

4.2 General Outline of the Experimental Set-up

Fig. 5 shows the schematic of the two-coil proton maser devised and investigated by the author. It is a magnetometer maser which oscillates in the magnetic field of the earth ($H_o \approx 0.48$ gauss) at a frequency near to 2.04 kHz.

The maser medium is distilled water. The active particles utilized are the protons (hydrogen nuclei) contained in the water.

As Fig. 5 shows, the water flows through a tube into a container of volume V_p located between the pole faces of a strong prepolarizing magnet. The average field in the inter-polar space of this magnet is $H_p = 2400$ gauss. The water remains in this large field for a time τ_p long compared with the relaxation time T_1 so that the protons approach thermal equilibrium.

In order to ensure that the water flowing through a certain volume in the pole gap remains there as long as possible with the same flow rate F_p, a distributing device has been arranged in the prepolarization container.

On leaving the prepolarization container the water passes into a plastic tube through which it moves rapidly out of the large field and flows into the magnetic field of the earth, in a time short compared with the relaxation time T_1.

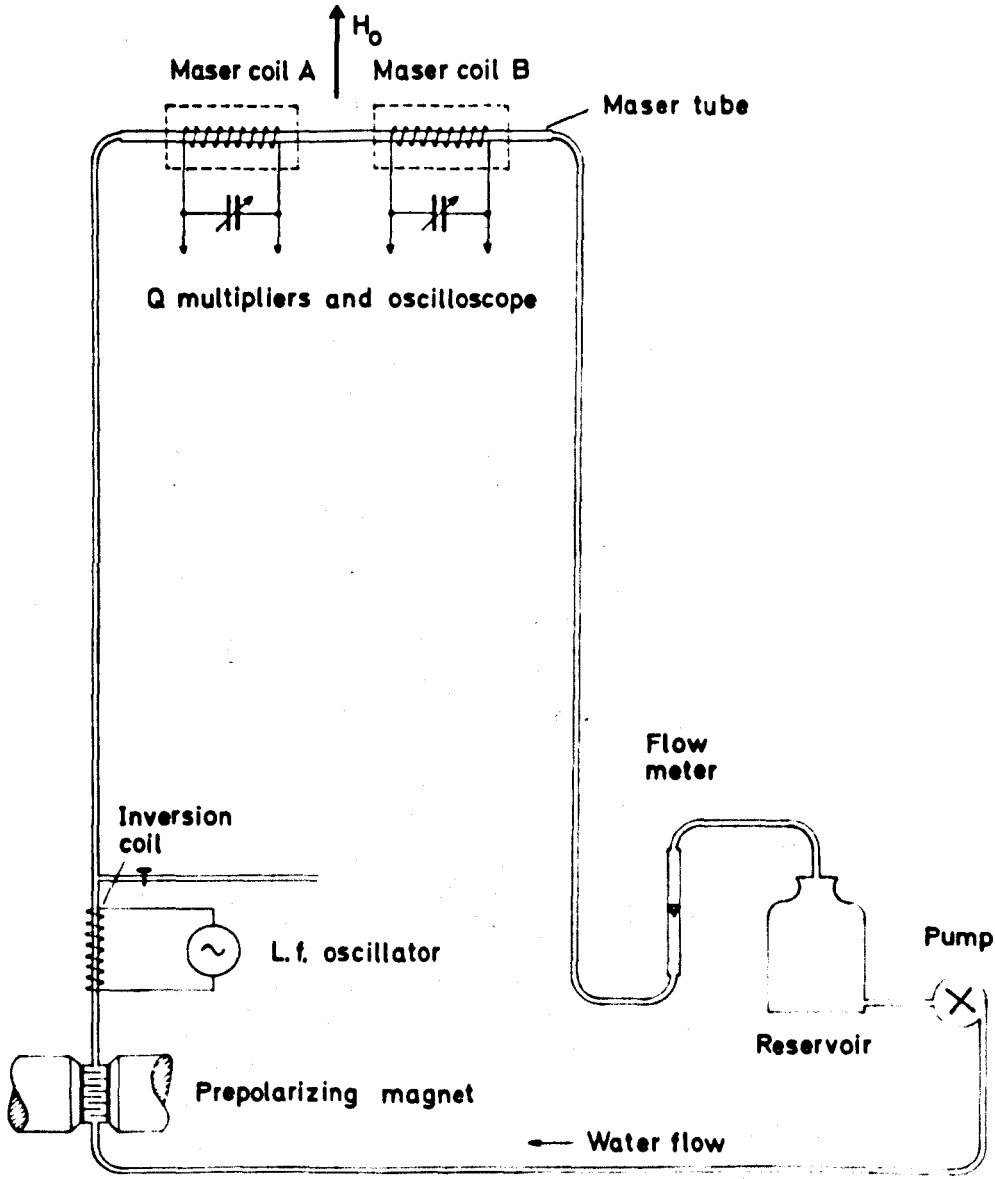

FIG. 5. Schematic of the two-coil proton maser.

At the edge of the magnet an auxiliary radio-frequency coil is wrapped around the connecting tube to produce a low-frequency magnetic field in the flowing water. If the frequency of this field is such that $\omega_1 = \gamma H$ at some point near the centre of the coil then as the water flows through this l.f. field from a strong field region where $\gamma H > \omega_1$ to a weak field region where $\gamma H < \omega_1$ the proton spins are inverted by "adiabatic fast passage".

At the exit of the auxiliary coil the water possesses a magnetization which is aligned antiparallel to the local constant magnetic field.

The water carrying the negative longitudinal macroscopic moment flows now through the plastic tube into the maser tube, a glass tube having a larger inner diameter.

The two maser coils are identical and are arranged coaxially on the maser tube.

In order to avoid direct electromagnetic coupling between the two maser coils, both coils are screened by means of aluminium cylinders.

The quality factor of each coil can be enhanced by means of a separate variable Q multiplier.

The voltages available from the two maser coils are observed by means of a two-channel oscilloscope. For frequency measurements a digital counter has been used.

Part of the water emerging from the prepolarizing field can be deviated into a second flow circuit. This allows to keep the flow rate F_p constant, while altering the flow rate F in the maser tube.

The principal difference between conventional nuclear masers and the new two-coil proton maser is that the latter utilizes separated emission fields: the normal maser coil is followed downstream by a second emission coil.

4.3 Choice of Experimental System

As far as literature indicates, magnetic masers with separated emission fields have not been devised or been discussed previously.

However, during a general investigation of a liquid-flow nuclear maser oscillating in a large field of H_o = 7000 gauss at a frequency near to 30 MHz, FRIC (1961) had attempted to measure the residual magnetization of the water emerging from the maser coil. The water passed through a second coil, the terminals of which were connected to a NMR detector circuit. The residual moment was found to be so weak that it was impossible to determine either its magnitude or its sign. It was also found difficult to avoid direct electromagnetic coupling between the two coils. In 1967 LAINÉ proposed, independently of FRIC, to use the same arrangement (high-field BENOIT-type of liquid flow maser with a successive coil) in order to clarify experimentally

whether this system shows eventually a similar complicated behaviour as a two-cavity molecular beam maser.

A preliminary estimate performed by the author, showed that a nuclear maser with separated emission fields should behave quite analogously to a two-cavity molecular beam maser, provided the relaxation time T_2^* be at least of the order of magnitude of the total transit time the nuclei need to pass through both coils in succession.

The relaxation time T_2^* is largely dependent on the inhomogeneity of the field $\vec{H}_o$. In an inhomogeneous field the individual moments of the different nuclei dephase more rapidly because the local fields are different. The situation is usually worst in large fields since a large field with a good homogeneity is difficult to realize in practice. In FRIC's experiment the transverse relaxation time of the protons in water was only about 2msec, although the natural relaxation time of protons in water is of the order of magnitude of seconds. The residence time of the nuclei in the maser coil was about 20 msec.

The compensation of the field inhomogeneity by means of auxiliary static magnetic fields is not very convenient for a two-coil nuclear maser. The same holds for the method of averaging out the field inhomogeneity by rotating the sample (BLOCH 1954).

A good homogeneity can however usually be expected from the magnetic field of the earth. Inside laboratory buildings the transverse relaxation time of protons in water would be typically of the order of

magnitude of a tenth of a second, but away from buildings utilizing ferromagnetic materials in their construction T_2^* can be considerably larger.

For this reason the experiment to be described in the following was performed in a small magnetic observatory erected inside the University campus away from the main buildings. With $H_o \approx 0.48$ gauss the frequency of oscillation of the maser is about 2 kHz.

A conventional one-coil liquid flow maser oscillating in the earth's magnetic field and utilizing also the method of prepolarization in a large magnetic field was devised by HENNEQUIN (1961). Under laboratory conditions at the Sorbonne, T_2^* was 0.1 sec and by injecting the water tangentially into the sample container such that a rotation of the water occurred T_2^* could be enhanced by a factor of three. The residence time of the nuclei in the coil was about 1 sec.

In the new two-coil maser devised by the author the water is not rotated artificially but passes straight through both emission coils. When the transit time τ for which the protons remain in one coil was altered between 0.45 sec and 0.23 sec then the measured relaxation time T_2^* varied between 0.64 sec and 0.43 sec, respectively. These relaxation times are long enough for coherent spontaneous emission to occur in the second coil.

4.4 Prepolarization

In the earth's magnetic field the observation of NMR phenomena is hampered by the smallness of the equilibrium magnetization $M_o = \chi_o H_o$. However, the long thermal relaxation time T_1 of liquids makes it possible to prepolarize the nuclei in a large field H_p where the equilibrium value $M_p = \chi_o H_p$ is approached, and then, after the suppression of H_p in a time short compared with T_1, to observe the NMR phenomenon in a weak magnetic field. In flowing liquids, prepolarization can be achieved continuously.

As indicated in Fig. 5, the water passes first through a container fitting closely between the pole faces of the prepolarizing magnet, then the water flows through a connecting tube into the earth's magnetic field where it passes through the maser tube sticking through the two maser solenoids. For the prepolarization process to be efficient the field in the interpolar space of the magnet has to be large and the water has to remain there for a time comparable with T_1.

The magnet available for this project was a permanent magnet which provides a maximal field of approprimately 3000 gauss between its pole faces. The average magnetic field across the container was measured by means of a Cambridge fluxmeter furnished with a single copper wire loop having the same diameter as the container, the result being $H_p = 2400$ gauss. The container, made from copper, has deflection sheets inside it, so ensuring that the water flowing through a certain volume remains in that volume as long as possible with the same flow rate.

By draining the container into a measuring cylinder, its volume was found to be V_p = 237 cm^3. For comparison, HENNEQUIN's earth-field maser operated with V_p = 295 cm^3 and a considerably larger field, H_p = 22000 gauss.

On leaving the container located between the pole faces, the water passes into a nylon tube of 4mm inner diameter and about 150 cm length. After a length of 30 cm, beyond the inversion coil arranged at the edge of the magnet, part of the prepolarized water deviates into a second tube short-circuiting the maser tube. The flow rate F of the water which passes through the maser tube sticking through the two emission coils was controlled by allowing a certain amount of water to flow through the second circuit. Flow rates F between 17 cm^3/sec and 35 cm^3/sec were used.

The maser tube is a glass tube of 11.8 mm inner diameter, 12.3 mm outer diameter and 50 cm length. At both ends of the maser tube the connection with the plastic tube was performed by means of a rubber stopper sticking in the maser tube and a short glass tube reaching through the rubber stop. The strong turbulence establishing itself near the entrance of the maser tube was found to have a slightly diminishing effect on the maser voltage across the first coil. In order to avoid this effect, the first coil was displaced by 8 cm away from the entrance of the maser tube. Herewith the volume of the tubing and the connecting pieces present between the point where the water deviates into the second circuit and the entrance of the maser tube adds to about 40 cm^3.

During operation, the flow rate in the container located in the pole gap of the magnet was kept at $F_p = 34$ cm^3/sec so that the protons remained for $\tau_p = V_p/F_p = 7$ sec in H_p.

The evolution of the longitudinal moment M_z in the field H_p is governed by the equation

$$\frac{dM_z}{dt} = -\frac{M_z - M_p}{T_1}$$

which gives

$$M_z = M_p + (M_{zo} - M_p)\exp(-t/T_1)$$

where M_{zo} is the initial value of M_z, i.e. the equilibrium magnetization in the earth's field, M_o, and can be neglected. Hence at the exit of the prepolarization container the longitudinal moment is

$$M_z' = M_p\left[1 - \exp(-\tau_p/T_1)\right]$$

In the subsequent flow towards the two-coil system M_z' decreases according to

$$\frac{dM_z}{dt} = -\frac{M_z - M_o}{T_1}$$

which gives

$$M_z = M_o + (M_z' - M_o)\exp(-t/T_1)$$

The value of M_o is again negligible. If the time the water needs to travel from the exit of the prepolarization container to the entrance

of the first maser coil is denoted by τ_t, then the static polarization available at the entrance of the first maser coil, M_o', is given by

$$M_o' = M_p\left[1 - \exp(-\tau_p/T_1)\right] \exp(-\tau_t/T_1) \qquad (1)$$

The longitudinal relaxation time of distilled water was measured to be $T_1 = 2.07$ sec. Under those conditions the magnetization in the container reaches 97% of its equilibrium value M_p. With the tubing as described above, at the point where part of the water deviates into the second flow circuit bridging the maser tube the magnetization is decreased to 92% of the value M_p. With $F_p = 34$ cm^3/sec the longitudinal magnetization available at the entrance of the first maser coil is given by

$$M_o' = 0.92 M_p \exp(-19.5/F) \qquad (2)$$

where the flow rate in the maser tube, F, is measured in cm^3/sec.

The pump utilized had originally an iron connecting piece, and some arrested screws reached inside the pump into the water pass. This led to corrosion which spoiled the relaxation properties of the distilled water utilized. Hence the connecting piece was replaced by one made from brass, and the iron screws were covered with araldite.

4.5 Inversion Technique

According to BLOCH (1946), if a macroscopic nuclear magnetization is subjected to a transverse field of amplitude h_1 and constant angular frequency ω_1, and the direction field $\vec{H}$ changes its magnitude and passes through the resonance condition, then the magnetization vector will invert, if the inequality $\gamma h_1^2 >> \frac{dH}{dt}$ is satisfied. Here it is assumed that the relaxation effects are negligible. This method of "adiabatic fast passage" has been discussed in depth by POWLES (1958) and by BENOIT (1959); the latter devised the first liquid-flow nuclear maser utilizing this method.

In BENOIT's technique the flowing liquid passes through an a.c. magnetic field established inside a long solenoid located in the inhomogeneous fringe field $\vec{H}$ of a strong magnet. If the frequency of the a.c. driving field is such that $\omega_1 = \gamma H$ at some point near the centre of the coil, then as the liquid flows through the a.c. field from a strong field region where $\gamma H > \omega_1$ to a weak field region where $\gamma H < \omega_1$, the nuclear magnetization changes sign.

This principle is illustrated in Fig. 6. In a frame rotating with an angular frequency ω_1 about the direction of the field $\vec{H}$ it can be seen that there exists an effective field, of amplitude $H_e = \left[(H - \frac{\omega_1}{\gamma})^2 + h_1^2 \right]^{\frac{1}{2}}$, which turns through an angle of π in a plane parallel to the direction of the field $\vec{H}$. BENOIT has shown that already under the condition $\gamma h_1^2 = 3\frac{dH}{dt}$ the macroscopic moment $\vec{M}$ follows nearly perfectly this effective field, so ensuring that after the fast passage

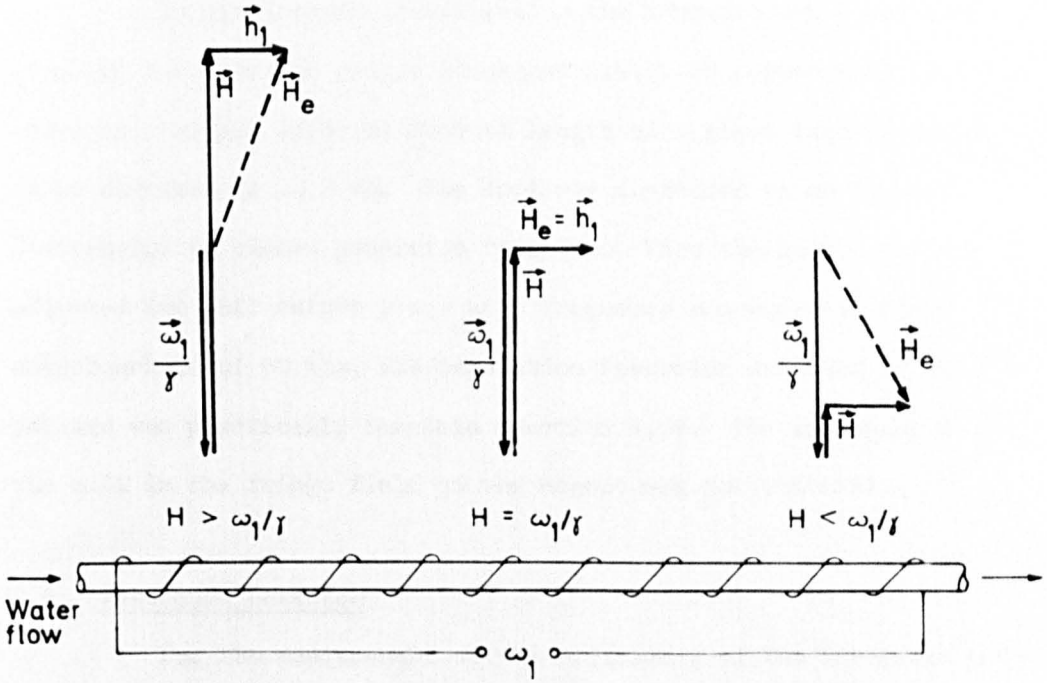

FIG. 6. Principle of BENOIT's inversion technique. The vector $\vec{M}$ follows $\vec{H}_e$.

the inversion is practically complete. Because of the inhomogeneity of the fringe field and the consequent shortness of the transverse relaxation time the liquid emerging from the inversion coil has no residual transverse rotating moment.

In the present investigation the inversion coil used consisted of about 900 turns of single enamelled s.w.g. 32 copper wire (0.274 mm^{ϕ}) wound in a single layer of 25.5 cm length on a glass tube having an outer diameter of 13.7 mm. The coil was connected to an Advance Electronics AF signal generator type J2C. When the oscillator was adjusted for full output power at a frequency somewhere in the neighbourhood of 60 kHz, the population inversion achieved by fast passage was practically complete (Section 4.6). The arrangement of the coil in the fringe field of the magnet was not critical.

4.6 Resonance Detector

For the measurement of the efficiency of the inversion method and in the determination of the relaxation time T_1 by a method to be described in Section 4.7, one of the maser coils connected to its Q multiplier was used as an NMR detector. The protons in water flowing through the detector coil were irradiated by means of an external exciter coil having about 3000 turns and a diameter of about 9 cm. The exciter coil was placed about 1 m away from the detector coil. The coil axes were arranged such that the detector and exciter coils were decoupled. The screening cylinder was not removed from the

detector coil. It was found that the exciter and detector coils could be decoupled in different relative positions, also in a position with the coil axes parallel to each other. This can be explained by the distribution of the eddy currents produced by the exciter field in the symmetrical screening cylinder of the detector coil.
The detector signal was read on the oscilloscope screen. When the frequency of the 2 kHz oscillator connected to the exciter coil was tuned to the NMR resonance condition, the resonance signal appeared at the output of the Q multiplier. The detector signal was read on the oscilloscope screen for different frequencies of the exciter field. (The resonance signal can also be obtained when the detector and exciter coils are weakly coupled; in this case the voltage induced by the exciter field in the detector coil is superimposed on the resonance signal.)

Using this method, the proton resonance in the earth's magnetic field was measured with the inversion coil connected to the 60 kHz oscillator, and with the inversion coil disconnected. Fig. 7 shows two typical resonance lines measured for these different cases. In order to achieve a reasonable signal amplitude it is necessary to use a large exciter field, and hence the resonance lines shown are saturation broadened.

The resonance line for stimulated emission is slightly higher than for absorption.. This effect becomes more distinct at larger quality factors of the detector circuit. Also, the lines have

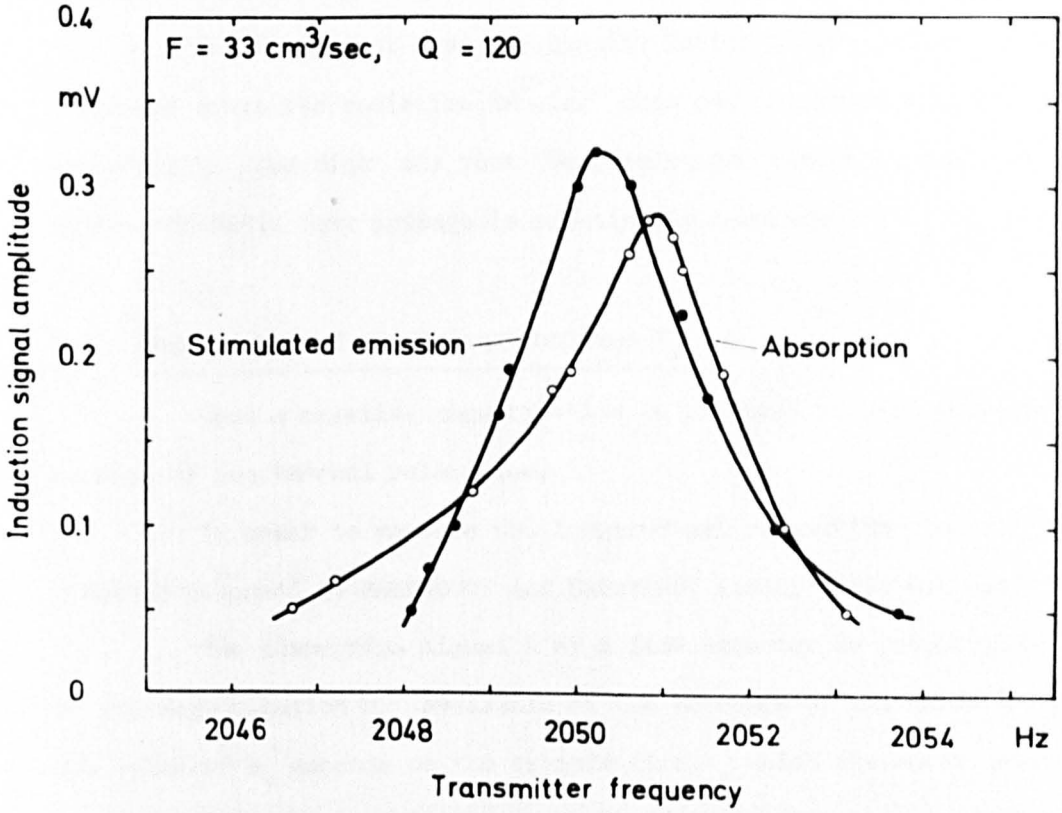

FIG. 7. Measured NMR lines of the protons in water.

a slightly different width. Both these phenomena arise because the phenomenon of "radiation damping" occurs in the tuned detector coil (BENOIT 1960).

In the present case the quality factor of the detector was small and hence the radiation damping does not introduce a large uncertainty. One might say that the population inversion achieved by the adiabatic fast passage is practically complete.

4.7 Measurement of the Relaxation Time T_1

Once a negative magnetization is produced it will decrease because of the thermal relaxation.

In order to measure the longitudinal relaxation time T_1, a method proposed by ZHERNOVOI and LATHYSHEV (1958, 1965) was used.

The absorption signal A of a flow detector is proportional to the magnetization M_o' available at the entrance of the detector coil. The value of M_o' depends on the transit time τ_t which the water needs to travel from the prepolarizing magnet to the detector coil located in the earth's magnetic field, see Eq.(1). Hence for a constant flow rate F_p the dependence of A on τ_t can be expressed by

$$A = \text{const.} \exp(-\tau_t/T_1)$$

By measuring A for different transit times τ_t it is possible to determine T_1. A semi-logarithmic plot of A against τ_t should yield

a straight line of slope $-1/T_1$, from which T_1 can be found.

In measuring T_1 the same detector arrangement as described in Section 4.6 was used. The transit time τ_t was altered by pulling the maser tube out of the detector coil.

Fig. 8 shows the decay of the absorption signal measured when the transit time τ_t was altered by increasing intervals $\Delta\tau_t$. The measurements were repeated for different flow rates T in the detector coil. According to the slope of the curves shown in Fig. 8, the relaxation time of the distilled water utilized is

$$T_1 = 2.07 \text{ sec}$$

For comparison, GRIVET and MALNAR (1967) quote 2.1 sec as the relaxation time of distilled water.

For tap water a relaxation time of about 1.7 sec was measured.

4.8 Summary

In the two-coil maser devised population inversion of the ZEEMAN energy levels is achieved by BENOIT's liquid flow method. The working substance, distilled water, is prepolarized in a strong field where a large equilibrium magnetization is approached, and population inversion is obtained by adiabatic fast passage through an auxiliary coil arranged in the fringe field of the prepolarizing magnet. With H_p = 2400 gauss the field of the magnet is considerably

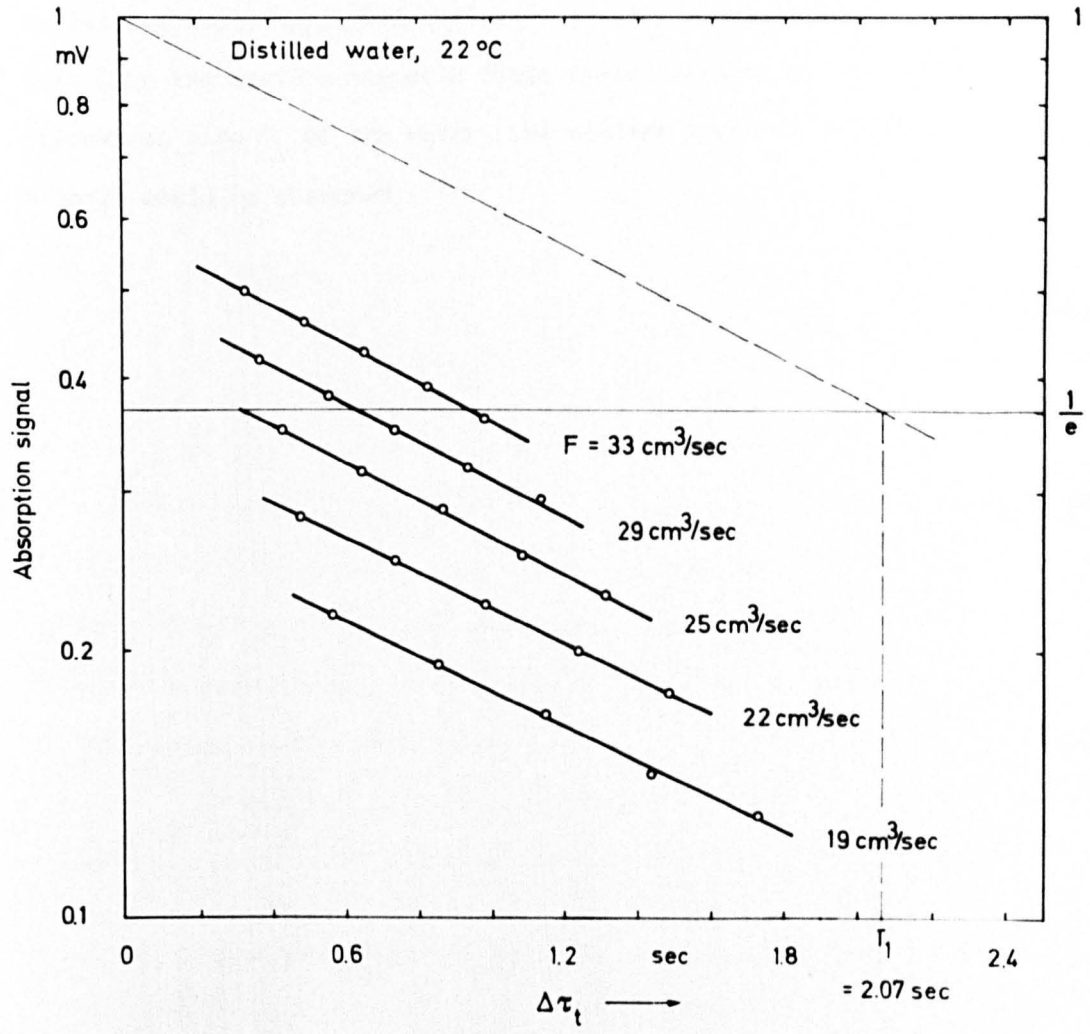

FIG. 8. The relaxation time T_1 as determined by the method of varying the demagnetizing volume.

smaller than in experiments described previously by other authors. On leaving the prepolarizing field the water flows through a plastic tube into the earth's magnetic field where, because of the long relaxation time T_1 of the water, the nuclear magnetic resonance signals could be observed.

CHAPTER V

REALIZATION OF THE TWO-COIL SYSTEM OF THE PROTON MASER

5.1 Introduction

The discussion in Chapter IV was limited to the experimental technique utilized in order to achieve a large negative longitudinal magnetization. The method which was described is a conventional one.

In this chapter the experimental details of the two-coil system of the proton maser devised by the author shall be described. This part of the experimental set-up is original and differs from conventional nuclear masers in that the normal emission coil is followed downstream by a second emission coil. On the other hand, this arrangement of separated emission fields resembles that used in two-cavity ammonia beam masers.

We shall now give the experimental details of the two-coil system and also discuss how this arrangement compares with a two-cavity ammonia beam maser.

5.2 The Emission Coils

For auto-oscillations to occur in the first coil of the two-coil proton maser the quality factor of this solenoid, Q, must be larger than the threshold value $Q_{\ell o} = (2\pi\eta\gamma T_2^* M_o')^{-1}$. Here $\eta = V/V_c$ is the filling factor of the solenoid, V_c is its volume and V is the sample volume.

In order for the threshold quality factor to be as low as possible, the filling factor η should have a value as large as possible (the theoretical maximum value of η is unity). This would require to choose a large coil because in practice it is difficult to construct a small solenoid which allows a large filling factor and which has also a reasonable natural quality factor. As an empirical rule, at a frequency of 2 kHz coil quality factors between 26 and 130 can be achieved if the sample volume is varied between 35 cm^3 and 8 dm^3, respectively (GRIVET 1960).

The emission coils for the two-coil proton maser were devised such that for a constant flow rate F the ratio T_2^*/τ be greater than unity. Here $\tau = V/F$ is the time for which the protons remain in the solenoid. If a coil is constructed along this line then this leads to a small sample volume V. On the other hand, a small sample volume leads to a small filling factor and/or to a low natural quality factor. Hence compromises had to be made.

For the two-coil proton maser two identical coils have been used; the coil dimensions are shown in Fig. 9. Each coil has 5650 turns of enamelled 30 s.w.g. copper wire (0.315 mm^{ϕ}), an inductance of L = 0.230 henry, and a rather low natural quality factor of 20. However, with the inner diameter of the maser tube equal to 1.18 cm, the sample volume of each coil is only V = 7.6 cm^3 and herewith about 5 times smaller than for conventional low-field nuclear masers.

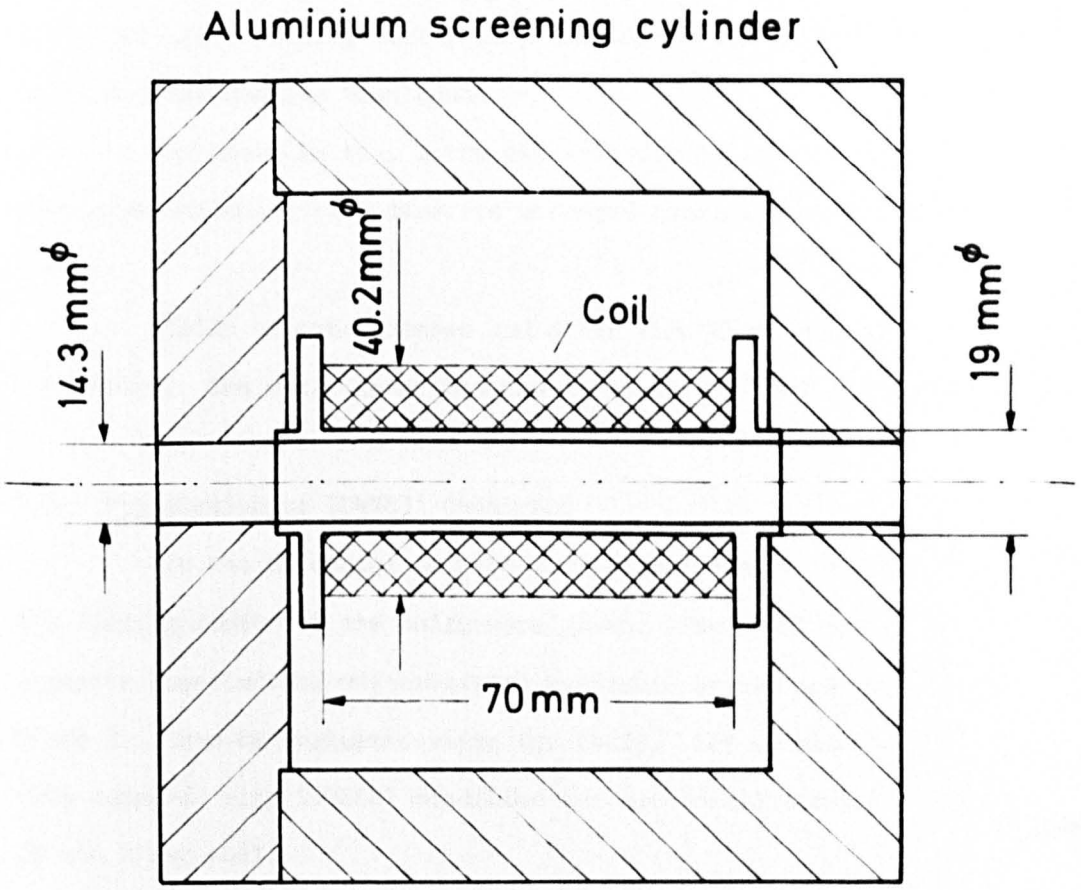

FIG. 9. Coil dimensions .

Each coil has a filling factor such that $2\pi\eta \approx 1$, and herewith η is about 4 times smaller than usual.

As shown in Fig. 5 the two emission coils with their aluminium screening cylinders are arranged coaxially on the maser tube.

Coils of other shapes and other wire diameters have also been tried. The coils described proved to be the most efficient ones.

5.3 Realization of TOWNES' Condition

In the preceding section the natural quality factor and the filling factor of the coils were given. The magnitude of the negative longitudinal magnetization available at the entrance of the first coil can be evaluated using Eq. (4.2). Let us now find out how this compares with TOWNES' condition for auto-oscillations to occur in the first coil.

TOWNES' condition for the first coil can be written as

$$Q > Q_{\ell o} = (2\pi\eta y \chi_o \omega_p T_2^*)^{-1}$$

where $y = M_o'/M_p$ is the prepolarization efficiency which can be evaluated from Eq. (4.2), and $\omega_p = \gamma H_p$ is the resonance angular frequency corresponding to the prepolarizing field.

The magnetogyric ratio of protons is $\gamma = 2.67513.10^4$ gauss/sec (BENDER and DRISCOLL 1958), while the static nuclear magnetic susceptibility of water is $\chi_o = (3.1 \pm 0.3)10^{-10}$ UEM cgs (BENOIT, FRANCOIS, POZZI, THELLIER and KASTLER 1967).

Since the emission coil is arranged in the homogeneous earth's magnetic field in a magnetically clean part of the observatory, it appears to be reasonable to assume $T_2^* = 0.5$ sec. A typical value of y is 0.5. With $H_p = 2400$ gauss, one finds $Q_{\ell o} = 270$, i.e. the threshold quality factor for auto-oscillations to occur is more than 10 times larger than the natural quality factor of the first maser coil. Hence auto-oscillations cannot be obtained from this system without an artificial enhancement of the quality factor of the first coil. (With a prepolarizing field about 10 times larger and with a larger coil and filling factor, auto-oscillations can be obtained in the earth's magnetic field without an artificial enhancement of the quality factor of the coil; HENNEQUIN 1961.)

In order to overcome the problem of too small a natural quality factor, BENOIT (1959) introduced a negative resistance parallel to the resonant circuit by means of a unit-gain vacuum tube amplifier and the use of positive feedback (HARRIS 1951). This is equivalent to a Q multiplication.

Let us briefly recall the principle of a Q multiplier. Suppose the tuned circuit has an equivalent parallel resistance r. The natural quality factor would be $Q = \frac{r}{\omega L}$. If an active network having a negative resistance characteristic is put in parallel to this tuned circuit, then the negative resistance can be combined with the positive resistance of the circuit by the usual laws of combination of parallel resistances. The effective parallel resistance is given by

the relation

$$r_{eff} = \frac{(-r_n)r}{(-r_n) + r} = \frac{r\, r_n}{r_n - r}$$

and is obviously greater than the original r by a factor $r_n/(r_n - r)$. The corresponding quality factor is

$$Q_{eff} = \frac{r\, r_n}{\omega L(r_n - r)} = Q\,\frac{r_n}{r_n - r}$$

Hence by letting r_n approach r in principle the Q multiplication can be made arbitrarily large.

The author applied the same method as BENOIT, however, instead of a vacuum tube amplifier a transistorized unit-gain amplifier utilizing a field effect transistor in the input stage was used (see Fig. 10). The circuit of the transistorized unit-gain amplifier was copied from a Texas Instruments source (MILLER, Ed., 1967), and positive feedback was introduced around this amplifier by means of two potentiometers connected in series. The 50 kohm potentiometer serves for coarse adjustment of the quality factor Q, the 5 kohm potentiometer serves for fine tuning.

The amplifier has a very high input impedance and is well stabilized. In practice the performance of this Q multiplier was very satisfactory. A stable Q up to about 10000 can be obtained. A comparison with BENOIT's vacuum tube Q multiplier which was re-built by the author showed that this latter circuit had a considerable zero

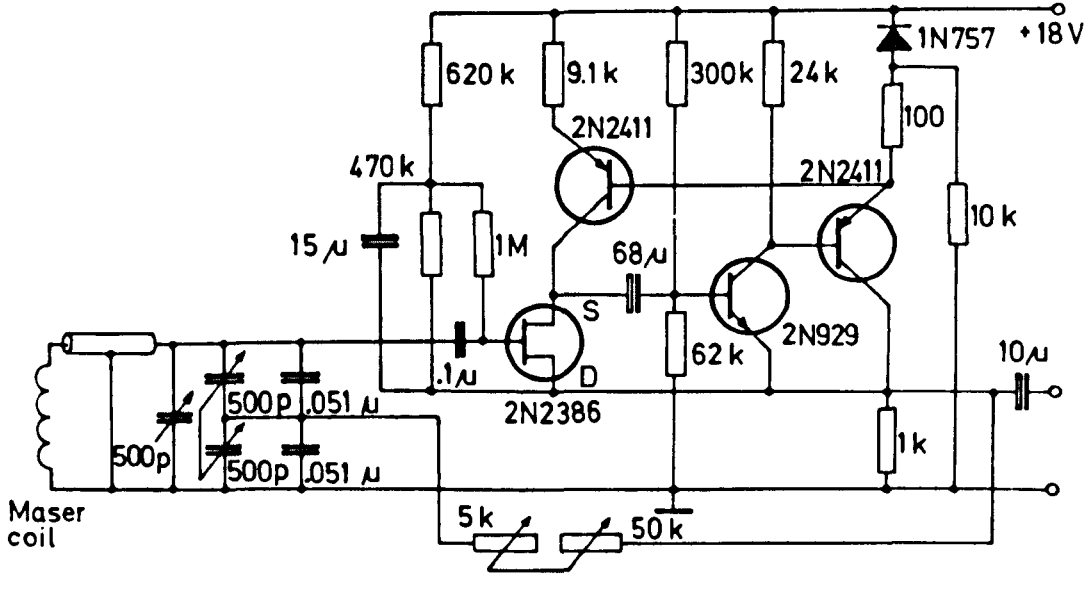

FIG. 10. Circuit diagram of the Q multipliers.

drift , possibly due to the unrest of the cathode, which was completely absent in the transistorized circuit. However, the transistorized circuit showed a little more electronic noise which was, however, not disturbing. Otherwise no difference in the performance of the circuit was found. The maser coil is tuned by two low-leakage polystyrene condensers of 0.051 μfarads each. Coarse tuning over a frequency range of 36 Hz is achieved by 500 pfarad tunable condenser connected parallel to the coil; fine tuning over a frequency range of 6 Hz can be achieved by a tunable 2 x 500 pfarad condensers.

An identical transistorized Q multiplier is used in order to enhance the quality factor of the second coil.

The transistorized Q multiplier has also been operated successfully at frequencies larger than 2 kHz. The highest frequency checked was 30 kHz.

We are not aware of a case where a nuclear maser has been previously operated with a transistorized Q multiplier. This can be explained by the fact that with normal transistors no high Q multiplication can be obtained and that the field-effect transistor came historically after the invention of the nuclear maser.

5.4 Decoupling of the Emission Coils

In order to avoid direct electromagnetic coupling, each maser coil is placed inside a screening cylinder made from aluminium. The walls of the cylinder are 25 mm thick, and since the skin depth of

aluminium at the operation frequency of 2 kHz is about 2 mm, the direct coupling through the space between the coils is negligibly small.

However, during the operation of the two-coil maser it was found that there existed a source of indirect coupling due to the ionic current in the distilled water flowing through both solenoids in succession. It was found that this disturbing coupling could be suppressed completely by connecting the distilled water flowing through the first emission coil towards earth. For this purpose an earthed insulated copper wire of 1 mm diameter and the length of the screening cylinder was arranged inside the water flowing through the first coil. It is essential that this wire does not stick out beyond the first screening cylinder by more than about 1 cm, the optimum position, otherwise the coupling towards the second coil increases again. A wire much thinner than 1 mm does not decouple sufficiently.

The decoupling wire is arranged along the inner wall of the maser tube where the velocity of the water is nearly zero. The connection of the wire with the earth is achieved by means of a thin wire leading through the rubber bung stuck in the entrance of the maser tube.

With the decoupling wire connected to earth, the decoupling is, even for the highest quality factor of the second circuit, more than 60 dB and hence much more than sufficient.

In Chapter VIII the influence of direct electromagnetic coupling between the two coils will be demonstrated by comparing corresponding experimental results.

5.5 Practical Design of the Two-Coil System

Fig. 11 shows photographs of the experimental set-up. The two screening cylinders are put on rollers and can be shifted along a U shaped aluminium bar which is screwed on a wooden stand by means of aluminium screws. The minimum inter-coil distance is 6 cm and the maximum coil distance is about 28 cm. The screening cylinder accommodating the first maser coil can be arrested on the aluminium guide rail. This trestle which supports the two screening cylinders is of robust design for it must withstand vibrations in the mode of operation where the distance between the coils is modulated.

In this design no magnetic materials have been used, and also no brass parts since brass contains usually ferromagnetic impurities. Any small iron part located near the maser coils would affect the field homogeneity across the system and hence the relaxation time T_2^*.

The modulation of the distance between the two coils is made possible by transferring the pendulum motion of a normal wind-screen wiper motor by means of an aluminium axis of 150 cm length and 6 mm diameter to a simple lever mechanism driving the second screening cylinder. Although this modulation method was sufficient for the two-coil maser to show the effect looked for, a wind-screen wiper motor is

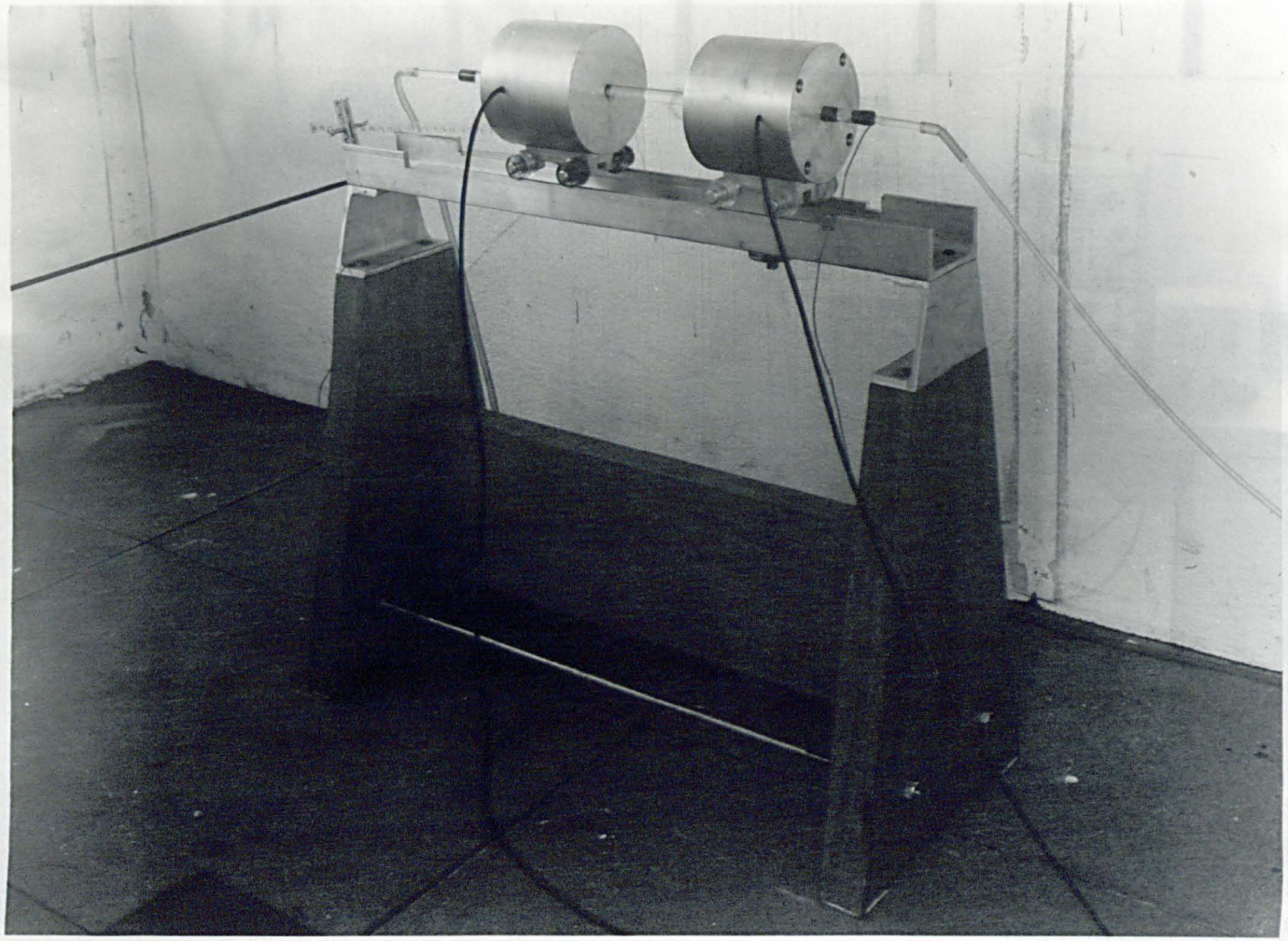

Fig. 11a. View of the two-coil system of the experimental proton maser. *Total height of the instrument: 81 cm.*

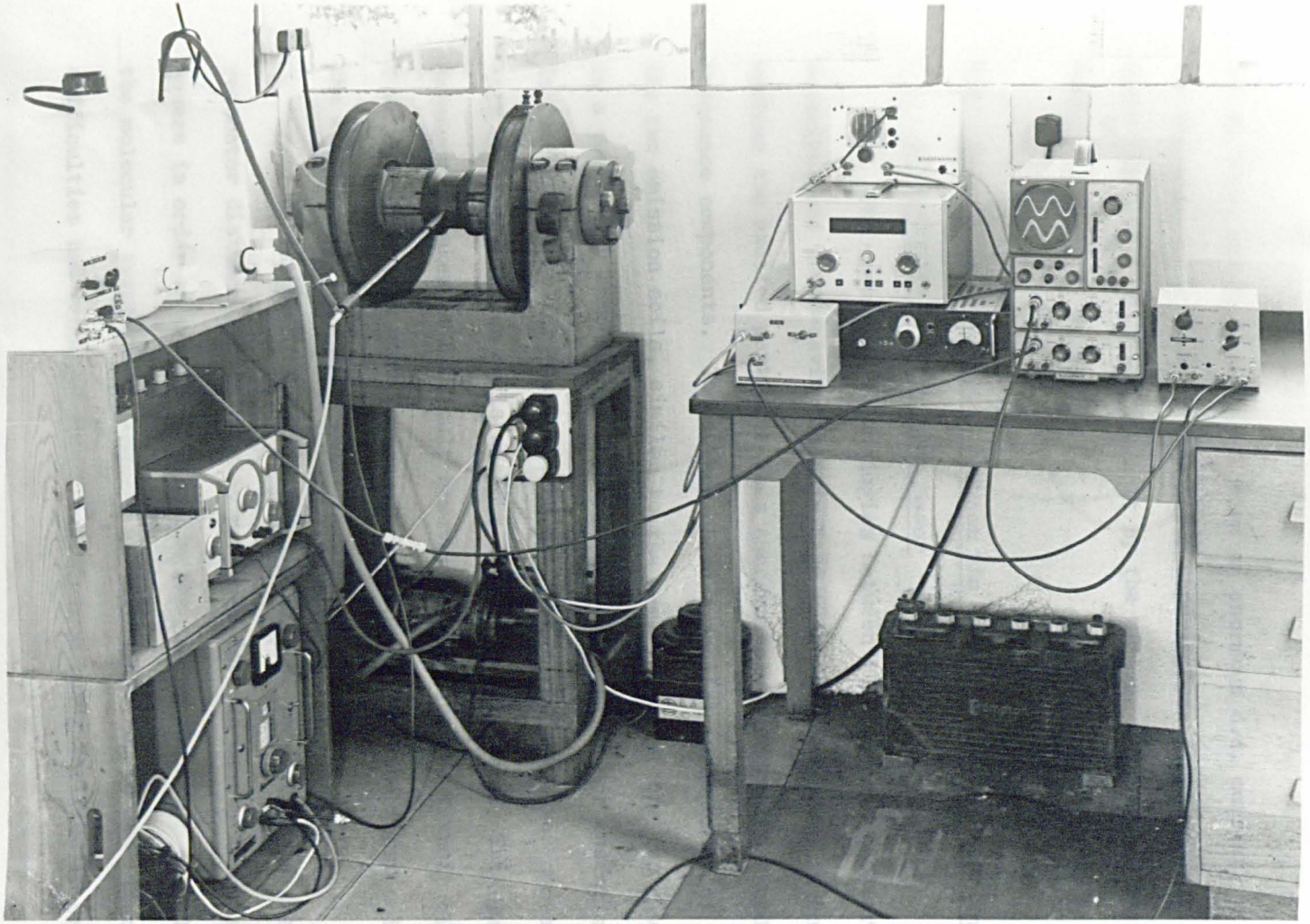

Fig. 11b. Part of the experimental set-up, with view of the prepolarizing magnet and the inversion coil in its fringe field.

not an ideal solution since it draws an enormous d.c. current. The magnetic stray field of the motor superimposes itself on the earth's magnetic field and is felt by the nuclear maser some distance away.

5.6 Systematic Differences between the Two-Coil Proton Maser and a Two-Cavity Ammonia Beam Maser

The constructive analogies between the two-coil nuclear maser described and a two-cavity ammonia beam maser are obvious: in both systems the excited particles pass successively through two tuned resonance components. The author chose a coaxial arrangement of the two emission coils, similar to the arrangement of the two cavities in a two-cavity ammonia beam maser. This is however not essential. In fact in an earlier stage of the experiment the maser was operated with crossed emission coils without screening cylinders. This latter arrangement makes it difficult however to modulate the transit time T which the protons need to travel from the exit of the first coil to the entrance of the second coil.

As was pointed out in Chapter II, the modulation of the inter-resonator distance was originally proposed for two-cavity ammonia beam masers in order to obtain a criterion for tuning the maser exactly to the molecular transition (VESELAGO et al. 1965). Up to now experimental difficulties had hindered this proposal from being verified in practice.

The great experimental advantage of a proton maser is of course that it does not require a vacuum housing. In a two-cavity maser the vacuum housing can act as an "external" multimode-resonator, an effect which is completely absent in the new two-coil proton maser.

Another advantage of the two-coil proton maser is that the quality factors of both resonant circuits can be varied within large limits. In a two-cavity maser the quality factors of the resonators are fixed.

Furthermore, in the proton maser the water flow rate can be measured directly by means of a flow-meter, and hence it is possible to determine precisely the average velocity of the protons passing through the coils in succession. In two-cavity masers it is difficult to determine the velocity of the molecular beam by means of a direct measurement. An accurate measurement is here also in principle difficult to obtain because the molecules slow down as they pass through the two-cavity system.

Furthermore, a molecular beam spreads out, and because of this molecules are lost between the two cavities, an effect which also is not present in the two-coil proton maser devised.

Apart from the different nature of the quantum transitions utilized and apart from the unimportant distinctions connected with the totally different frequencies of operation (2 kHz compared with 23.870 GHz), there remains still another small difference which cannot be avoided: the molecules establishing a molecular beam have a "thermal" velocity distribution, while a laminar flow has a parabolic

velocity profile. In the experimental system devised the flow is slightly turbulent which means that the parabolic velocity distribution is slightly flattened out near the axis of the maser tube.

5.7 The Observatory

The two-coil maser was operated in a small magnetic observatory which was erected on a magnetically clean place some distance away from the next laboratory building inside the University Campus. Before the erection, cable net plans were checked by the Architects' Department against the eventuality of current-carrying cables being buried in the place chosen. All critical steel bolts were removed from the hut and replaced by aluminium bolts. Assuming the absence of eddy currents flowing through the ground, and these precautions taken, the field inhomogeneity left should be due to the presence of the prepolarizing magnet. The stray field of this magnet decreases with the cube of the distance and was measured by means of the maser to be about 0.002 mG/cm at a distance of 160 cm away from the magnet.

5.8 Summary

A description of the experimental details of the two-coil system of the proton flow maser devised has been given. The two emission coils are arranged coaxially and the water passes through these coils in succession. This arrangement resembles that of a two-

cavity ammonia beam maser where the molecular beam passes through two resonators in series. The two-coil proton maser devised is original in that up to now nuclear masers have been operated exclusively with one emission coil only. The quality factors of the two resonant circuits can be changed continuously by means of Q multipliers. Here transistorized circuits have been used instead of the conventional vacuum tube circuit. The inter-coil distance can be modulated mechanically, so allowing a mode of operation which was previously proposed for two-cavity ammonia beam masers.

CHAPTER VI

SOME GENERAL EXPERIMENTAL RESULTS

6.1 Introduction

In Chapters IV and V the experimental set-up of the new proton maser with separated emission fields was described. Before we proceed with investigating this maser in more detail it shall first be clarified whether this system actually fulfils the most fundamental condition to be an analogue of a two-cavity maser; the frequency of the oscillation in the second coil must follow precisely the frequency of the auto-oscillations in the first coil (Chapter II).

In the subsequent chapters VII and VIII, the maser voltage across the first and second coils will be evaluated and the results will be compared with the experimental data. For the quantitative analysis the transverse relaxation time T_2^* must be known. Hence in this chapter the measurement of T_2^* shall also be reported.

First some general remarks on the behaviour of the two-coil maser will be made, and its reaction on a transient disturbance of the earth's field near the second coil will be discussed.

6.2 General Behaviour of the Two-Coil Proton Maser

When the nuclear maser was taken into operation it was found that oscillations occurred simultaneously in both emission coils if the quality factor of the first circuit, Q, was larger than about 500. The appearance of oscillations in the second coil was not dependent on the quality factor of the second resonant circuit, Q_B. Oscillation could be observed in the second coil when Q_B was as low as 20. The amplitude of the oscillation in both coils could be enhanced by increasing the quality factors of the coils.

Fig. 12 shows a typical oscilloscope trace of the sinusoidal voltage oscillations available from the two maser coils. They are typically of the order of magnitude of millivolts. If the quality factors of both emission coils are equal the amplitude of the voltage available from the terminals of the second coil is typically one order of magnitude smaller than the amplitude of the voltage across the first coil.

If the quality factor of the first coil, Q, is smaller than the threshold value Q_ℓ for auto-oscillations to occur, then the second emission coil behaves as if the first coil had been omitted, i.e. if Q_B is larger than a certain threshold value $Q_{\ell B}$ auto-oscillations occur in the second coil. The second coil behaves then like a normal one-coil nuclear maser.

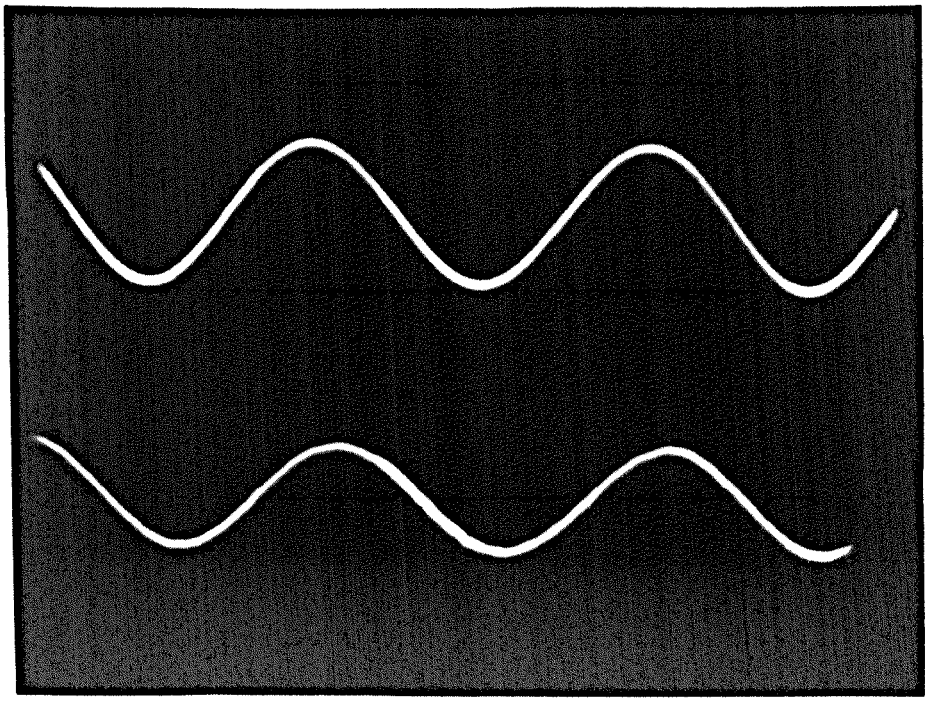

FIG.12. Typical oscilloscope traces of the voltage oscillations of the proton magnetometer maser with separated emission fields. Upper trace: first emission coil. Lower trace: second emission coil. Frequency: ≈ 2 kHz. Amplitudes: millivolts.

6.3 Reaction of the Maser on a Field Disturbance near the Second Coil

In order to prove experimentally that the oscillation in the second coil is produced by the residual nuclear magnetization of the water emerging from the first coil, and is not produced by direct pick-up, a small iron piece, a few millimeters thick and a few centimeters long, was brought near the exit of the second solenoid.

Fig. 13 shows the behaviour of the two amplitudes of the two-coil maser during this artificial disturbance of the field $\vec{H}_o$ near the second coil. As the field homogeneity is distorted, the voltage across the second coil, E_B, decreases. After the intervention E_B overshoots slightly and falls back to its normal level.

The quality factor of the second circuit, Q_B, was here adjusted below its value for auto-oscillations for at larger Q_B's the transient phenomena are very slow and were difficult to record with the oscilloscope utilized.

That nevertheless oscillations are observed in the second coil and that these oscillations are sensitive to field inhomogeneity, must necessarily mean that the radiation in the second coil is produced by the macroscopic transverse rotating moment of the coherently precessing protons emerging from the first coil. As the field $\vec{H}_o$ is made inhomogeneous the individual moments of the different protons dephase and the macroscopic transverse rotating moment shrinks, allowing only a poor nuclear magnetic induction in the second coil.

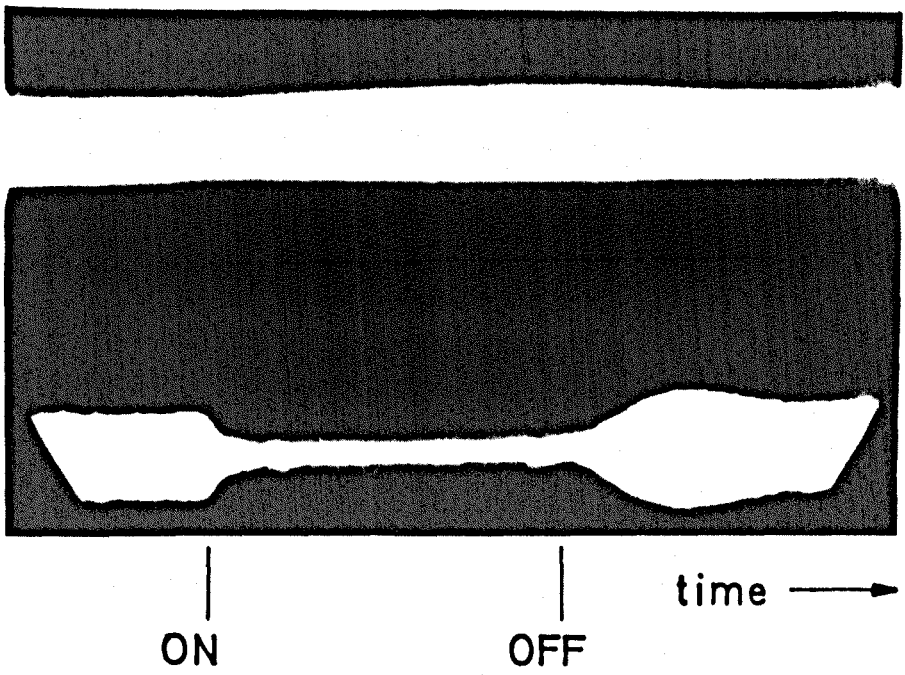

FIG. 13. Reaction of the two-coil proton maser on a transient disturbance of the homogeneity of the earth's magnetic field near to the second coil. Upper trace: voltage across the first coil. Lower trace: voltage across the second coil. Total display time: ≈ 5 sec.

In other words, the phenomenon of the free precession of the residual magnetization about $\vec{H}_o$ is responsible for the oscillations observed in the second coil.

Concerning the overshooting of E_B recorded in Fig. 13, transient processes in conventional one-coil nuclear masers have been discussed by COMBRISSON (1960) and SOLOMON (1961) and in molecular beam masers by GRASYUK and ORAEVSKII (1964). However, the phenomenon observed here is rather different because when the first coil oscillates the behaviour of the second coil cannot be compared with that of a normal maser.

6.4 Frequency of Oscillations

It is clear that the analogy between the system under discussion and a tandem-cavity molecular beam maser (Chapter II) could only be established if upon a frequency detuning of the first maser coil the frequency of oscillation in the second coil would follow precisely the frequency of oscillation in the first coil. That a nuclear maser with separated emission fields could behave in this way is at first sight not obvious since it would mean that the frequency of the e.m.f. induced in the second coil by the precessing magnetization would not equal the precession frequency of the nuclei, ω_L but equal the frequency of the oscillating magnetic field in the first coil.

However it was observed experimentally that as the first coil was detuned the frequency of the oscillating potential available

from the terminals of the second coil followed precisely the frequency of the auto-oscillation in the first coil, independently on the exact frequency tuning of the second coil.

In other words, the phenomenon observed here is in complete qualitative agreement with the analogous effect found by HIGA (1957) in a two-cavity ammonia beam maser (Chapter II).

This suggests that the phenomenon of the free coherent precession of protons in the flow emerging from the first emission coil is in fact analogous to the phenomenon of "molecular ringing" as observed in a molecular beam maser with tandem resonators.

The comparison of the two frequencies was first made by observing the phases of the oscillating potentials available from the terminals of the two coils on the screen of a double-beam oscilloscope. Since both channels of the oscilloscope derive their horizontal deflection from the same synchronization unit, only one sine wave can be kept stationary on the screen if the frequencies of the two signals fed into the two channels are slightly different. The mean phases of the two maser signals displayed on the screen did not change with respect to each other, also not over very long observation periods. The random phase changes of the second maser oscillation due to irregularities in the liquid flow rate, did never exceed a few degrees.

The equality of the two frequencies of oscillation was also not cancelled when the second coil was tuned away from the LARMOR precession frequency ω_o, or when the earth's magnetic field in the environment of the second coil was slightly disturbed artificially.

During the time of investigation the local earth's magnetic field changed such that the centre frequency of the proton resonance fluctuated slowly between 2035 Hz and 2060 Hz. The oscillation was usually to be found between 2040 Hz and 2045 Hz. This corresponds to an average magnetic field of the earth at Keele University of 0.48 gauss. The daily variations of the maser frequency due to changes of the earth's magnetic field were usually a few hertz and not found to be disturbing in the experimental investigation of the maser.

For frequency measurements an Advance Electronics digital counter, type TC5 was used. This instrument indicates 2 kHz on 5 digit places.

6.5 Explanation of the Frequency Behaviour of the Two-Coil Maser

The frequency behaviour of the two-coil maser may be understood as follows. At the exit of the first solenoid the transverse rotating moment changes its phase according to the law $\psi_1 = \omega_A t + \Delta\psi_A$, where ω_A is the frequency of the auto-oscillation in the first coil and $\Delta\psi_A$ is some constant phase angle between the oscillating potential across the first coil and the rotating magnetization at its exit. In the subsequent flow of the water the phase of the freely precessing magnetization changes in correspondence with the local LARMOR precession frequency $\omega_o(x) = \gamma H_o(x)$, where the coordinate x is measured from the end of the first maser coil. The transit time is $T = \ell/\bar{v}$ where ℓ is the distance between the end of the first coil and the entrance of the

second coil, and $\bar{v}$ is the mean velocity of the fluid. After the distance ℓ, the phase of the precessing magnetization is given by

$$\psi(t) = \omega_A t + \Delta\psi_1 + \gamma \int_0^T H_o(x(t))dt - \omega_A T$$

$$= \omega_A t + \Delta\psi_1 + \frac{\gamma}{\bar{v}} \int_0^T H_o(x)dx - \omega_A T$$

$$= \omega_A t + \Delta\psi_1 + (\overline{\omega_o(x)} - \omega_A)T \qquad (1)$$

where

$$\omega_o(x) = \frac{\gamma}{\ell} \int_0^\ell H_o(x)dx$$

is the average LARMOR precession frequency of the magnetization in the tube section between the two coils. The integral expression represents the phase accumulated over the distance ℓ. The integral expression minus the term $\omega_A T$ is the accumulated phase difference.

It may be noted that in Eq. (1) only the first term on the right hand side depends on the time t. The phase shift between the precessing magnetization at the entrance of the second coil and the oscillating voltage across it is a constant. Adding this constant phase shift to Eq. (1) does not alter its meaning, and therefore it must be concluded that the frequency of the oscillation in the second coil, ω_B, is given by

$$\omega_B = \omega_A = \omega$$

as the experiment showed. Hence it is not necessary to make a distinction between ω_A and ω_B; the frequency of oscillation of the two-coil nuclear maser shall in the following simply be denoted by ω.

From the above one may also conclude that, as far as the equality of the frequencies are concerned, a two-coil nuclear maser behaves in much the same way as a passive two-coil liquid flow device where the first coil is connected to an external oscillator and the freely precessing magnetization is detected downstream in a successive coil. Such systems have been realized previously in a large field (SHERMAN 1957) and in the earth's magnetic field as well (SKRIPOV 1958).

6.6 Measurement of the Relaxation Time T_2^*

In Chapters VII and VIII a quantitative analysis will be attempted, for which it is necessary to know the transverse relaxation time T_2^*.

The standard methods of measuring T_2^* are the "spin echo" method (HAHN 1950) which can also be applied in the earth's magnetic field (POWLES and CUTLER 1957, POWLES 1958) and the method of the "wiggles" (GABILLARD 1955). The latter are a decaying beat signal which can be observed by means of an NMR spectroscope after sweeping through the resonance condition. The wiggles are produced by the interference of the external driving field, with the radiation field

from the coherently precessing spins which preserve their phases for some time after the external field swept through the resonance condition. The method of the wiggles is easier to realize in practice.

However, in a flowing liquid the decay of the wiggles is no longer exponential and the results need a more complex re-interpretation. The same holds for the spin echo method (HERMS 1961, ARNOLD and BURCKART 1965).

A possible method of determining T_2^* experimentally for a liquid-flow nuclear maser is to investigate the pulling phenomenon expressed by Eq. (3.21) and to extrapolate T_2^* from the experimental data (FRIC 1961).

A nuclear maser with separated emission fields offers a further method. If the phenomenon of "radiation damping" is negligible in the second coil then the voltage E_B is directly proportional to the transverse rotating moment appearing at the second coil (Chapter VIII), and for a given flow rate, E_B falls with the transit time $T = \ell/\bar{v}$ according to the law

$$E_B = \text{const.}\exp(-T/T_2)$$

Hence T_2^* can be measured by altering the inter-coil distance. A semi-logarithmic plot of E_B against T should yield a straight line of slope $-1/T_2^*$, from which T_2^* can be found.

This method has been used in order to determine T_2^* for flow rates between 17 cm^3/sec and 33 cm^3/sec of the distilled water; the

result is shown in Figs. 14 and 15.

The fall of T_2^* with increasing flow rates can be explained by the non-infinite residence time of the protons in the second coil, τ, which leads to a frequency spread proportional to $1/\tau$, and hence to a more rapid dephasing of the individual moments of the different protons. If this is the only reason for the fall of T_2^* at higher flow rates, F, (see Fig. 15), then an extrapolation of this dependence towards $F = 0$ ($\tau = \infty$) should yield the relaxation time $T_2^{*\prime}$ which is valid in the tube section in the space between the two coils. From Fig. 15 one would obtain $T_2^{*\prime} \approx 1$ sec.

In order to check the dependence shown in Fig. 15 the method of the wiggles was applied. For this the spin inversion was switched off and the spins were irradiated externally by an auxiliary coil (Chapter IV) which was placed about 50 cm away from the first screening cylinder. Modulation of the earth's magnetic field was achieved by means of a small U shaped permanent magnet located about 2 m away from the first coil (the second coil is not used in this experiment). Fig. 16 shows the phenomenon of the wiggles for water flow rates of 17 cm^3/sec and 33 cm^3/sec. The relaxation time T_2^* is longer for the lower flow rate, in agreement with the experimental result obtained before.

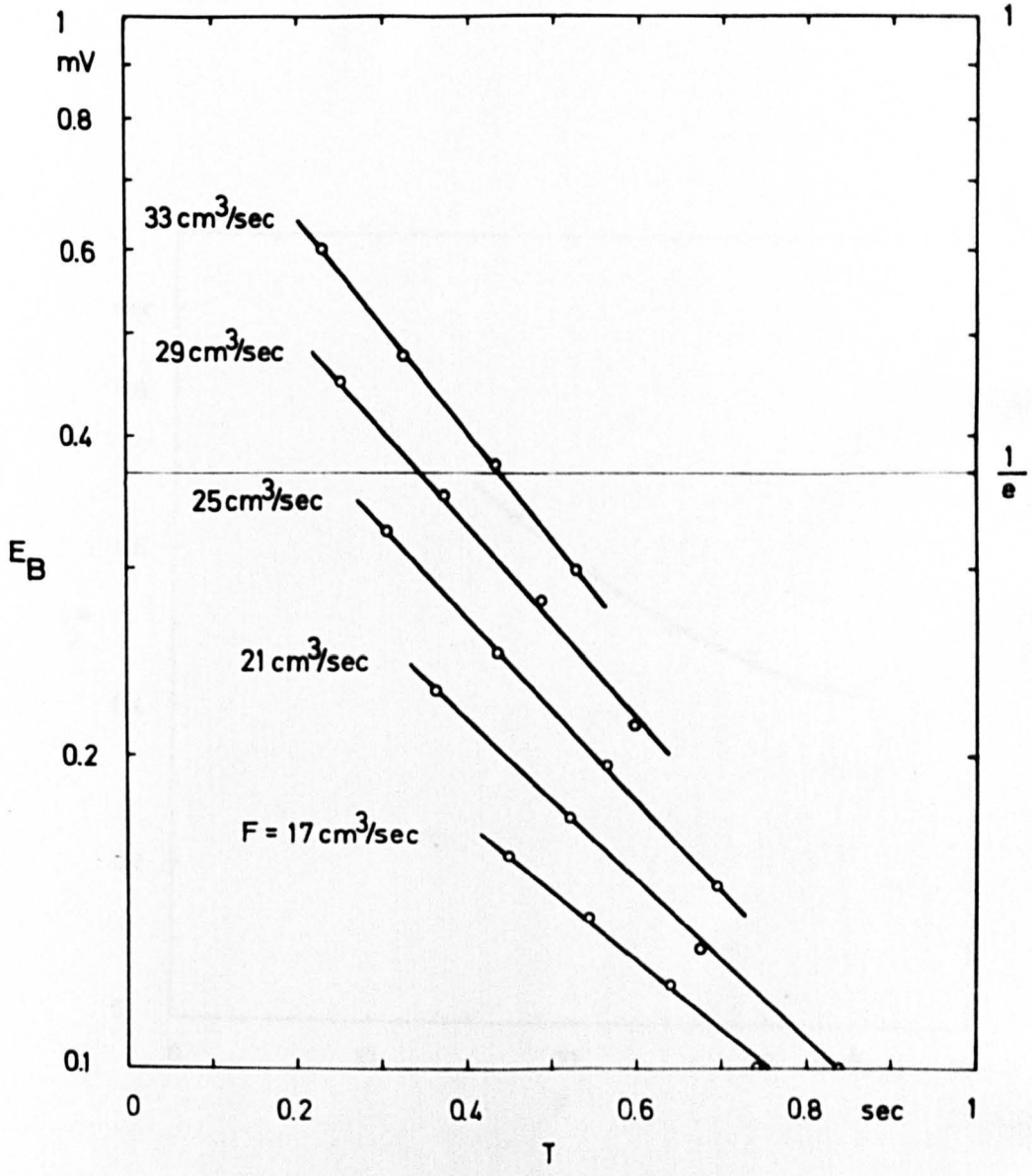

FIG. 14. Voltage across the second emission coil, E_B, as a function of the transit time T, for different flow rates F.

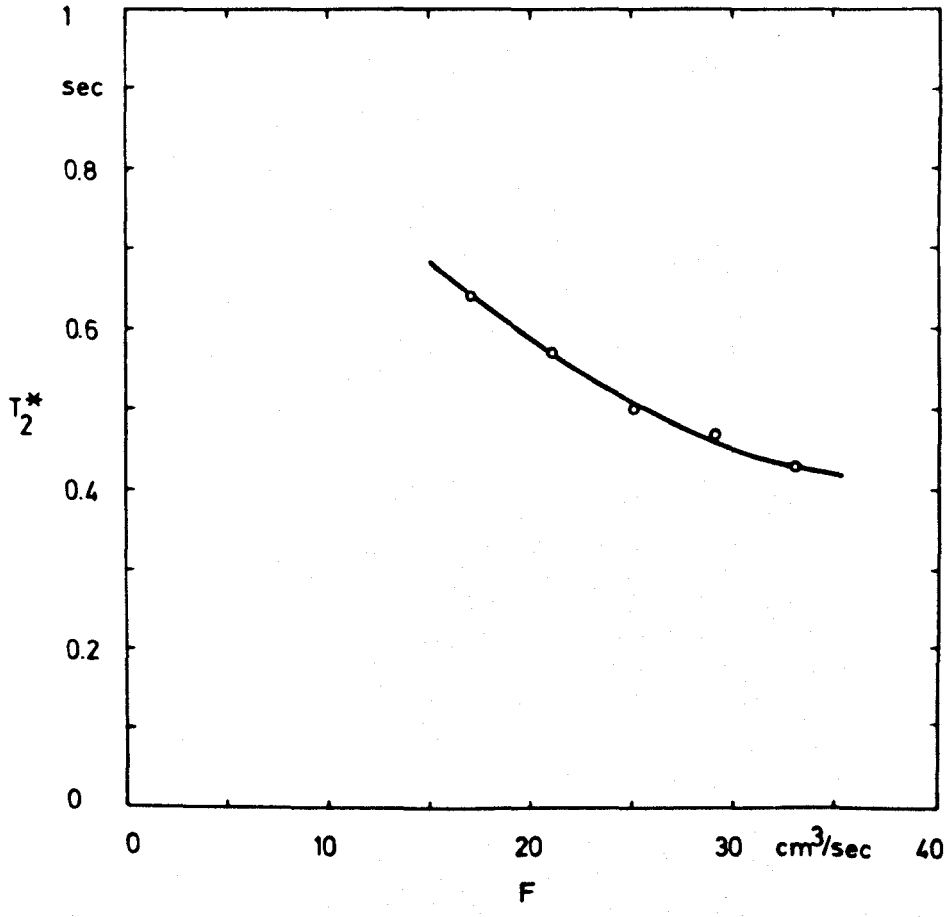

FIG.15 . Effective transverse relaxation time as a function of the water flow rate F.

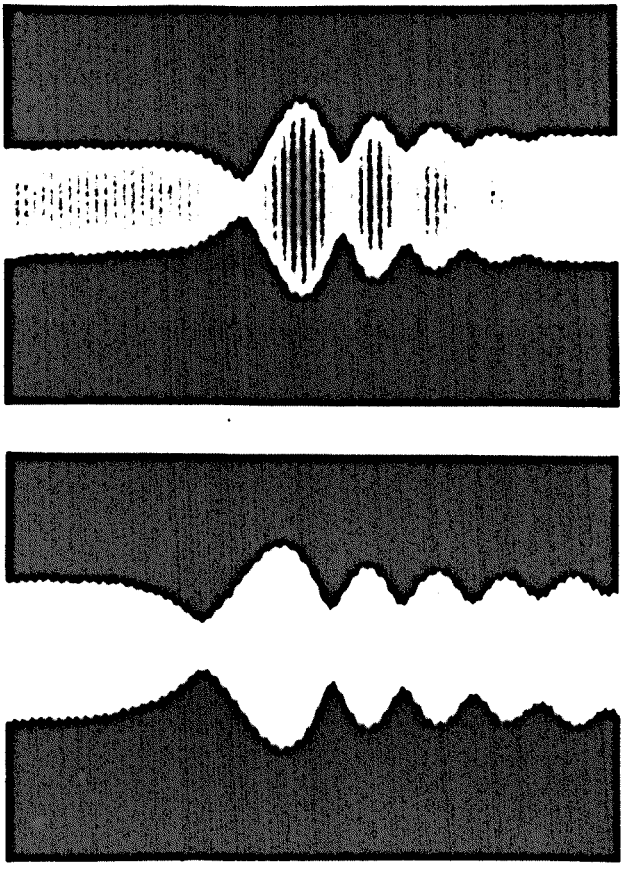

FIG. 16. The phenomenon of the "wiggles" as observed in the earth's magnetic field. Upper trace: water flow rate $F = 33\ cm^3/sec$. Lower trace: $F = 17\ cm^3/sec$. Total display time: ≈ 1.4 sec. 2 kHz not resolved (50 Hz modulation superimposed).

Table I : Residence Times and Transverse Relaxation Times

F (cm^3/sec)	$\tau = \tau_A = \tau_B$ (sec)	T_2^* (sec)	T_2^*/τ
17	0.45	0.64	1.4
21	0.36	0.57	1.6
25	0.30	0.50	1.7
29	0.26	0.47	1.8
33	0.23	0.43	1.9

As Table I shows, the ratio T_2^*/τ grows slightly with the flow rate, and hence higher flow rates are more favourable in the operation of a two-coil nuclear maser. However, if the water does not remain long enough in the pole gap of the prepolarizing magnet, then the prepolarization efficiency decreases again.

Whilst measuring T_2^* by altering the coil distance, an interesting effect was observed when the decoupling wire in the maser tube was bent, and created turbulences along the maser tube. When the second coil was shifted, there was a certain region, about 2 cm long, for which the voltage across the second coil remain unchanged. This region moved towards the first coil when the flow rate was decreased. The wire produced obviously a vortex in the water. This vortex averaged out the inhomogeneity of the magnetic earth's magnetic field such that at the point of the vortex the transverse relaxation was considerably longer than usual.

Unfortunately, in the reports on the two-cavity maser experiments (Chapter II) which concern us, relaxation times are not specified so that a quantitative comparison of a two-cavity maser and the new two-coil proton maser in this respect is difficult. However it is well known that the phase memory time of the ammonia molecules is considerably longer than the total transit time which the molecules spend in the two-cavity system.

6.7 Summary

The experimental investigation has shown that, as far as the frequency of oscillation is concerned, the two-coil proton maser behaves in much the same way as a two-cavity ammonia beam maser, i.e. the frequency of the oscillation in the second resonant circuit follows precisely the frequency of the auto-oscillation in the first resonant circuit. In the case of a two-coil nuclear maser this phenomenon can be understood by an elementary examination of the phase relations existing between the oscillation in the two coils.

The transverse relaxation time T_2^* has been measured by altering the inter-coil distance. This is an unorthodox method. It was found that T_2^* decreases as the flow rate increases. This result was checked experimentally using the method of the "wiggles".

CHAPTER VII

INVESTIGATION OF THE VOLTAGE ACROSS THE FIRST COIL

7.1 Introduction

As was pointed out in Chapter III the behaviour of a nuclear maser can be described by classical equations. The different parameters of the two-coil proton maser under investigation were given in Chapters IV and V. In the present chapter the voltage across the first emission coil will be examined. At the entrance of the first emission coil the macroscopic moment is aligned antiparallel to the direction of the earth's magnetic field. The radiation of magnetic energy in the first emission coil must necessarily result in a tilting of the moment towards its position of lowest energy parallel to the earth's magnetic field. It will be shown that this tilting and the voltage across the emission coil are dependent on each other and that this dependence is the more distinctive the larger the amplitude of the voltage available from the terminals of the coil. We are especially interested in the case of a large maser voltage across the first coil for in Chapter II it was stated that the double-hump detuning phenomenon of two-cavity ammonia beam masers can occur if the amplitude of the auto-oscillation in the first cavity is large. These should be analogous situations. The voltage across the first emission coil evaluated for different flow rates and quality factors will be compared with the corresponding experimental results.

7.2 Power of a Nuclear Maser

The power of an oscillating nuclear maser can be found from a conservation of energy argument as follows.

The energy of the spin system is $\vec{M}.\vec{H} = H_o M_z$. The power radiated per unit volume of the maser medium is therefore $H_o \frac{dM_z}{dt}$. Hence the effective power radiated by the volume V of the flowing liquid during the residence time τ is given by

$$\frac{VH_o}{\tau} \int_0^{\tau} dM_z = \frac{VH_o}{\tau} \left(M_z(\tau) - M_z(0) \right)$$

This power must be equal to the JOULE heat dissipated per unit time by the current in the tuned circuit, $\frac{1}{2}I^2R$, or

$$\frac{E^2}{2L\omega Q} = \frac{VH_o}{\tau} \left(M_z(\tau) - M_z(0) \right) \qquad (1)$$

Here E is the amplitude of the maser voltage across the first coil for zero detuning. Hence this conservation-of-energy argument allows the evaluation of the maser voltage, provided the equation of motion of the longitudinal magnetization M_z is known. The latter can be found by the aid of BLOCH's phenomenological equations.

For the moment we are interested in the case that the circuit be exactly tuned to the proton resonance such that $\omega = \omega_o = \omega_c$, for the detuning characteristic of the voltage across the first coil is already known to be a semi-ellipse (Chapter III).

7.3 Motion of M_z in the First Emission Coil

For the system under investigation the longitudinal relaxation time is $T_1 = 2.07$ sec, while the longest residence time of the nuclei in the first coil is $\tau = 0.45$ sec. Hence for the sake of simplicity one can regard T_1 as infinite without making too large an error.

If one studies now the motion of the macroscopic moment $\vec{M}$ in a frame XOZ rotating with the angular velocity $\omega = \omega_o$ about the direction of the field $\vec{H}_o$ applied parallel to the Z axes and chooses the phase of the rotating frame such that $M_x = 0$, then $\vec{M}$ can be studied in the YOZ plane, and the situation is that illustrated in Fig. 17a.

The motion of $\vec{M}$ can be described by two velocities, $\vec{v}_1 = \gamma H_1 \vec{M}$ being perpendicular to $\overline{OM}$, and $\vec{v}_2 = -M_y/T_2^*$ being parallel to $\overline{OY}$.

The corresponding BLOCH equations are

$$\frac{dM_z}{dt} = \gamma H_1 M_y \tag{2}$$

$$\frac{dM_y}{dt} = \gamma H_1 M_z - \frac{M_y}{T_2^*} \tag{3}$$

Eliminating M_y, the motion of M_z is given by the equation

$$\frac{d^2M_z}{dt^2} + \frac{1}{T_2^*}\frac{dM_z}{dt} + (\gamma H_1)^2 M_z = 0$$

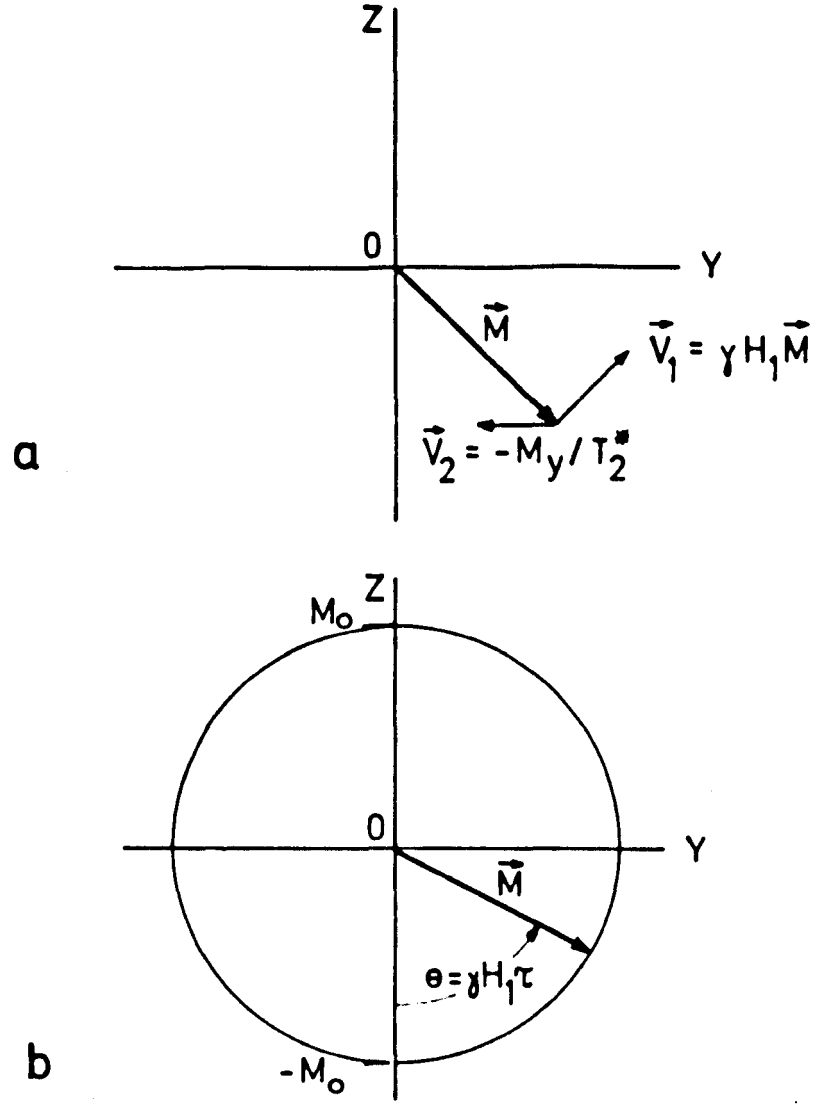

FIG. 17. a) Motion of $\vec{M}$ as seen in the rotating frame ($T_1 = \infty$). b) Motion of $\vec{M}$ in the case $2T_2^* \gg \tau$, $1/(2T_2^*) \ll \gamma H_1$.

which has three different types of solutions, depending on whether $\frac{1}{2T_2^*} > \gamma H_1$ (overdamped solution), $\frac{1}{2T_2^{*Q}} = \gamma H_1$ (critical damped solution) or $\frac{1}{2T_2^*} < \gamma H_1$ (underdamped or oscillatory solution).

We are interested in analogues of the phenomena which are observed in two-cavity masers when the level of oscillations in the first cavity is large (Chapter II).

If the voltage across the first emission coil is large the relation $\frac{1}{2T_2^*} < \gamma H_1$ will hold. With the initial conditions $M_z(0) = -M_o'$, $\dot{M}_z(0) = 0$ the corresponding solution is given by

$$M_z(t) = -M_o' \frac{\omega_1}{\omega_1^*} e^{-t/2T_2^*} \cos(\omega_1^* t - \alpha) \qquad (4)$$

where

$$\omega_1 = \gamma H_1$$

$$\omega_1^* = \omega_1 \left(1 - \frac{1}{4T_2^{*2}\omega_1^2}\right)^{\frac{1}{2}}$$

$$\tan \alpha = \frac{1}{2T_2^* \omega_1^*}$$

For the system under consideration τ is small compared with $2T_2^*$, and if only the case of strong excitation for which $\frac{1}{2T_2^*} \ll \gamma H_1$ is considered the above equation reduces to $M_z = -M_o' \cos \omega_1 t$. This corresponds to the case where the locus of the vector $\vec{M}$ in the YOZ plane is a circle (see Fig. 17b).

7.4 Voltage across the First Emission Coil

BENOIT and FRIC (1959) have used the relation $M_z = -M_o' \cos \omega_1 t$ in Eq. (1) in order to describe the voltage level available from a high-field nuclear maser oscillating in the megahertz range. If this approximation is made the voltage equation for the first emission coil can be written as

$$\frac{E^2}{2L\omega Q} = M_o' V H_o \frac{1 - \cos \gamma k E \tau}{\tau} \qquad (5)$$

where $k = H_1/E$ is a proportional constant depending on the geometry of the emission coil.

A nuclear maser with separated emission fields offers a simple method of determining the coil constant k, if the relaxation time T_2^* is long enough. The quality factor of the first coil, Q, can be adjusted such that $\theta = \gamma k E \tau = \pi$, (see Fig. 17b). Then the voltage across the second coil is zero (in fact this is the adjustment where the gap in the double-hump detuning phenomenon occurs, Chapter VIII). By measuring the voltage across the first coil and the residence time $\tau = V/F$ for zero voltage across the second coil, one can determine k. The experimental result was

$$k = \frac{H_1}{E} = 0.11 \text{ gauss/volt}$$

(For a long solenoid one can evaluate this constant from $k = \frac{1}{2\omega A}$ where A is the total mean geometrical turn area. For the coils used this approximation would give $k = 0.1$). What can be determined by this

method is the product $H_1\tau$ rather than the mean field amplitude $H_1 = kE$. The above value of k depends somewhat on the usual assumption that the effective length of the coil is identical with its geometrical length (see Fig. 18).

The voltage equation, Eq. (5), can be solved graphically, e.g. in the form

$$\frac{c_1}{(Qy\tau)^{\frac{1}{2}}} = \frac{\sin \theta/2}{\theta/2}$$

Here c_1 is an experimental constant given by

$$c_1 = \frac{1}{k\omega_o (L\omega_p \chi_o V 10^{-7})^{\frac{1}{2}}} = 12.0 \text{ sec}^{-\frac{1}{2}}$$

Remark: since χ_o is measured in UEM cgs, the unit of $M_p = \chi_o H_p$ is 1 erg/(gauss cm^3) corresponding to 10^{-7} joule/(gauss cm^3) in the practical system, where the unit of L is 1 henry.

The quantity $y = M_o'/M_p$ is the prepolarisation efficiency and can be evaluated by means of Eq. (4.2). The result of such a calculation is presented in Table II.

Table II : Prepolarization Efficiencies

F (cm^3/sec)	17	21	25	29	33
y (%)	29	36	42	47	51

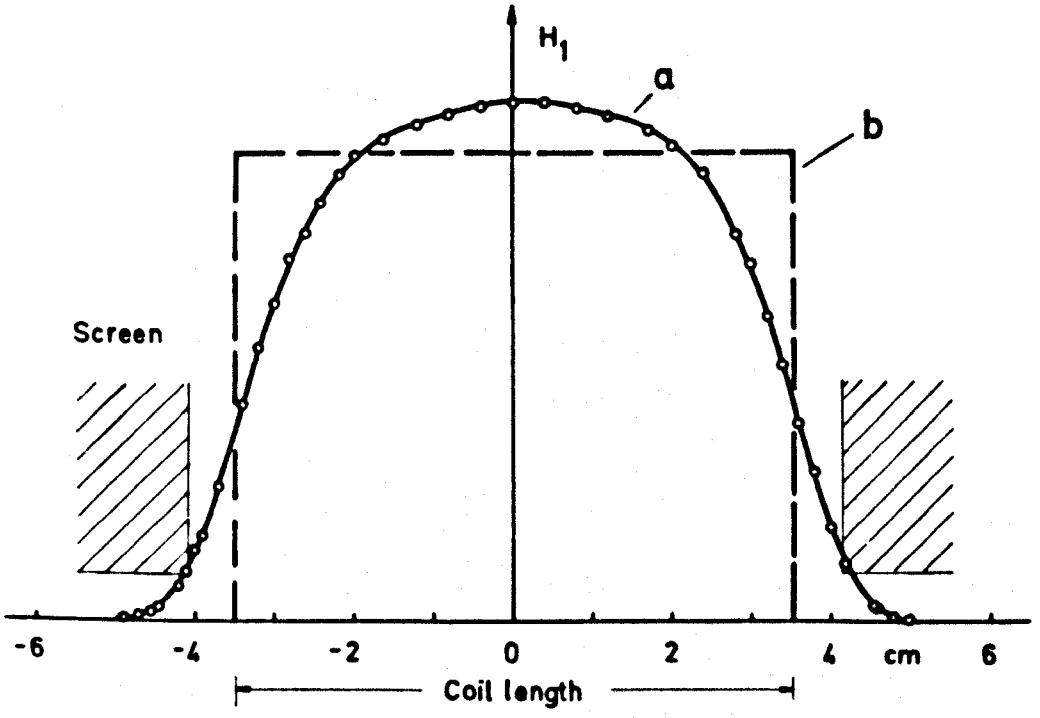

FIG.18. Field profile inside the emission coils, a) measured, b) assumed.

The calculated dependence of the voltage across the first coil, E, on the quality factor Q and the water flow rate F is shown in Fig. 19.

Fig. 20 shows the experimental result. The voltage amplitude was read on the oscilloscope screen, while the quality factor was measured through the relation

$$Q = \frac{\nu_o 3^{\frac{1}{2}}}{\Delta\nu_c}$$

where $\Delta\nu_c$ is the half-voltage bandwidth of the tuned circuit. The bandwidth $\Delta\nu_c$ was measured with the aid of an external oscillator and the digital counter.

7.5 Comparison of Theory and Experiment

In Fig. 19 the approximate voltage level is indicated for which, due to the non-infinite relaxation times T_2^* given in Table I, the condition $\frac{1}{2T_2^*} \approx \gamma H_1$ is fulfilled. Since Eq. (5) holds only for $\frac{1}{2T_2^*} \ll \gamma H_1$ the maser voltage predicted for the first coil can only be correct for voltages $E \gg E' = \frac{1}{2k\gamma T_2^*}$. A comparison of the theoretical curves shown in Fig. 19 with the experimental curves presented in Fig. 20 reveals that there is a fair agreement between theory and experiment for voltages above roughly 2mV. However, the voltages observed experimentally are about 25% lower. This is partly because the relaxation processes have been neglected entirely, and partly because at higher voltages the saturation effect enters the scene.

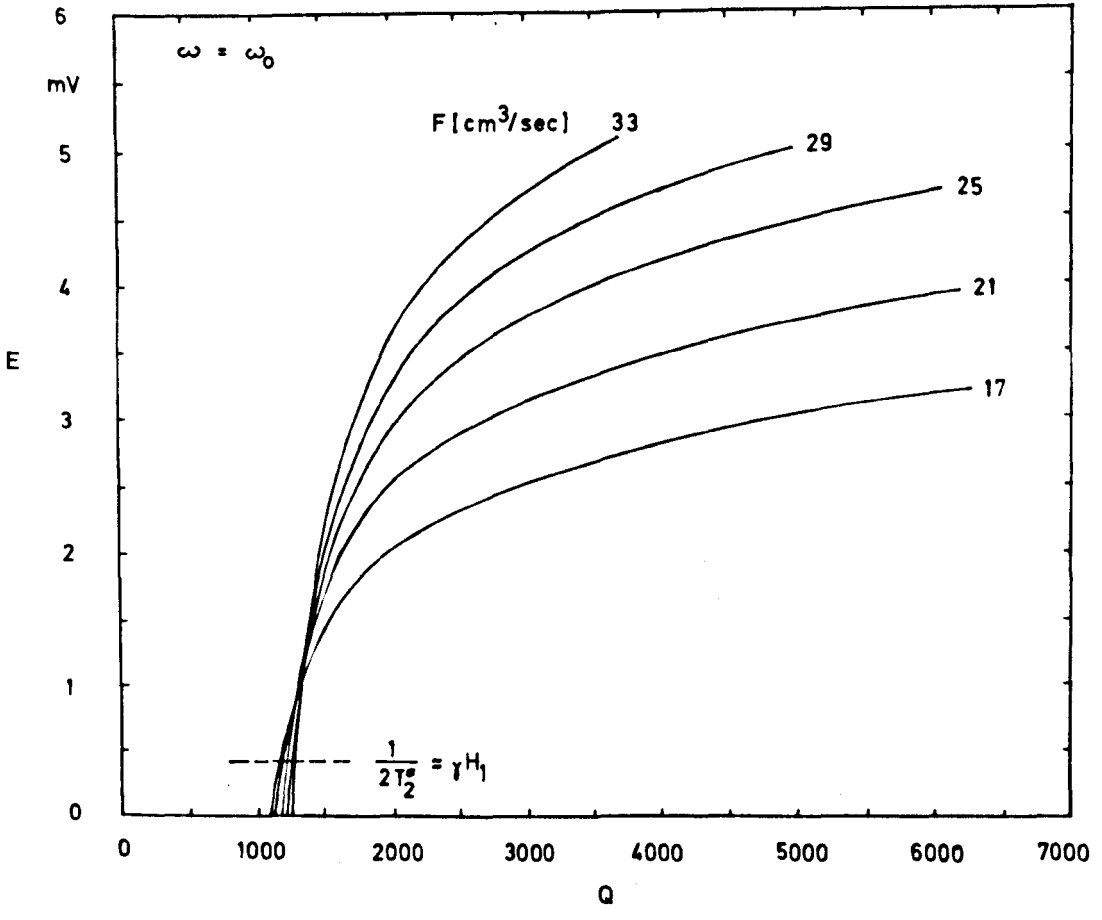

FIG. 19. Theoretical relation between the voltage across the first coil, E , its quality factor Q, and the water flow rate F , for $T_2^* = \infty$.

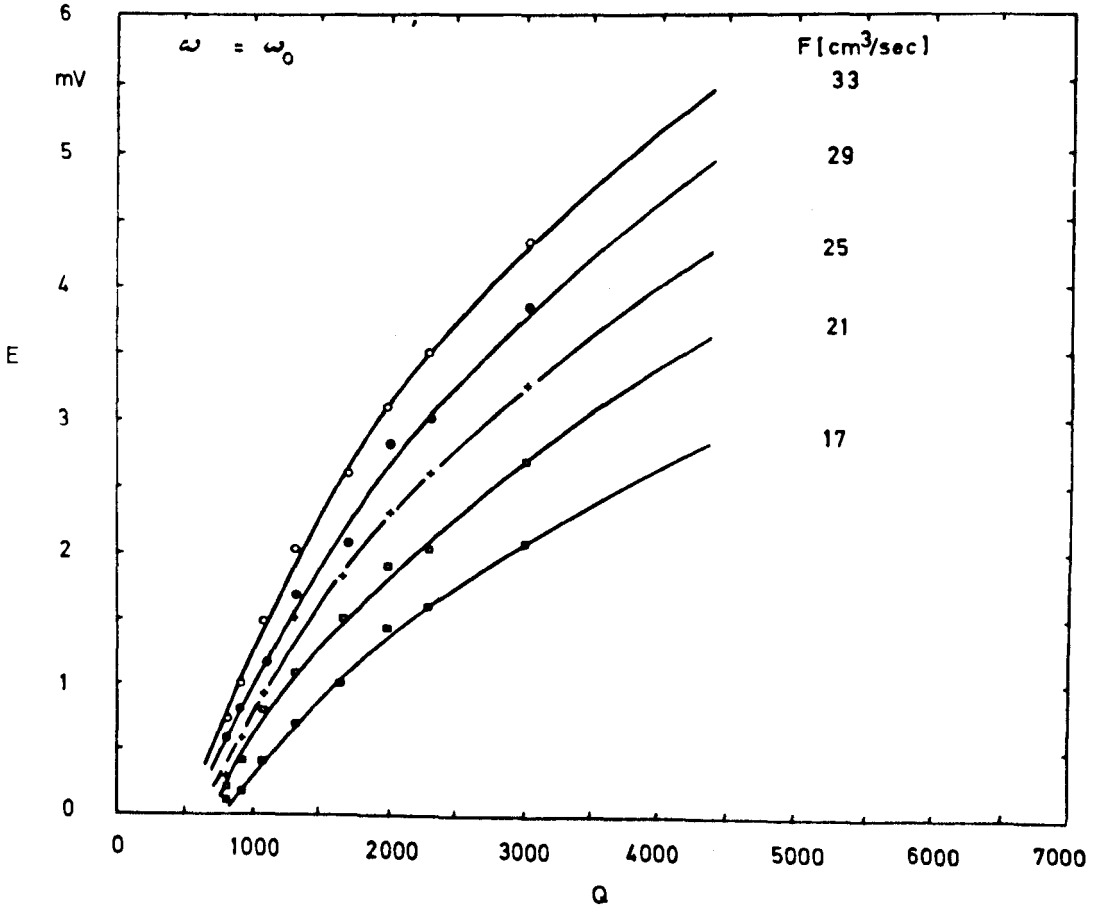

FIG.20 . Relation between the maser voltage across the first coil, E , its quality factor Q , and the water flow rate F (experimental).

The influence of the spin saturation will be seen more clearly in Chapter VIII.

A large discrepancy exists between the threshold quality factor predicted by Eq. (5) and the threshold quality factor observed experimentally. The reason for this is again that Eq. (5) is not valid near the threshold of oscillation. If the quality factor is so low that the condition $\frac{1}{2T_2^*} > \gamma H_1$ is fulfilled then the voltage across the maser coil can be described by another approximative formula (BENOIT 1959, ZHEROVOI and LATYSHEV 1965):

$$\frac{E^2}{2L\omega_o Q} = M_o' V H_o \frac{1 - \exp(-T_2^* \gamma^2 k^2 E^2 \tau)}{\tau} \qquad (6)$$

By evaluating the limit

$$\frac{\tau}{2L\omega_o Q_\ell M_o' V H_o} = \lim_{E^2 \to 0} \frac{1 - \exp(-T_2^* \gamma^2 k^2 E^2 \tau)}{E^2}$$

the threshold quality factor is found to be

$$Q_\ell = (2M_o' H_o V T_2^* L\omega_o \gamma^2 k^2)^{-1} \qquad (7)$$

On the other hand, evaluating the threshold value Q_ℓ' from Eq. (5) in the same manner,

$$\frac{\tau}{2L\omega_o Q_\ell' M_o' V H_o} = \lim_{E \to 0} \frac{1 - \cos \gamma k E \tau}{E^2}$$

one finds

$$Q_\ell' = (M_o' H_o V \tau L\omega_o \gamma^2 k^2)^{-1}$$

This latter value is larger than the more correct $Q_{\ell o}$ given by Eq. (7) by a factor of $2\tau/T_2^*$. This explains why the Q_ℓ's observed experimentally are only about half as large as those predicted (wrongly) by Eq. (5).

For nuclear masers oscillating in the magnetic field of the earth up to now only Eq. (6) has been of importance, the reason being as follows. Those masers are applied as magnetometers, and in this applicationthe actual frequency of oscillation should always be as near to the LARMOR precession frequency as possible. In fact up to now a suitable tuning criterion for nuclear masers does not exist (GRIVET and MALNAR 1967). If the quality factor of the circuit is too large then the frequency pulling phenomenon (Chapter III) becomes dangerously high, and in order to avoid this one adjusts a quality factor as low as possible. If one does the latter then the voltage across the maser coil is very low so that Eq. (6) holds.

In fact as far as literature indicates, for an earth-field nuclear maser up to now Eq. (5) which holds only for high levels of oscillation has not been compared with experimental results. The agreement of theory and experiment found for a high-field nuclear maser by FRIC and BENOIT is of the same order of magnitude as that obtained here.

7.6 Summary

The voltage across the first emission coil has been evaluated assuming that the motion of M_z be governed by the relation $M_z = -M_o \cos \gamma H_1 t$, i.e. the relaxation processes have been neglected entirely. This leads to a voltage equation which has been derived previously by other workers and been checked experimentally using a strong-field nuclear maser. In the present case, for larger quality factors the theoretical predictions for different flow rates are in a fair quantitative agreement with the corresponding experimental results. This proves that the formula utilized has also meaning for a nuclear maser oscillation in a weak magnetic field, if the level of oscillations is large enough. On the other hand, we are mainly interested in the case of a strongly excited first emission coil for this should be analogous to the situation where in a two-cavity maser the oscillation level in the first resonator is high.

CHAPTER VIII

INVESTIGATION OF THE VOLTAGE ACROSS THE SECOND COIL

8.1 Introduction

In Chapter VII the maser voltage available at the terminals of the first emission coil of the two-coil proton maser was investigated. The present chapter deals with the voltage induced in the second coil by the transverse rotating moment of the residual nuclear magnetization of the water emerging from the exit of the first emission coil.

The voltage across the second emission coil has been investigated for the case that both coils be precisely tuned to the LARMOR frequency ω_o. As was pointed out in Chapter VI, if the first coil is tuned to ω_o the frequency of the maser oscillation occurring in each coil is given by $\omega = \omega_o$. Measurements of the voltage available at the terminals of the second coil have also been carried out when the first coil was mistuned such that the frequency of oscillation of the whole system differed from ω_o.

The main purpose of this chapter is to give both theoretical and experimental evidence that the analogue of the double-hump detuning phenomenon which was previously observed during experiments performed with two-cavity ammonia beam masers (Chapter II) and which is still under dispute (Section 2.4) can be observed using a two-coil nuclear maser.

First some general aspects of the free LARMOR precession of the residual nuclear magnetization of the water emerging from the exit of the first maser coil shall be discussed.

8.2 The Residual Magnetization of the Water emerging from the Exit of the First Emission Coil

At the entrance of the first emission coil the macroscopic magnetization is aligned antiparallel to the earth's magnetic field $\vec{H}_o$. If TOWNES' condition (Eq. (3.16)) is fulfilled for the first emission coil, then the protons in the water flowing through this emission coil radiate in it part of their magnetic energy away. This can only happen if the resultant moment $\vec{M}$ tilts during the residence time τ towards its equilibrium position of lowest energy parallel to the direction of the field $\vec{H}_o$. At the exit of the first emission coil the moment $\vec{M}$ precesses in a cone about the direction of the field $\vec{H}_o$, the angle between the negative z axis and $\vec{M}$ being θ. The angle θ depends on the couple $\vec{M} \times \vec{H}_1$ which is exerted on the magnetization vector by the proper circularly polarized component $\vec{H}_1$ of the linearly polarized reaction field H_x produced by the circulating current in the coil. In the preceding chapter it was shown that if the relaxation effects are negligible, the final angle of the precession in the first coil is given by $\theta = \gamma H_1 \tau = \gamma k E \tau$.

During the transit time T which the water needs to travel from the exit of the first screened emission coil to the entrance of

the second screened emission coil, the magnetization vector does not cause and hence not experience a reaction field. Consequently, if the relaxation effects are negligible, during the transit time T the angle θ will remain constant. This is the phenomenon of the free LARMOR precession, as discussed in Chapter III.

Because of the spin-spin interaction and the spin-lattice relaxation the phenomenon of the free LARMOR precession of the macroscopic moment $\vec{M}$ about the direction of $\vec{H}_o$ cannot go on forever.

It follows from BLOCH's equations (comp. Section 4.4) that in the subsequent flow of the water emerging from the exit of the first coil the component M_z changes with the relaxation time T_1 according to the relation

$$M_z = M_{zex} e^{-t/T_1} + \chi_o H_o (1 - e^{-t/T_1})$$

Since the strength of the earth's magnetic field $\vec{H}_o$ in which the water flows after emerging from the first emission coil is low, the inequality $\chi_o H_o << M_z$ holds, and the above equation reduces to

$$M_z = M_{zex} e^{-t/T_1}$$

The components M_x and M_y fall with the transverse relaxation time $T_2^{*'}$ which differs from the transverse relaxation time T_2^* valid inside the solenoids:

$$M_x = M_{xex} e^{-t/T_2^{*'}}$$

$$M_y = M_{yex} e^{-t/T_2^{*'}}$$

The relaxation time $T_2^{*'}$ is primarily determined by the degree of the homogeneity of the earth's magnetic field, whilst the relaxation time T_2^{*}, which is valid inside the coils, is in addition shortened due to the non-infinite residence time τ for which the water remains inside the coils (Chapter VI).

A time T after the emergence of the water from the first emission coil, the magnetization M is decreased to a value given by the expression

$$M = (M_{zex}^2 e^{-2T/T_1} + (M_{xex}^2 + M_{yex}^2) e^{-2T/T_2^{*'}})^{\frac{1}{2}}$$

If the inter-coil distance is short and the water flow-rate is sufficiently large such that the inequalities $T << T_1/2$, $T << T_2^{*'}/2$ hold, then the magnetization available at the second coil will equal approximately the magnetization emerging from the first solenoid. Also, during the transit time T_1 the angle of the cone in which the vector $\vec{M}$ precesses about the direction of the field $\vec{H}_o$ will remain approximately the same.

The transverse component of the freely precessing magnetization of the water emerging from the first coil provokes the oscillation in the second coil. This is the mode of operation for which the two-coil proton maser is designed.

There is also another mode of operation possible. Suppose the imhomogeneity of the earth's magnetic field in the inter-coil space is very large. In this non-uniform external field the different magnetic

moments of the individual protons precessing in a field with slightly different strength get out of phase, and this leads to a rapid fall in the resultant transverse moment, i.e. to a low value of the relaxation time $T_2^{*\prime}$. If now the transit time T is large enough such that the transverse moment is completely cancelled before the water enters the second coil, then only the longitudinal component of the magnetization is left. If the level of the auto-oscillation in the first coil is very low then in the first coil the tilting of $\vec{M}$ towards its equilibrium position of lowest energy parallel to the direction of $\vec{H}_o$ will amount to only a few degrees, i.e. the component M_{zex} and hence the magnetization available at the entrance of the seconc coil will have a negative sign. The second resonant circuit will respond to this negative magnetization in much the same way as the first coil reacts to the magnetization $-M_o'$, i.e. if TOWNES' oondition is fulfilled for the second coil an auto-oscillation will build up in it. Since the transverse rotating component is suppressed there exists no phase dependence between the auto-oscillations in the first and the second coils. Since the coils oscillate individually, this possible mode of operation of the two-coil proton maser is in no way similar to the mode of operation of a two-cavity ammonia beam maser, and hence we shall not consider this case any further. It should be remarked, however, that in the two-coil maser devised this mode of operation can be verified by disturbing artificially the homogeneity of the earth's magnetic field in the inter-coil space.

8.3 Estimate of the Voltage across the Second Coil for Zero Detuning of Both Coils

In Chapter VII it was shown that the voltage available from the terminals of the first emission coil can be evaluated on the basis of a conservation of energy argument. The same must also be true for the second emission coil.

There is, however, a difference in the operation of the two emission coils. The maser action in the first coil is always connected with a tilting of the moment $\vec{M}$ away from its initial position of largest energy antiparallel to the main field $\vec{H}_o$, and the resulting change of the component M_z is linked to the power emitted by the spin system. The tilting of $\vec{M}$ in the first emission coil is an essential part of the maser action itself. In the second coil the situation is slightly different. Here an e.m.f. is induced by the freely precessing magnetization emerging from the exit of the first solenoid, independently from whether TOWNES' condition is fulfilled for the second coil or not. The appearance of this e.m.f. in the second circuit is not causally connected to a further tilting of $\vec{M}$ in the second coil. However, since the e.m.f. produces an electric current which dissipates JOULE heat, there will be a tilting of $\vec{M}$ towards its position of lowest energy parallel to $\vec{H}_o$ in the second solenoid also.

Let us first consider the case when the quality factor of the second circuit, Q_B, is very small. In this situation the current circulating in the second coil will be very weak, and so therefore the

reaction field produced by this current. Consequently the torque exerted on the spins will be very small, i.e. the tilting of $\vec{M}$ in the second solenoid will be negligible.

If the relaxation effects are neglected the e.m.f. induced in the second coil by the precessing magnetization is found from the FARADAY law to be

$$\varepsilon_B = 4\pi\eta\omega_o A M_o' \sin\theta$$

Hence the voltage $E_B = Q_B \varepsilon_B$ available at the terminals of the second coil is given by

$$\varepsilon_B = 4\pi\eta\omega_o A Q_B M'_o \sin\theta \qquad (1)$$

Here $M_o' \sin\theta$ is the transverse component of the precessing magnetization and the angle $\theta = \gamma k E \tau$ is determined by the degree of excitation of the first maser coil, see Fig. 17b. If the quality factor of the second circuit is very small then the angle θ will remain nearly constant throughout the whole length of the second solenoid, and Eq. (1) is valid.

On the other hand, if the quality factor of the second resonant circuit is large then in the second solenoid the angle between $\vec{M}$ and $\vec{H}_o$ will not remain constant, but increase continuously as the water passes through the coil. The voltage available at the terminals of the second emission coil can now be found from the power relation

$$\frac{E_B^2}{2L\omega_o Q_B} = VH_o \frac{M_{zB}(\tau) - M_{zB}(0)}{\tau} \qquad (2)$$

where $M_{zB}(0)$ and $M_{zB}(\tau)$ are the longitudinal components of the magnetization at the entrance and at the exit of the second coil, respectively. This equation is valid independently from whether relaxation effects play a role or not.

In order to find the connection between Eq. (1) and Eq. (2) let us neglect the relaxation effects in Eq. (2) also. The tilting angle of $\vec{M}$ in the first coil is given by $\theta = \gamma k E \tau$. The equation of motion of M_z in the second coil is of the same form as the equation of motion of M_z in the first coil, only the boundary conditions differ. Under the influence of the reaction field produced by the circulating current in the second identical coil, the macroscopic moment $\vec{M}$ will tilt further by an angle $\theta_B = \gamma k E_B \tau$. This is illustrated in Fig. 2 1 from which it might be seen that $M_{zB}(0) = -M_o' \cos\theta$, $M_{zB}(\tau) = -M_o' \cos(\theta + \theta_B)$. Hence the voltage across the second coil is for the ideal case of negligible nuclear relaxation given by

$$\frac{E_B^2}{2L\omega_o Q_B} = M_o' VH_o \frac{\cos\theta - \cos(\theta + \theta_B)}{\tau} \qquad (3)$$

If TOWNES' condition is not fulfilled for the first emission coil, then the second coil behaves as if the first coil would be switched off. In this particular case we have $\theta = 0$, and Eq. (3) takes the same form as Eq. (7.5).

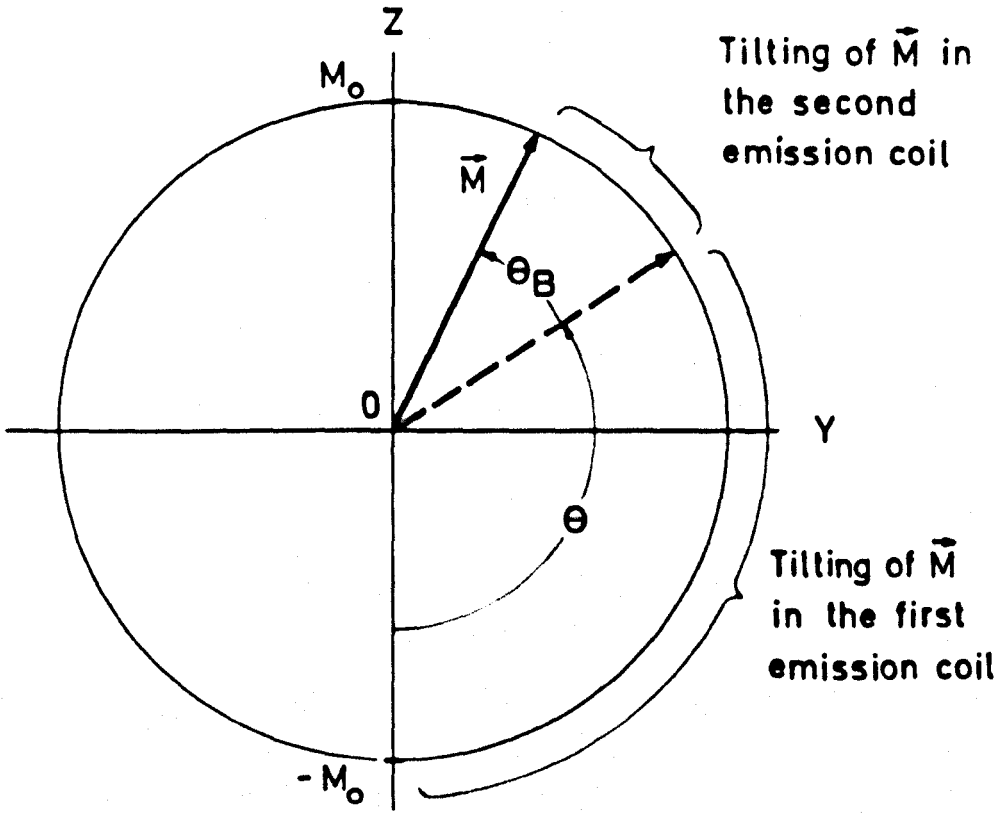

FIG. 21. Tilting of $\vec{M}$ in the two-coil maser as seen in the rotating frame, for $T_1 = \infty$, $T_2^* = \infty$.

The value of θ_B depends on the quality factor of the second coil, Q_B, for the voltage across the second coil depends on Q_B. By adjusting a low value for Q_B the tilting angle θ_B can be made arbitrarily small.

Let us investigate the voltage E_B for the case $\theta_B \to 0$. We first re-arrange Eq. (3) in the form

$$\frac{E_B}{2L\omega_o Q_B \gamma k} = M_o' V H_o \frac{\cos\theta - \cos(\theta + \theta_B)}{\theta_B}$$

and evaluate

$$\frac{E_B}{2L_o\omega_o Q_B \gamma k V H_o M_o'} = \lim_{\theta_B \longrightarrow 0} \frac{\cos\theta - \cos(\theta + \theta_B)}{\theta_B}$$

which gives

$$E_B = 2\omega_o L Q_B \gamma k V H_o M_o' \sin\theta \qquad (4)$$

In fact, this latter equation is identical with Eq. (1). This can be seen easily if the second emission coil has the shape of a long solenoid. In this case the magnetic field produced by the circulating current in the coil is uniform inside it, and the relations $\eta \approx V/V_c$, $k = \frac{1}{2}\omega_o A$ $L = 4\pi A^2/V_c$ hold. Introducing these relations into Eq. (4) gives Eq. (1).

In summarizing, if in the second solenoid the tilting of the moment $\vec{M}$ is sufficiently weak, the voltage across the second coil, E_B, is related to the voltage across the first coil, E, through a simple

sine law, and in this particular case it will not be necessary to evaluate E_B starting from a conservation-of-energy argument.

Eq. (4) is idealized in that the relaxation effects have been neglected. In the experimental two-coil proton maser the minimum inter-coil distance is limited by the thick screening cylinders and is about 6 cm. Hence the entrance of the second solenoid is rather far away from the entrance of the first solenoid where the magnetization $-M_o'$ arrives; the corresponding transit time of the water is typically 0.5 sec for a medium flow rate used in the experiment. Since the transverse relaxation time is also of this order of magnitude, the transverse relaxation will have a considerable diminishing effect on the voltage across the second coil, E_B, and cannot be neglected, i.e. in Eq. (4) the term $M_o \sin\theta$ which represents the transverse component of the precessing magnetization must be replaced by a term which takes the transverse relaxation into account.

In Chapter VII the motion of the macroscopic moment $\vec{M}$ damped by the influence of T_2^* was studied in the rotating frame. The phase of the rotation of the frame was chosen such that $\vec{M}$ was confined to the YOZ plane. Using this technique, an equation of motion of M_z given by Eq. (7.4) was derived.

In this rotating frame the transverse component of $\vec{M}$ is given by M_y. The equation of motion of the transverse magnetization M_y damped by the influence of the transverse relaxation is connected to the motion of M_z expressed by Eq. (7.4) through Eq. (7.2):

$$\frac{dM_z}{dt} = \omega_1 M_y$$

Evaluating M_y gives

$$M_y = M_o' \frac{\omega_1}{\omega_1^*} e^{-t/2T_2^*} \sin \omega_1^* t$$

where ω_1 and ω_1^* are the same as in Eq. (7.4). This expression for the transverse component of the magnetization is valid for spin systems inside the first emission coil, if the relaxation time T_1 has a negligible effect.

If the damping of M_y due to $T_2^{*\prime}$ in the section of the maser tube between the two emission coils is taken into account by a factor $e^{-T/T_2^{*\prime}}$ the transverse component of $\vec{M}$ available at the entrance of the second coil will be given by

$$M_y = M_o \frac{\omega_1}{\omega_1^*} e^{-(\tau/2T_2^* + T/T_2^{*\prime})} \sin \omega_1^* \tau$$

If in Eq. (4) the term $M_o' \sin \theta$ is replaced by this expression for M_y the voltage across the second coil for negligible radiation damping ($\theta_B \approx 0$) and zero detuning of both coils is approximately given by

$$E_B = c_2 y Q_B \frac{\omega_1}{\omega_1^*} e^{-(\tau/T_2^* + T/T_2^{*\prime})} \sin \omega_1^* \tau \qquad (5)$$

where

$$\omega_1 = \gamma H_1 = \gamma k E$$

$$\omega_1^* = \omega_1 \left(1 - \frac{1}{4T_2^{*2}\omega_1^2}\right)^{\frac{1}{2}}$$

and c_2 is an experimental constant given by

$$c_2 = 2\omega_o{}^2 LkV\chi_o H_\rho .10^{-7} = 4.7 \times 10^{-6} \text{volts}$$

Using Eq. (5) the dependence of E_B on the voltage across the first coil, E, for zero detuning of both coils has been evaluated for an inter-coil distance ℓ = 7.2 cm, a quality factor of the second circuit Q_B = 380 and water flow rates of F = 17 cm^3/sec and F = 33 cm^3/sec, the result being shown in Fig. 22.

The functions $E_B(E)$ are essentially sinusoidal. E_B is zero if the voltage across the first coil, E, is such that $\omega_1{}^* \tau = n\pi$, n = 1, 2, ...

If the first emission coil is adjusted such that $\omega_1{}^* \tau = \pi$ then at its exit the moment $\vec{M}$ is aligned parallel to the direction of the main field $\vec{H}_o$, and the transverse magnetic moment in the water emerging from the first coil is zero, i.e. the second coil cannot be excited. The question is whether an adjustment $\omega_1{}^* \tau \geq \pi$ for the first emission coil is actually possible in principle. If the moment $\vec{M}$ tilts in the first emission coil by an angle larger than π then this means that at some point in the first solenoid the moment $\vec{M}$ is aligned parallel to the earth's magnetic field $\vec{H}_o$, and in the subsequent flow through the remaining section of this solenoid the spin system would absorb energy. That the flow could absorb part of its own radiation appears to be paradoxical at first glance, and, as far as the author is aware, that this could eventually happen has not been discussed previously in the literature on nuclear masers.

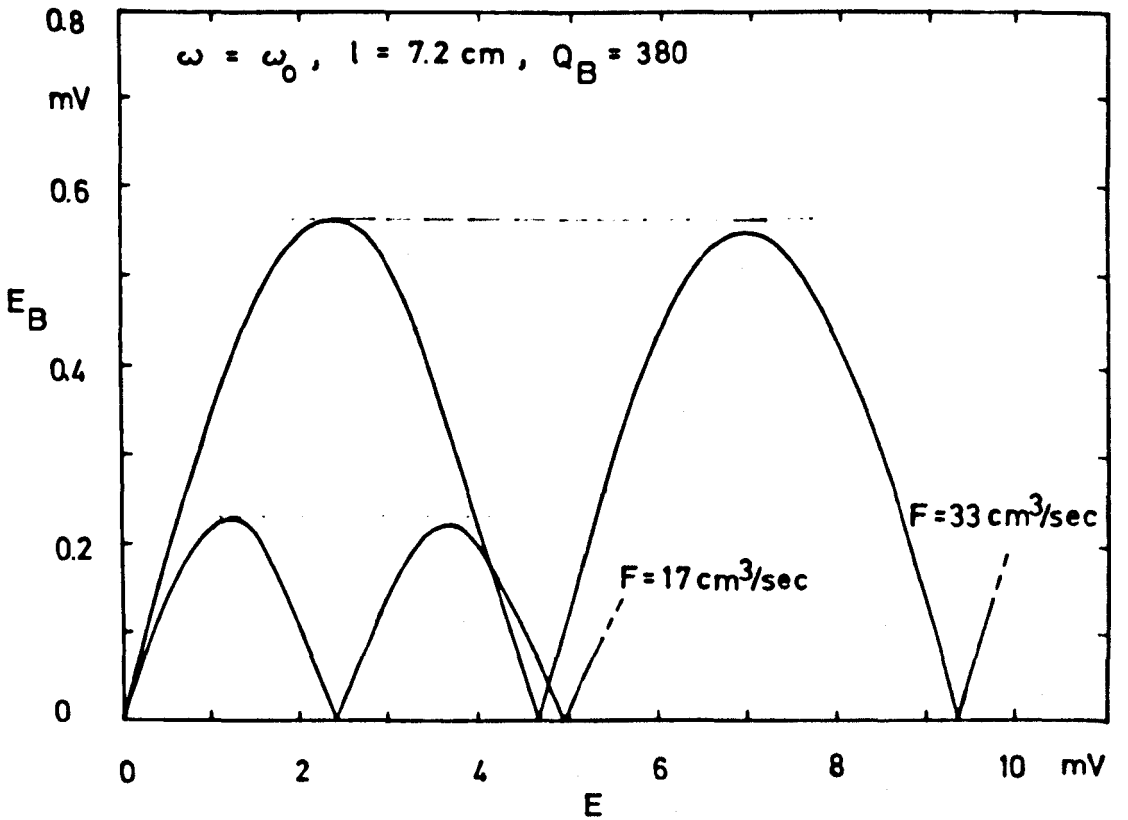

FIG. 22. Theoretical relation between the voltage across the second coil, E_B , the voltage across the first coil, E , and two different values of the water flow rate F ($T_1 = \infty$).

The answer to this question is hidden in the power relation for the first emission coil, Eq. (7.5). Suppose the quality factor of the first emission coil, Q, is infinite. In this case no JOULE heat would be dissipated by the current in the tuned resonant circuit, i.e. the left-hand side of Eq. (7.5) would be zero. In order for the right-hand side of this equation to become zero too, the angle $\theta = \gamma k E \tau$ must equal 2π. In other words, if no JOULE heat is dissipated in the first emission coil, the moment $\vec{M}$ which is initially aligned antiparallel to $\vec{H}_o$ approaches in the middle of the first coil the angle $\theta = \pi$ and at its exit the angle $\theta = 2\pi$ with $\vec{H}_o$. The spin system confined to the second half of the first solenoid would absorb all energy radiated away by the spin system confined to the first half of the solenoid. In practice we will not be able to produce this idealized situation; however, from the experimental results to be reported in the following section, it can be concluded that in the two-coil maser devised the moment $\vec{M}$ can tilt by an angle considerably larger than π.

Since it follows theoretically that for $\theta = \pi$ the oscillation in the second coil ceases, it would be a close assumption that this is the adjustment analogous to that where the radiation intensity in the second resonator of a two-cavity beam maser becomes zero (Fig. 2).

8.4 Experimental Investigation of the Voltage across the Second Coil for Zero Detuning of Both Coils

We recall that the double-hump detuning phenomenon of two-cavity ammonia beam masers (Chapter II, Fig. 2) is marked by the fact that for zero detuning of the first cavity the level of oscillations in the second cavity can become zero if the focusser voltage is increased to a certain value. Several more or less contradicting theories have been produced in order to explain this effect (Section 2.4).

On the other hand, from the theoretical estimate of the voltage across the second coil of the two-coil nuclear maser, it follows quite naturally that this voltage can become zero if the first coil is sufficiently excited.

In the second cavity of the two-cavity ammonia beam maser the level of oscillations becomes zero at a high focusser voltage, i.e. when a large electric polarization is present at the entrance of the first cavity and when, consequently, the level of oscillations in the first cavity has a certain value. Hence in order to find in the two-coil proton maser the analogous phenomenon by means of corresponding experimental manipulations, strictly speaking, one would have to enhance the magnetization $-M_o'$ available at the entrance of the first coil. With the flow system as described, the latter can however not be done arbitrarily, but it is easy to enhance the quality factor of the first circuit, Q, instead. In fact Eq. (7.5) shows that the functional dependence of the voltage across the first coil, E, on its quality

factor Q is the same as that of E on M_o'. The variability of the quality factors of the circuits of the two-coil maser is a great advantage; in the two-cavity beam maser the quality factors of the resonators are fixed.

The experimental relation between the voltage across the second coil, E_B, and the voltage across the first coil, E, for zero detuning of both coils has been measured for water flow rates between 17 cm^3/sec and 33 cm^3/sec. Fig. 23 shows the experimental results obtained for an inter-coil distance ℓ = 7.2 cm and a quality factor of the second circuit Q_B = 380. These are the same parameters on which the theoretical curves shown in Fig. 22 are based. In measuring the curves in Fig. 23 the voltage across the first maser coil was altered by varying the quality factor Q of the circuit. The readings of the respective voltages were taken by means of the double-channel oscilloscope.

The results of the measurements show clearly that for a certain value of the voltage across the first emission coil, the voltage across the second coil becomes zero, in agreement with the theoretical prediction, see Fig. 22. The maxima of the experimental curves correspond to situations where the residual magnetization $\vec{M}$ of the water emerging from the exit of the first maser coil is aligned perpendicularly to the direction of the field H_o.

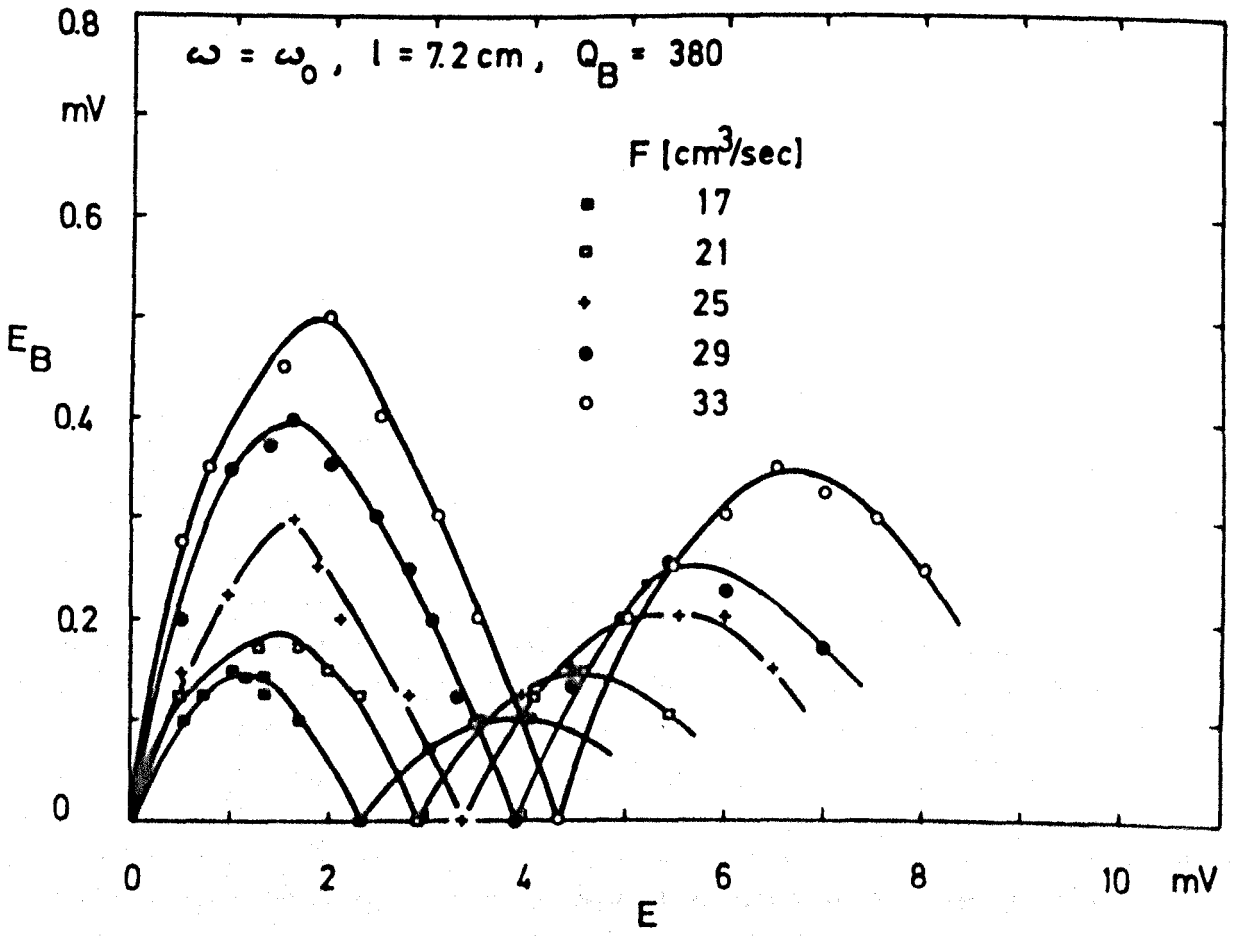

FIG. 23. Experimenal relation between the voltage across the second coil, E_B , the voltage across the first coil, E , and the water flow rate F.

A comparison with the theoretical curves shown in Fig. 22 indicates that the second maximum of each of the experimental curves is considerably lower than predicted. The reason for this is that if the voltage across the first coil is increased, the reaction field H_1 inside it grows in proportion, and if H_1 is large the power saturation of the spin system enters the scene (Chapter III). This effect which is dependent of the spin-lattice relaxation is not taken into account by Eq. (5).

Fig. 24 shows the results of a series of measurements which has been performed for a quality factor Q_B nearly twice as large as before and for flow rates between 19 cm^3/sec and 31 cm^3/sec. The maxima of E_B are now higher because of the larger quality factor of the second circuit, and the minima are shifted because other flow rates have been used.

In Chapter V it was mentioned that direct coupling between the two emission coils of the proton maser was prevented by means of a decoupling wire arranged inside the maser tube in the first solenoid. The curves shown in Fig. 25 were measured when the decoupling wire was removed and direct coupling due to the ionic current in the water passing through the maser tube was present. At smaller voltages across the first coil, E, the voltage across the second coil, E_B , still reveals the typical dependence known from Fig. 23 and Fig. 24; however, at higher E's this dependence is completely falsified due to the superimposition of direct pick-up. This clearly shows the need for the decoupling wire.

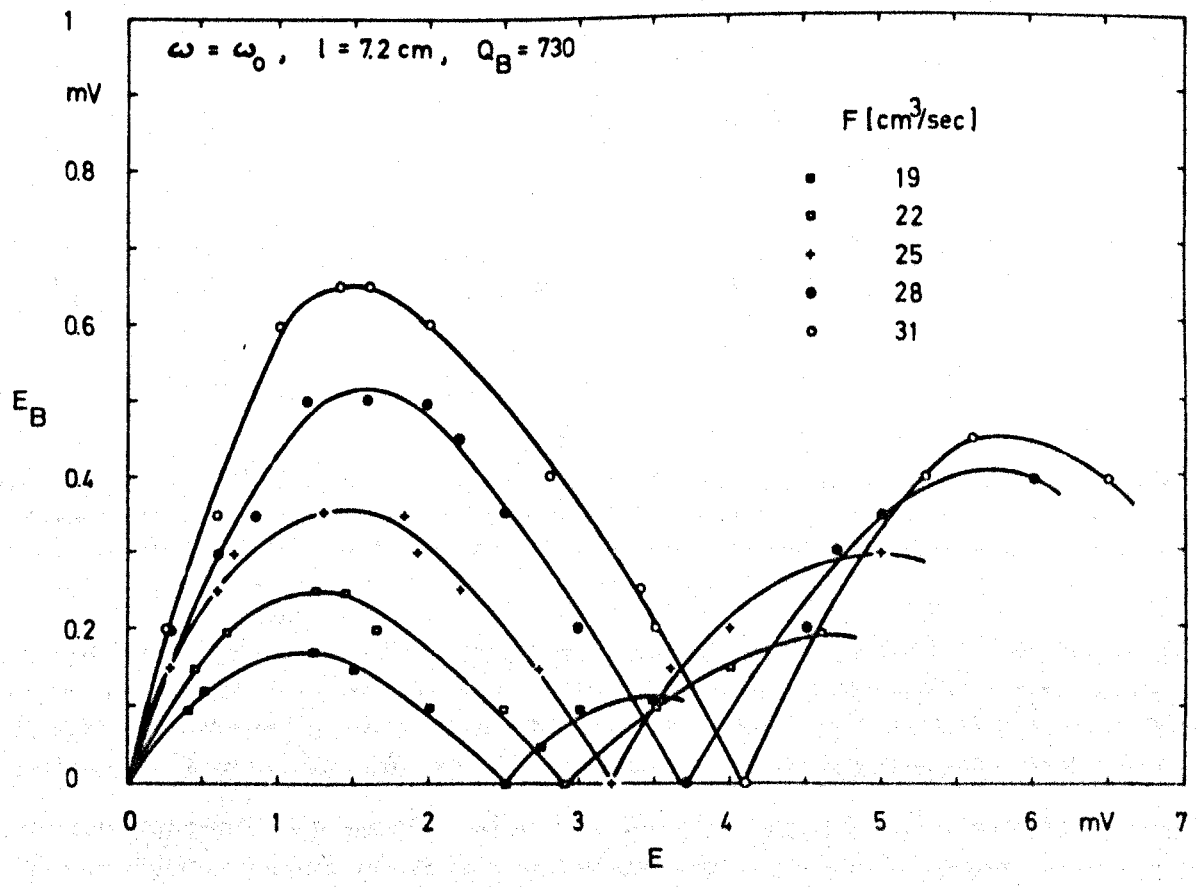

FIG. 24. Experimental relation between the voltage across the second coil, E_B, and the voltage across the first coil, E , for parameters different from those in FIG. 23.

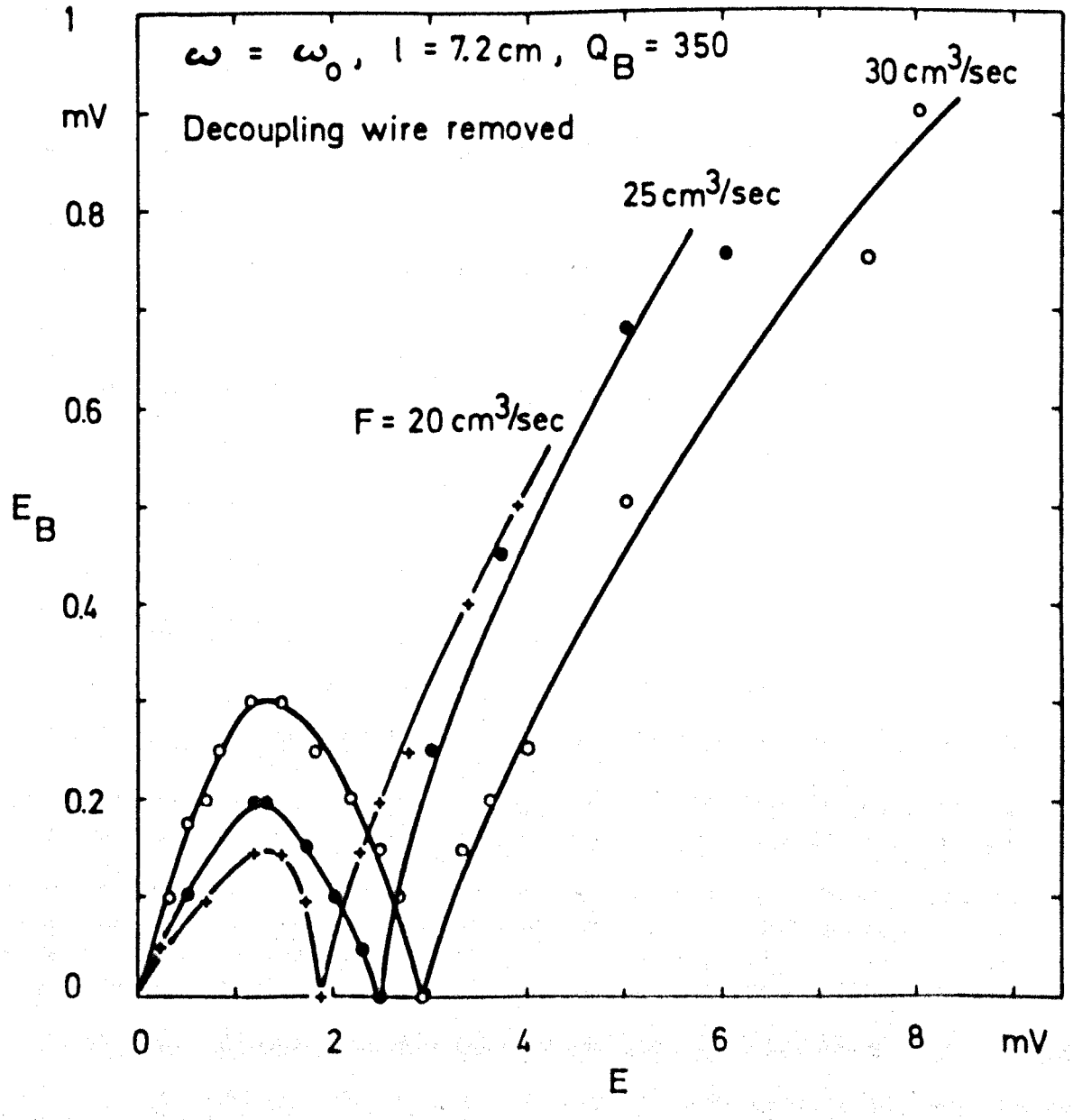

FIG. 25. Experimental result obtained with the decoupling wire removed from the maser tube.

Returning to the correct measuring results, Fig. 26 shows the relation between the critical voltage across the first emission coil, E_π, for which E_B becomes zero, and the water flow rate F. If E is adjusted to the value E_π then the residual moment $\vec{M}$ of the water emerging from the first emission coil is aligned parallel to the direction of the field $\vec{H}_o$. In this particular case the moment $\vec{M}$ tilts in the first emission coil by an angle $\theta = \omega_1^* \tau = \pi$. As Fig. 26 shows, the points of the measurements are all lying more or less on a straight line, although the dependence of ω_1^* on E is not a linear one (see Eq. (5)). The reason for this is that if the voltage across the first coil, E, is large, the inequality

$$\frac{1}{4T_2^{*2}\omega_1^2} \ll 1$$

holds such that $\omega_1^* \approx \omega_1 = \gamma k E$. In fact the critical voltage across the first coil, E_π, for which in the second coil the oscillation ceases, is with great accuracy given by

$$E_\pi = \frac{\pi}{\gamma k \tau} \qquad (6)$$

This is the condition for which the double-hump detuning phenomenon of the two-coil proton maser (Section 8.5) is most pronounced.

For $E > E_\pi$ the voltage E_B, available at the terminals of the second emission coil, approaches a second maximum which corresponds to a situation where $\vec{M}$ tilts in the first coil by an angle $\theta = 3\pi/2$.

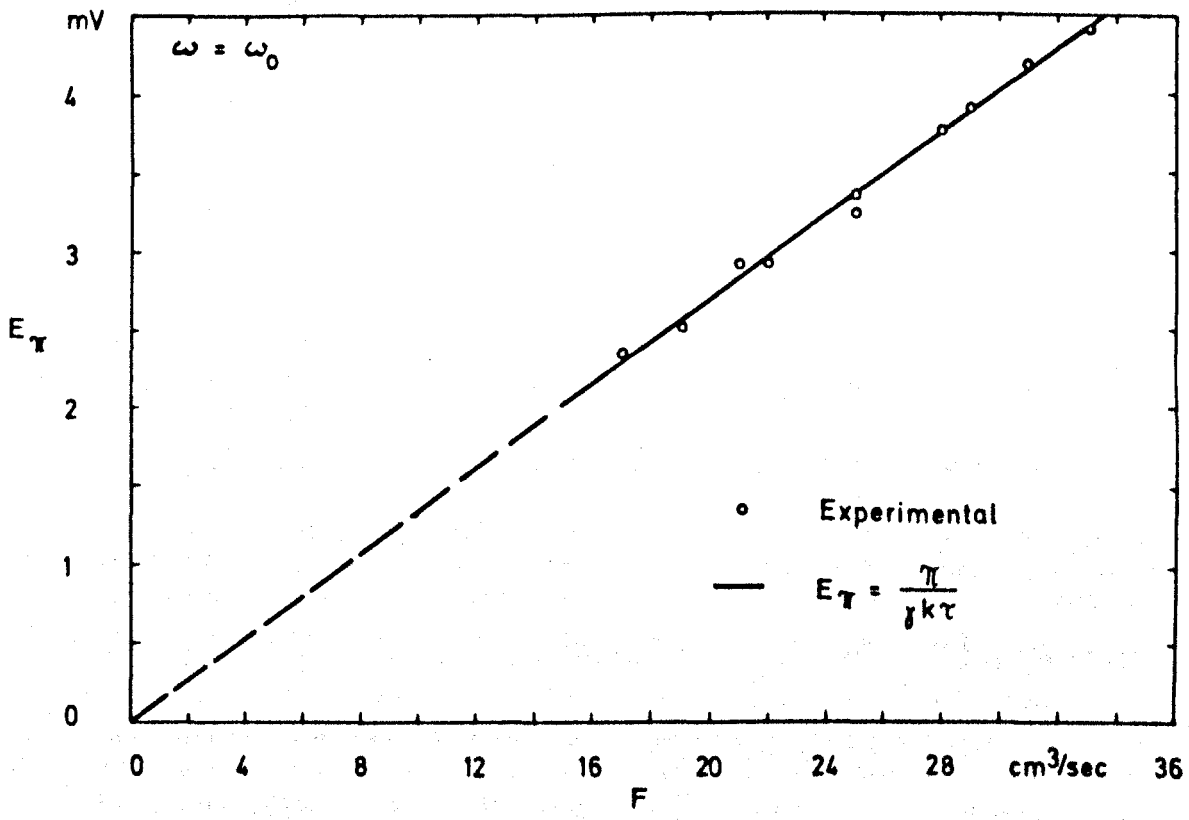

FIG. 26. Relation between the voltage across the first coil, E_π, for which the voltage across the second, E_B, becomes zero, and the water flow rate F.

The second maximum could of course also arise if $\vec{M}$, after tilting in the first coil by an angle θ, would, as E is further increased, tilt back to $\theta = \pi/2$. This is in contradiction with the theory, but it is also not difficult to prove experimentally that this is not the case. The experimental method used in order to show that $\vec{M}$ actually can tilt by an angle $\theta > \pi$ is illustrated in Fig. 27. By increasing the quality factor of the first circuit, Q, one can achieve that the voltage across the second coil takes a small value. If Q is further enhanced, then one can achieve that E_B, after becoming zero, takes the original small value again. It has been found experimentally that if this change in adjustment is made, the phase of the voltage across the second coil changes by 180°. This indicates that during the change of adjustment the phase of the transverse component of $\vec{M}$ exciting the second coil also changes by 180°. If one studies the situation in the rotating frame, see Fig. 27, it becomes obvious that during the change of the adjustment of the two-coil maser the moment $\vec{M}$ has tilted from an angle $\theta < \pi$ to an angle $\theta > \pi$.

Having found experimentally that the second maxima of the curves represented in Fig. 23 and Fig. 24 must correspond to situations where the residual moment $\vec{M}$ in the water emerging from the exit of the first emission coil makes an angle $\theta = 3\pi/2$ with $\vec{H}_o$, we are in the position to reconstruct the locus of $\vec{M}$ in the rotating frame on purely empirical grounds. In Fig. 28 a typical locus of $\vec{M}$ is shown, as it can be reconstructed from the experimental $E_B(E)$ dependence. As the voltage

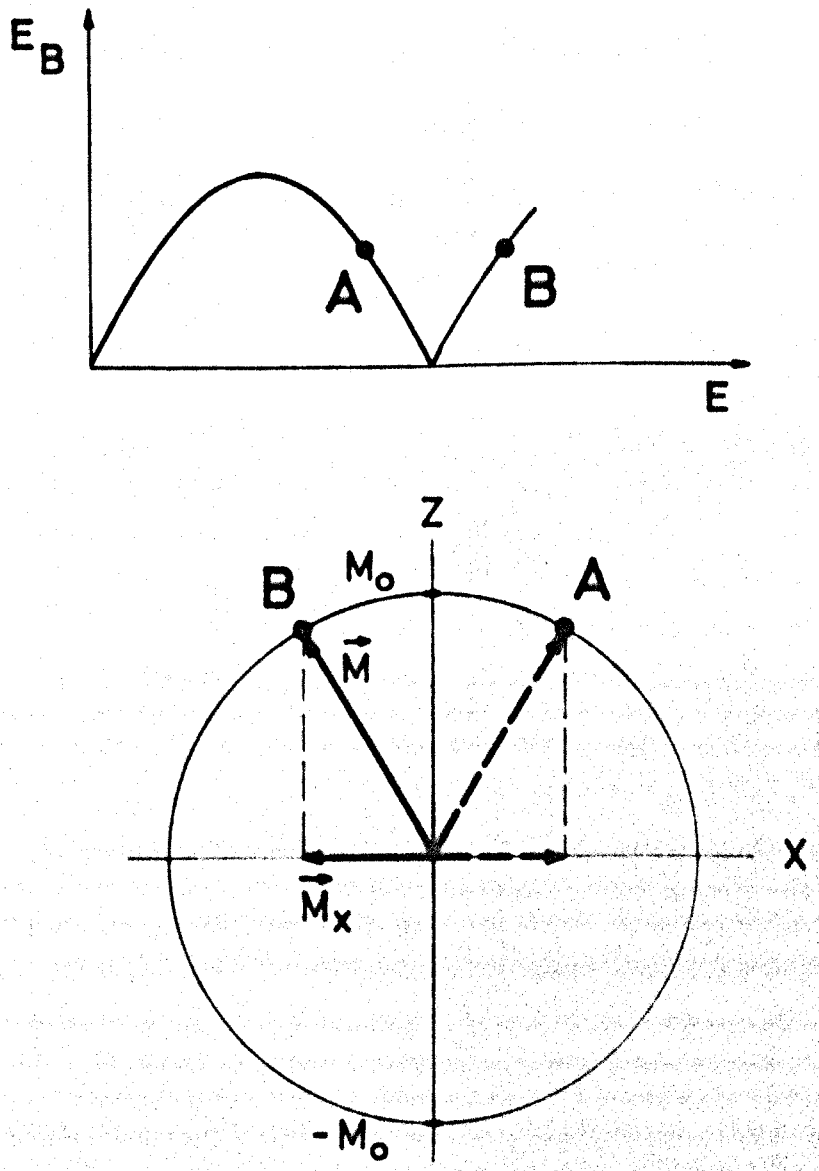

FIG. 27. If the voltage across the first coil, E , is increased such that the voltage across the second coil, E_B , changes from A to B (upper diagram) then it is observed experimentally that the phase of the voltage across the second coil changes by 180°. The lower diagram shows the corresponding positions of $\vec{M}$.

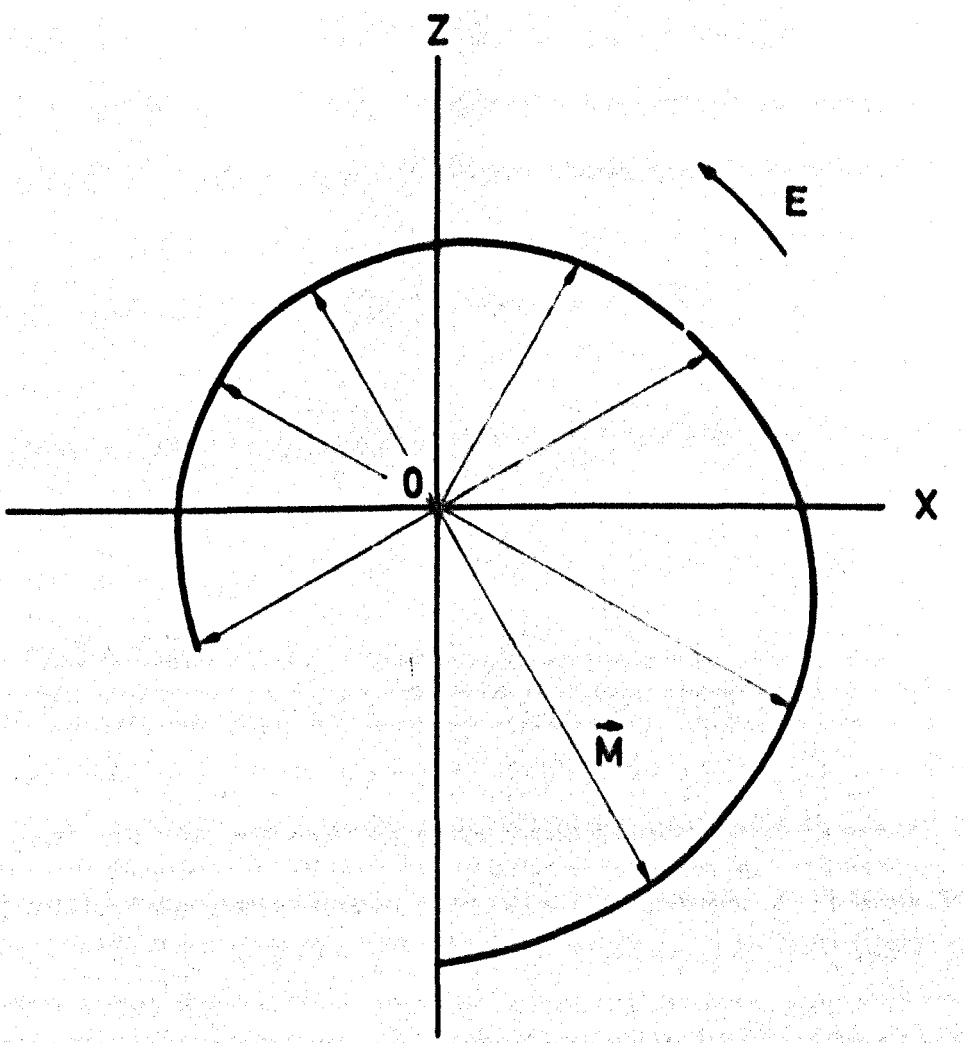

FIG. 28. Typical locus of the residual magnetization $\vec{M}$ exciting the second maser coil as the voltage across the first coil, E, is altered. Reconstructed from FIG. 24, F = 28 cm^3/sec.

across the first emission coil, E, is increased the tip of the residual magnetization $\vec{M}$ available in the second coil describes a spiral. The shrinking of the spiral is mainly caused by the saturation effect. It might be noted that according to the locus shown in Fig. 28 the residual transverse moment is not maximum for $\theta = \pi/2$, but for a somewhat lower angle. In determining the angle θ by means of the second emission coil there is of course an error involved, for even if Q_B is adjusted to a low value $\vec{M}$ tilts also in the second emission coil by a small angle. The locus of $\vec{M}$ has been reconstructed from the voltage curve measured for $F = 28\ cm^3/sec$ (Fig. 24). The maximum voltage across the second coil was here 0.52 mV, corresponding to a tilting angle of $\vec{M}$ in the second emission coil of $\theta_B = \gamma k E_B \tau = 2.67 \times 10^4 \times 0.11 \times 0.52 \times 10^{-3} \times 0.25 = 0.38$ rad, i.e. during this measurement $\vec{M}$ tilted in the second coil by about 22°. This explains why the locus of $\vec{M}$ shown in Fig. 28 is somewhat distorted at that angle where the transverse component of $\vec{M}$ is maximum. The additional tilting of $\vec{M}$ in the second solenoid shifts the maxima of E_B towards lower values of E. As Fig. 23 and 24 show, this effect is more distinct at higher water flow rates: at higher flow rates E_B is larger and, consequently, the additional tilting of $\vec{M}$ in the second emission coil is more pronounced.

If the quality factor of the first emission coil is enhanced such that the voltage E across it takes larger values than those for which the curves shown in Fig. 23 and Fig. 24 were measured, then the Q value becomes too large for the Q multiplier to remain stable.

If the Q multiplier of the first coil is gradually driven into its unstable range such that it becomes an auto-oscillator, then one can observe the voltage across the second coil following the same tendency of the curves shown in Figs. 23 and 24, with ever decreasing maxima, until the saturation effect hinders any voltage to be induced in the second coil. In the context of this thesis we are, however, not interested in the case that the spins be driven by an exciter field produced by means of an external oscillator.

8.5 The Double-Hump Detuning Phenomenon

In the preceding section voltage measurements have been reported which had been obtained when both emission coils of the two-coil proton maser were precisely tuned to the LARMOR frequency. We shall now discuss the case when the first emission coil is detuned.

Fig. 29 shows some typical detuning characteristics of the two-coil maser, including the double-hump detuning phenomenon. Each pair of oscilloscope traces shown (a, b and c) belongs to a certain adjustment of the Q multiplier of the first emission coil. In each case the first resonant circuit was detuned through the full frequency range in which maser oscillation occurs in the first emission coil. In recording these pictures the oscilloscope was switched over to the mode of operation where the horizontal deflection of the electron beam can be adjusted manually. The control knob serving for this latter purpose was removed from the front panel of the double-channel oscilloscope, and

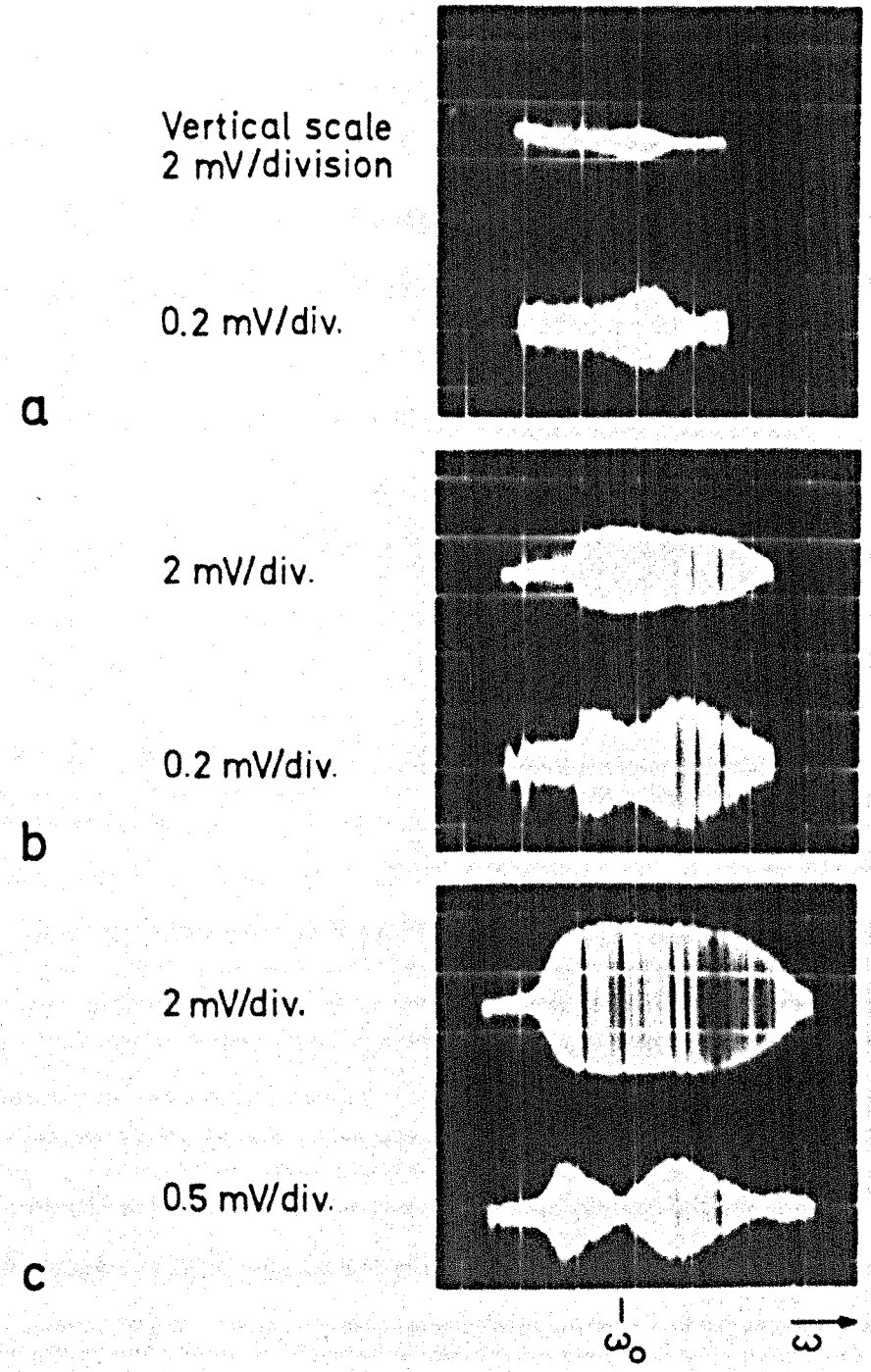

FIG. 29. The double-hump detuning phenomenon as observed with the two-coil proton maser. Upper traces in a), b) and c): voltage across the first coil. Lower traces: voltage across the second coil. Horizontal axes: frequency of auto-oscillation.

the spindle of the corresponding potentiometer was mechanically connected with the spindle belonging to the tuning condenser of the first Q multiplier. This allowed the simultaneous manual adjustment of the frequency detuning of the first emission coil and of the horizontal deflection of the electron beam.

The pictures show clearly that as the first coil is detuned through the full frequency range in which auto-oscillations are obtained, the dependence of the voltage across the first coil on the frequency of oscillation is always bell-shaped. In fact, according to Eq. (3.22) the detuning characteristic of the first emission coil should have the shape of a semi-ellipse, independently of the degree of excitation of this coil. On the other hand, Fig. 29 shows that as the first coil is sufficiently excited the level of the oscillations occurring in the second coil can go through two maxima with a gap in the middle. This is the double-hump detuning phenomenon which up to now had only been observed in two-cavity ammonia beam masers and for which up to now no cogent explanation had been found. Recently it was assumed that this phenomenon might arise in the two-cavity beam maser because of the interference which occurs between the emissions of ammonia molecules which move with different velocities and radiate fields with different phases (BASOV, ORAEVSKII and USPENSKII 1967, Section 2.4).

As was demonstrated in Chapter VII, as the quality factor of the first resonant circuit, Q, is increased the maser voltage across the first emission coil takes larger values (Fig. 20). Fig. 29 shows

that for larger Q's the oscillatory range of the proton maser increases also. This is in agreement with Eq. (3.19), Chapter III. The oscillatory range of the maser is typically a few hertz wide.

The double-hump detuning phenomenon is most pronounced if at zero detuning of the first coil, $\Delta\nu = \nu - \nu_o = 0$, the voltage across it equals E_π given by Eq. (6). Fig. 30 shows a set of detuning characteristics which was measured for a water flow rate F = 33 cm^3/sec. The double-hump detuning phenomenon occurs here for E_π = 4.2 mV, in good agreement with the $E_\pi(F)$ dependence represented in Fig. 26.

In fact the reproducibility of the phenomenon is excellent. In the course of the experimental investigation it has currently been used in order to tune the proton maser precisely to the LARMOR frequency ω_o. Because of the natural changes of the earth's magnetic field, this was often necessary in time intervals of less than one minute. Using the double-hump detuning phenomenon, the proton maser could be tuned to ω_o with an accuracy of at least 0.1 Hz which is the accuracy of the frequency counter utilized. If other working substances which have a longer natural relaxation time than distilled water, such as deoxygenated benzene for example, would be used the tuning accuracy available could be considerably enhanced.

Fig. 31 shows the appearance and disappearance of the double-hump detuning phenomenon as observed at the second coil when the first coil is detuned through the full oscillatory range and when the voltage appearing across the first coil is enhanced step-wisely by increasing

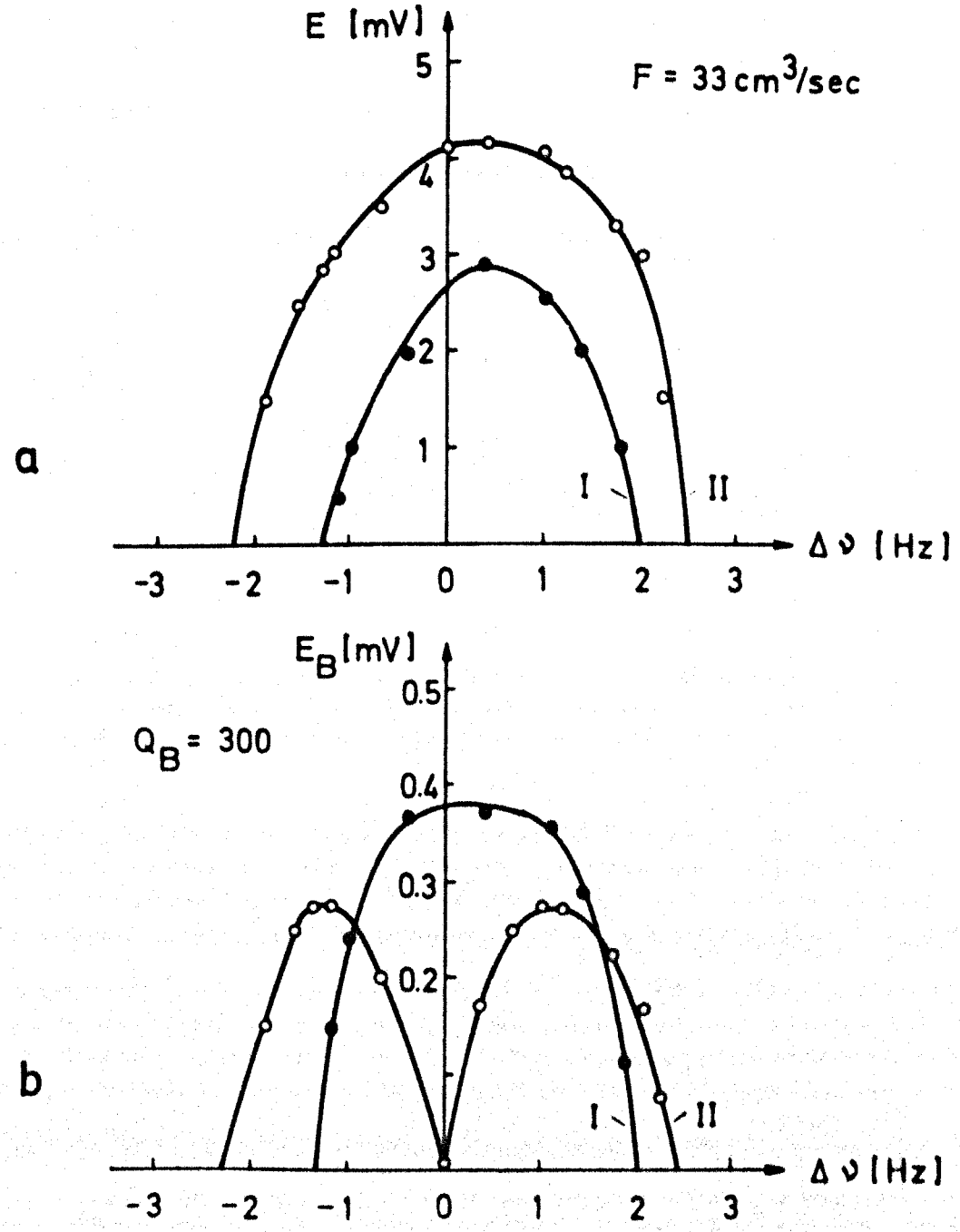

FIG. 30 . Typical detuning characteristics of the two-coil maser. a) Detuning characteristic of the first emission coil . b) Voltage across the second coil as the first coil is detuned. (Experimental.)

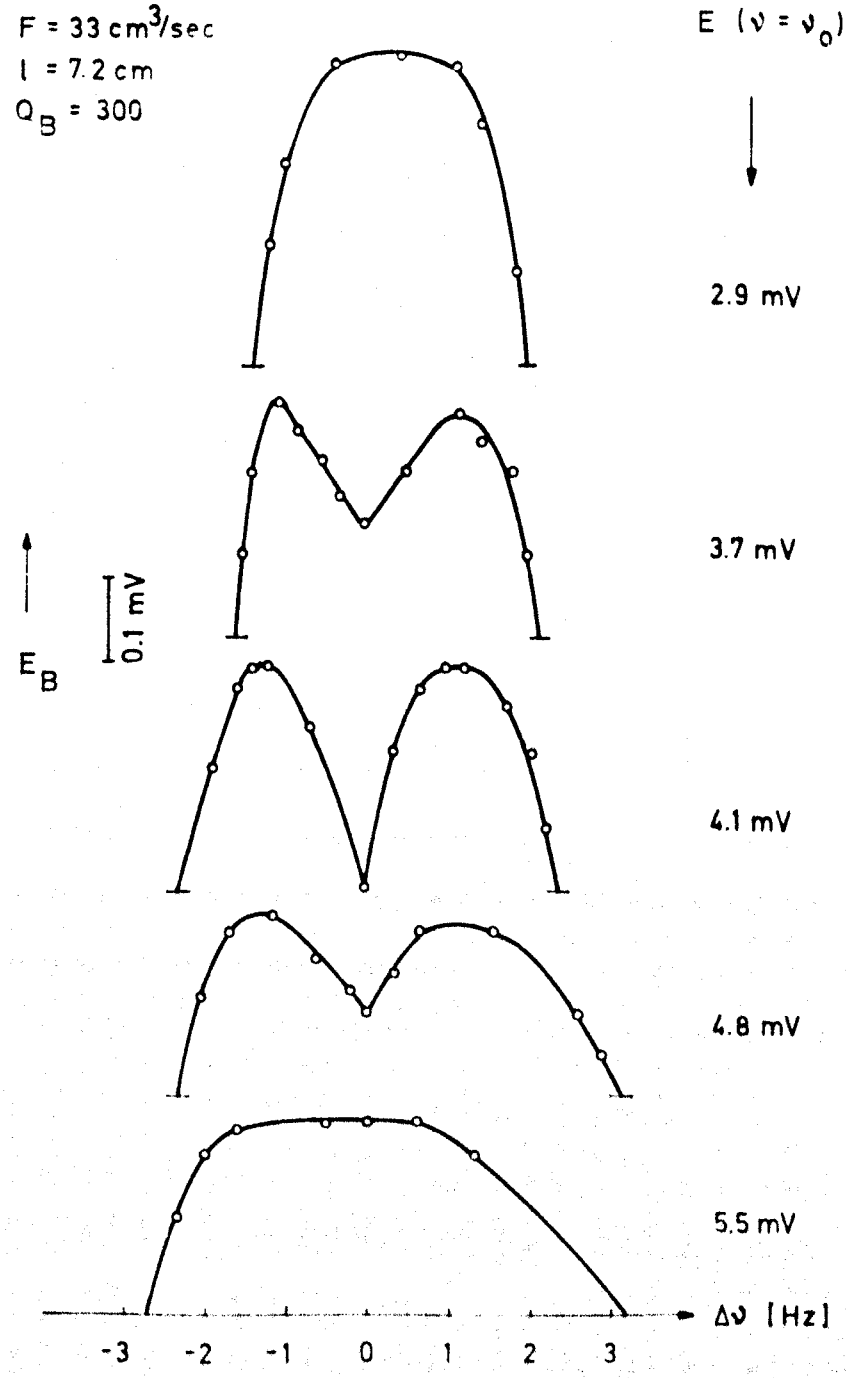

FIG.31. Experimental relation between the voltage across the second coil, E_B, and the voltage E and the frequency detuning $\Delta\nu$ of the first coil.

its quality factor. The gap opens at a medium voltage across the first coil and closes when the level of oscillations in the first coil is large. If the voltage across the first coil is increased even further, then one can observe the gap opening again. This is not shown in Fig. 31 for this large excitation of the first coil could not be produced without its Q multiplier becoming unstable, so hindering correct measurements from being taken.

If the first coil is detuned by a certain amount such that the frequency of oscillation of the system differs from ν_o by a fixed value $\Delta\nu = \nu - \nu_o$ then the voltage across the second coil, E_B, depends on the voltage across the first coil, E, in a manner different from that observed for zero detuning, (Figs. 23 and 24). This is shown in Fig. 32. Now E_B does not approach zero as E is increased by means of the Q multiplier of the first coil.

During the measurements reported up to this point the resonant frequency of the second circuit, ν_{c3}, was always equal to ν_o. Fig. 33 shows the typical dependence of E_B on the detuning $\nu_o - \nu_{cB}$ of the second resonance circuit as observed when the first maser coil oscillated. This curve was measured when the quality factor of the second circuit, Q_B, was large enough such that the second coil was itself capable of auto-oscillations when the first coil was switched off. (The critical quality factor $Q_{\ell B}$ for auto-oscillations to occur in the second coil when the first coil was switched off was about 800.) The curve has the typical shape of the amplitude transfer characteristic of a tuned

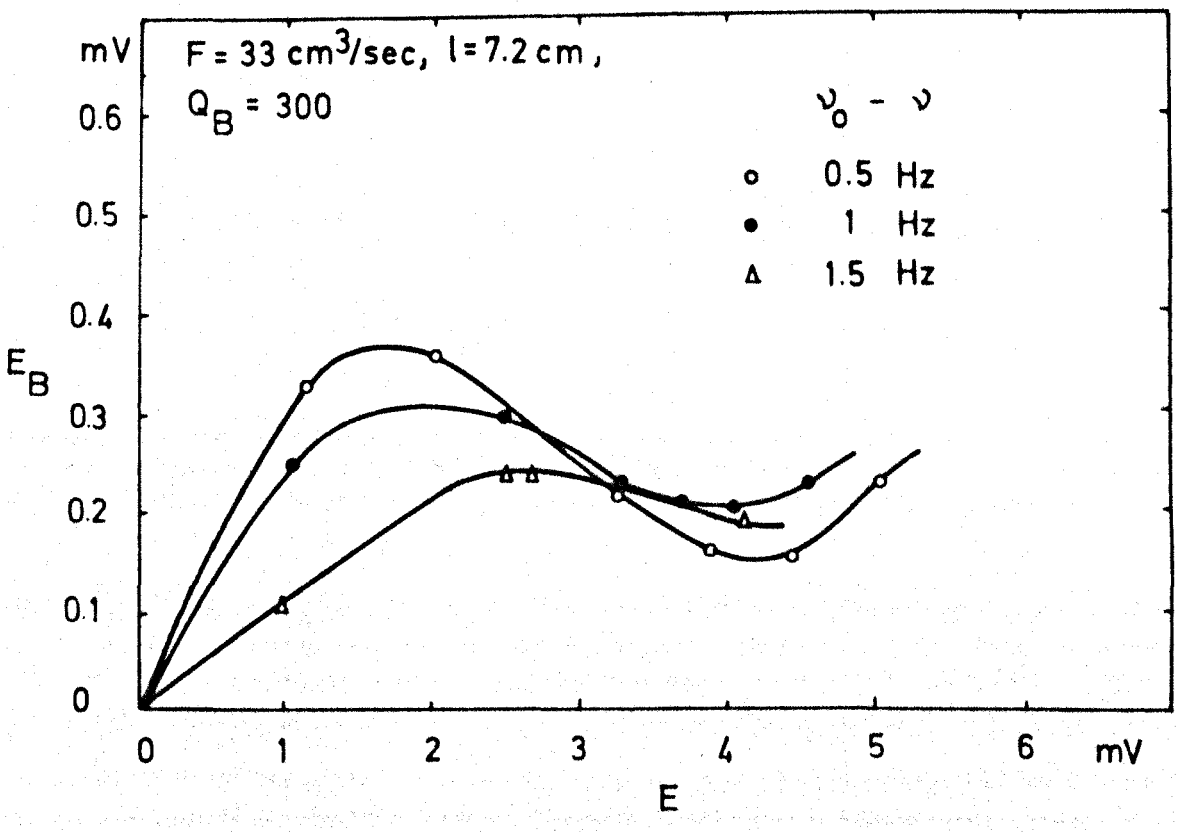

FIG. 32. Typical experimental dependence of the voltage across the second coil, E_B, on the voltage across the first coil, E, when the first coil is detuned.

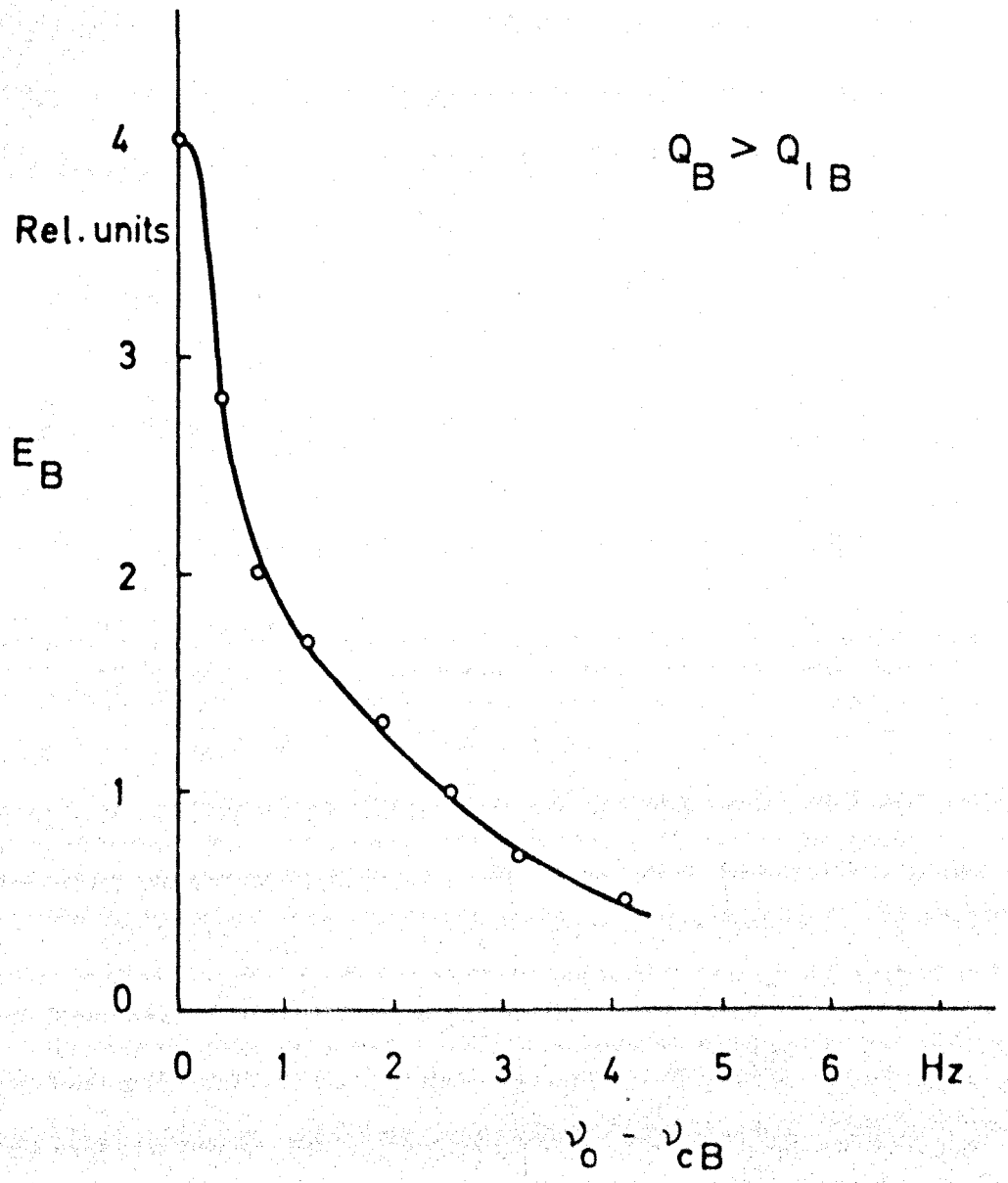

FIG. 33. Typical experimental relation between the voltage E_B across the second coil and its detuning $\nu_0 - \nu_{cB}$.

resonant circuit, and this shape is also observed for $Q_B < Q_{\ell B}$. Recently SMITH and LAINÉ (1968) have measured a corresponding curve for the second cavity of a two-cavity ammonia beam maser, their result agreeing qualitatively with the dependence represented in Fig. 33. If the first coil oscillates at a non-negligible level, even for $Q_B > Q_{\ell B}$ a detuning $\nu_o - \nu_{cB}$ of the second resonant circuit does only alter the voltage E_B, but not the frequency of oscillation which is determined by the frequency detuning of the first emission coil.

Concerning the explanation of the double-hump detuning phenomenon represented in Figs. 29 - 31, we have already shown why the voltage across the second coil can become zero when the first coil is sufficiently excited: if the macroscopic magnetic moment $\vec{M}$ of the water emerging from the first solenoid is aligned parallel to the direction of the main field $\vec{H}_o$ then the transverse moment is zero and the second coil cannot be excited. Suppose now that at the time $t = \tau$ (at the exit of the first emission coil) the moment $\vec{M}$ is actually in the position parallel to $\vec{H}_o$ and the first coil is subsequently detuned to a slightly higher or somewhat lower frequency $\omega \neq \omega_o$. Then the moment $\vec{M}$, as observed at the exit of the first coil, must necessarily tilt towards its initial ($t = 0$) position antiparallel to $\vec{H}_o$, for if the first coil is completely mistuned so that no auto oscillations occur in the first coil, the moment $\vec{M}$ must leave the first coil aligned exactly antiparallel to $\vec{H}_o$. If the first coil is sufficiently detuned then $\vec{M}$ will tilt back by an angle $\pi/2$, and this is the situation where the voltage across the

second coil is maximum. If the first coil is gradually detuned through the full oscillatory range then the transverse component of the residual magnetization of the water emerging from the exit of the first coil will be maximum twice, and therefore the voltage across the second emission coil.

We shall now show that the transverse component of the magnetization in a nuclear maser can become maximum if the maser is sufficiently detuned. Let us use the rotating frame introduced in Fig. 17(a) and choose the time origin such that in the laboratory frame the transverse component of $\vec{M}$ varies according to

$$M_y(t) = M_y \cos \omega t$$

If this equation is introduced into Eq. (3.8), then one finds that the stationary solution for the reaction field is given by

$$H_y(t) = 2H_1 \sin (\omega t + \delta)$$

where

$$\tan \delta = Q\frac{\omega_c^2 - \omega^2}{\omega\omega_c} \approx 2Q\frac{\omega_c - \omega}{\omega}$$

In other words, depending on the sense of the detuning, the reaction field lags behind the transverse moment by somewhat more or somewhat less than 90°. In the frame rotating with the frequency ω about the Z axis, the projections of the rotating field $\vec{H}_1$ on the X axis and the Y axis are given by

$$H_x = H_1 \cos \delta \ , \quad H_y = H_1 \sin \delta$$

Now the velocity $\vec{V}_1$ (Fig. 17(a)) is given by $\vec{V}_1 = \gamma H_1 \cos \delta \vec{M}$, and if the influence of T_1 is neglected this leads to the equation

$$\frac{d^2M_y}{dt^2} + \frac{1}{T_2^*} \frac{dM_y}{dt} + (\gamma H_1 \cos \delta)^2 M_y = 0$$

This equation can also be derived from the work of COMBRISSON (1960) and SOLOMON (1961). If the influence of T_2^* is neglected also, with the initial conditions properly chosen the transverse moment is given by

$$M_y = M_o' \sin (\gamma H_1 t \cos \delta)$$

If at the time $t = \tau$ for zero detuning ($\cos \delta = 1$) of the maser we have $\gamma H_1 \tau = \pi$ such that $M_y = 0$ (no voltage induced in the second coil) then, as the maser is gradually detuned towards a lower or higher frequency, both H_1 (Section 3.5) and $\cos \delta$ will decrease. For $\gamma H_1 \tau \cos \delta = \pi/2$ the transverse moment M_y and hence the voltage across the second coil will be maximum.

We shall conclude by remarking that in comparing the double-hump detuning of the two-coil proton maser (Figs. 29 - 31) with the double-hump detuning phenomenon of the two-cavity ammonia beam maser (Fig. 2) one has to take into account that in the latter case the radiation intensity in the second cavity is measured, not the amplitude

of the field induced by the ringing molecules. The absolute power output of an ammonia beam maser is of the order of magnitude of only 10^{-10} watts and hence difficult to measure. Therefore relative power units are usually given.

For the two-coil proton maser devised we can say with certainty that here the double-hump detuning phenomenon is not produced by interference effects arising from the velocity distribution of the excited particles, as was recently suggested for the two-cavity ammonia beam maser (BASOV, ORAEVSKII and USPENSKII, 1967). Since the two-coil nuclear maser behaves also in other respects analogously to the ammonia beam maser we can conclude that also in the two-cavity ammonia beam maser the double-hump detuning phenomenon is produced by a more fundamental mechanism: an "abstract" tilting of the electric-polarization vector about some "fictitious" effective electric field.

8.6 Summary

Expressions for the voltage across the second emission coil have been derived for the case that both coils be precisely tuned to the circular frequency $\omega_o = \gamma H_o$. These formulae (Eq. (2) and Eq. (4)) reveal that the voltage across the second coil is strongly dependent on the voltage across the first coil. If the second coil is strongly excited, then the voltage across it can be evaluated starting from a conservation-of-energy argument (Eq. (2)). If the second coil is only weakly excited then the voltage across the second coil depends on the

voltage across the first coil through a simple sine law (Eq. (4)). This latter case has been checked experimentally and a fair quantitative agreement has been found. For a certain critical voltage across the first coil (Eq. (6)) the voltage across the second coil becomes zero.

As the first coil is detuned through its full oscillatory range then it is observed experimentally that the voltage across the second coil can go through two maxima with a gap in the middle. The analogue of this double-hump detuning phenomenon has previously only been observed in two-cavity ammonia beam masers and up to now no cogent explanation had been found for its appearance.

CHAPTER IX

MODULATION EFFECTS IN A TWO-COIL NUCLEAR MASER

9.1 Introduction

Apart from the double-hump detuning phenomenon, another distinctive characteristic of the two-cavity ammonia beam is the amplitude modulation which can occur in the second cavity if the first cavity is sufficiently detuned. It remains to show that an analogous effect can be observed using a two-coil nuclear maser.

The purpose of this chapter is also to discuss the performance of the two-coil nuclear maser in that mode of operation where the inter-coil distance is mechanically modulated.

9.2 Self-Modulation in the Second Emission Coil

Using an ammonia beam maser with two resonators through which the excited molecules passed in series, HIGA (1957) was the first to observe that if the first cavity is sufficiently detuned the second cavity can oscillate simultaneously at two different frequencies. One of the frequencies coincides with the frequency of the auto-oscillation in the first cavity, the other frequency being determined by the tuning of the second cavity and its natural generation. This effect has also been observed by other workers (Chapter II). The region in which these generation conditions exist is pointed out in Fig. 2.

The phenomenon occurs near maximum detuning of the first cavity over a frequency range of about 0.5 MHz. The beat frequency produced by this amplitude modulation in the second cavity is usually a few kilohertz. A modulation depth as large as 25% has been observed (SMITH and LAINÉ 1968).

The analogous effect has been observed in the two-coil proton maser, indicating that the analogy between the two different types of systems can be carried even further.

Fig. 34 shows the result of a measurement which has been carried out for a quality factor of the second coil $Q_B = 2500$. This quality factor is so large that, if the first coil were switched off the second coil would produce maser oscillations on its own.

As Fig. 34, the modulation effect occurs in the second if the first coil is sufficiently detuned. In taking these measurements the two-coil maser was adjusted such that, as the first coil was gradually detuned, in the second coil not only the self-modulation effect but also the double-hump detuning phenomenon could be observed. There are also other adjustments possible where the self-modulation effect occurs and the double-hump detuning phenomenon is less pronounced or does not occur. The self-modulation effect and the double-hump detuning phenomenon are not causally connected to each other. The reason for presenting the particular experimental curve shown in Fig. 34 is to stress the analogy to the corresponding experimental curves measured by BASOV and coworkers for the two-cavity ammonia beam maser (Fig. 2).

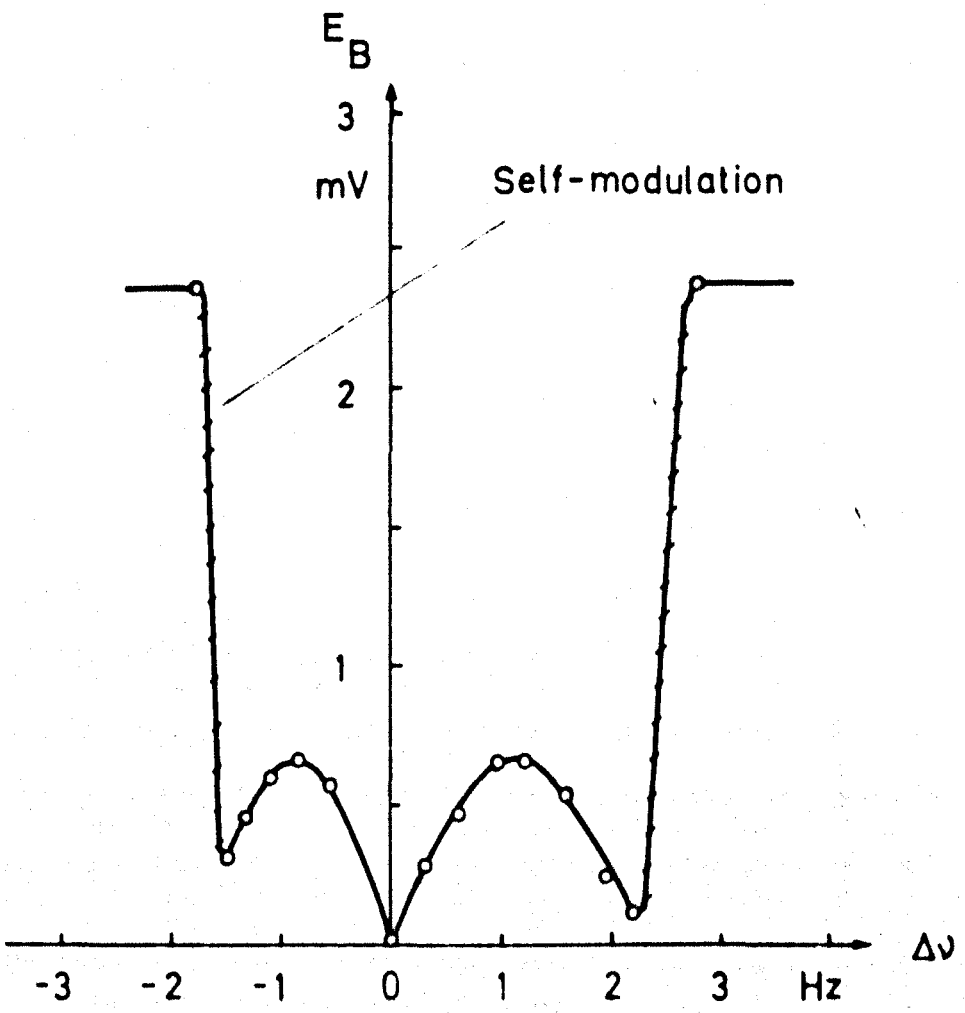

FIG.34. Example of the dependence of the voltage across the second coil, E_B, on the frequency detuning $\Delta\nu = \nu - \nu_0$ of the first coil, for a large quality factor Q_B of the second coil ($Q_B = 2500$, $F = 33\ cm^3/sec$, $l = 7.2\ cm$).

For the two-coil proton maser devised the range of frequencies in which the self-modulation effect could be observed in the voltage across the second coil was typically 0.3Hz. The beat frequencies of the voltage across the second coil were usually 0.5 ... 3 Hz.

It is obvious that since the effect is observed over a frequency range as small as 0.3 Hz, the beat frequency of the voltage across the second coil can hardly be varied by slightly further detuning or retuning the first emission coil. However, it was observed experimentally that by detuning the second coil the beat frequency could be brought to zero or be increased to about 10 Hz, depending on the sense of the tuning of this coil.

Fig. 35 shows a typical beat signal observed for zero detuning of the second coil when the first coil was sufficiently detuned. By detuning the first emission coil the modulation depth of the voltage across the second coil could be varied between 0 and 100%. As the first coil is tuned to that frequency where in the second coil the self-modulation starts then, as the first coil is further detuned, the modulation depth increases, takes a maximum of 100% and decreases again to zero. In recording the oscilloscope traces shown in Fig. 35 the first emission coil was adjusted such that the modulation depth of the voltage across the second coil was nearly 100%. This adjustment is a rather critical one: the frequency of oscillation of the first emission coil has to be set with an accuracy $\ll$ 0.1 Hz. Once the maser is adjusted for a certain modulation depth of the voltage across the second coil, the

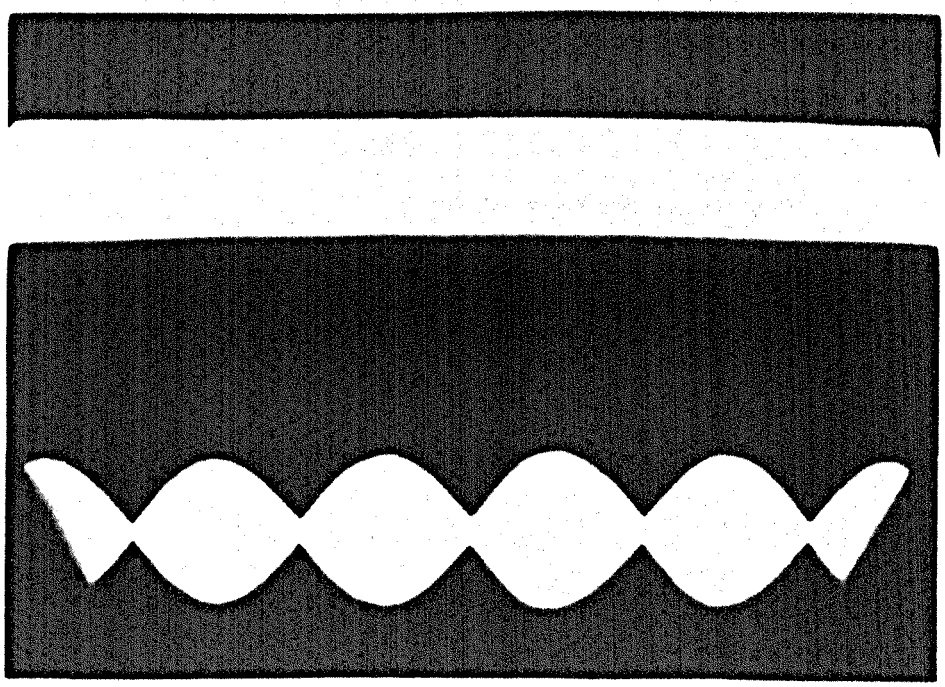

FIG.35. Typical amplitude modulation of the voltage across the second coil (lower trace) as observed when the first emission coil is sufficiently detuned. Beat frequency: ≈ 3 Hz. Upper trace: voltage across the first coil.

modulation depth changes after a short time, usually a few minutes, because of the natural variations of the earth's magnetic field H_o which determines the LARMOR precession frequency $\omega_o = \gamma H_o$ and hence alters the frequency of oscillation of the first emission coil.

The beat signal observed when the self-modulation occurs in the second cavity of a two-cavity ammonia beam maser has the characteristics of the beat signal of two superimposed sinusoidal signals of different frequencies. As Fig. 35 indicates, the same effect can be observed in a two-coil nuclear maser.

However, the two-coil proton maser showed the important feature that, for a certain adjustment of the experimental parameters, the beat signal available at the second coil did no longer exhibit the typical characteristics of a beat signal produced by two purely sinusoidally varying functions. Fig. 36 shows an oscilloscope trace which was recorded when the second coil was capable of a strong self-excitation (large quality factor Q_B) and when the first coil was so far detuned that in the second coil the natural generation was predominant. The phenomenon shown is reproducible. The shape of the beat signal shown reveals the existence of a non-linearity in the system. In fact if the level of oscillations in the second is high the saturation effect has a greater influence, and it is suggested that this might be the cause for the distortion of the beat signal. As far as the literature indicates, a similar modulation phenomenon has previously not been observed in two-cavity ammonia beam masers.

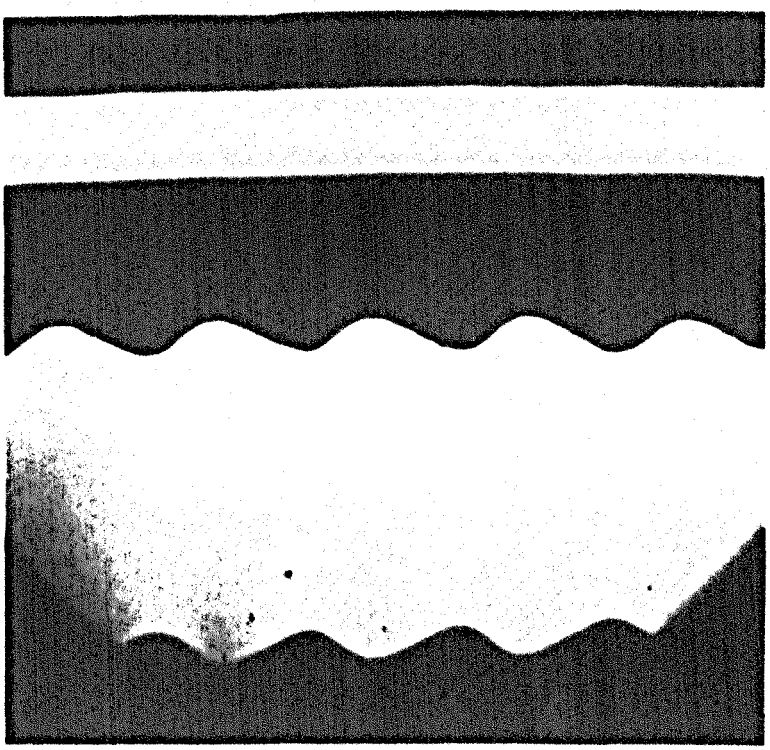

FIG.36. Non-sinusoidal amplitude modulation of the voltage across the second coil (lower trace) as observed when the first coil is sufficiently detuned and when the second coil oscillates predominantly at the centre frequency. Beat frequency: ≈ 3 Hz. Upper trace: voltage across the first emission coil.

9.3 Qualitative Explanation of the Amplitude Modulation

If auto-oscillations occur in the first emission coil then the frequency of oscillation in the second coil follows the frequency of oscillation in the first coil (Chapter VI). According to the experimental observations (Fig. 34), this picture does also not alter if the second coil is itself capable of auto-oscillations when the first coil is switched off.

Suppose now that the latter be actually the case, i.e. that TOWNES' condition be fulfilled for the second coil also ($Q_B > Q_{\ell B}$). As the first coil is gradually detuned, the macroscopic magnetic moment $\vec{M}$, as observed at the exit of the first emission coil, will tilt gradually back to its position antiparallel to the main field $\vec{H}_o$, for if the first coil is completely mistuned such that no generation takes place in it the moment $\vec{M}$ must appear at its exit in the position antiparallel to $\vec{H}_o$.

As soon as the maximum detuning of the first emission coil is reached, one would expect a sudden frequency jump of the oscillation in the second coil, because the mode of operation in this coil will change from forced oscillations at the frequency ν determined by the detuning of the first coil to auto-oscillations at the frequency ν_o (we assume that the second coil be precisely tuned to ν_o)

The appearance of the self-modulation effect in the second coil reveals that this change from one mode of operation to the other does in fact occur less suddenly. The circumstance that during this

change of the mode of operation there appear two oscillations in the second coil indicates that there are in this situation in the second solenoid two different macroscopic moments involved: the original moment $\vec{M}$ of the water passing into the second coil must have "split up".

This splitting process might be explained as follows. There is always a thermal radiation field produced by the thermal noise current present in each of the two coils. Let us first consider the thermal radiation field in the first coil. This field will produce a fluctuating torque on the magnetization, so not allowing a sharp definition of the tilting angle θ between $\vec{M}$ and $\vec{H}_o$. Clearly, the longer the magnetization remains in the first coil the more will $\vec{M}$ fluctuate. At the exit of the first solenoid the random motion of $\vec{M}$ will be maximum. Now assume the first coil has been nearly completely detuned such that the mean position of $\vec{M}$ as observed at the exit of the first solenoid is nearly antiparallel to $\vec{H}_o$. Then the water emerging from the exit of the first coil will still carry a small residual tranverse rotating moment with it which produces a weak forced oscillation in the second coil. On the other hand, the tilting angle θ vibrates with the thermal radiation field present in the first coil, and these vibrations will cause fluctuations of the e.m.f. induced in the second coil. The current produced by the e.m.f. will fluctuate and hence also the reaction field associated with this current. In addition there is the thermal radiation field which is

produced by the thermal noise current circulating in the second coil. Here the random vibration of the tilting angle of $\vec{M}$ will be even more pronounced than in the first coil. If $\vec{M}$ enters the second coil in a position nearly antiparallel to $\vec{H}_o$ there will be in the time average a macroscopic magnetization which is aligned antiparallel to $\vec{H}_o$ and which has no net transverse rotating moment. If for this magnetization TOWNES' condition is fulfilled, there also will appear an auto-oscillation at the frequency ν_o. The superimposition of the auto-oscillation at the frequency ν_o and of the forced oscillation at the frequency ν leads to a beat note which can be observed in the voltage available at the terminals of the second coil.

In practice the Q multiplier will add flicker noise, and shot noise if vacuum tubes are used. There is also the non-uniform velocity distribution of the nuclei, a further reason for the macroscopic magnetization to be distributed around the tilting angle.

9.4 Modulation of the Inter-Coil Distance

We shall now discuss a further analogy between the two-coil proton maser and the two-cavity ammonia beam maser.

In 1965 VESELAGO, ORAEVSKII, STRAKHOVSKII and TATARENKOV proposed the use of mechanical inter-cavity distance modulation as a means of tuning an ammonia beam maser precisely to the centre of gravity of the inversion line (Section 2.5). According to these workers, if the inter-cavity distance is varied by an amount $\Delta\ell$

then the phase of the oscillation in the second cavity changes by an amount

$$\Delta\psi = (\omega_1 - \omega_{21}) \frac{\Delta\ell}{\bar{v}}$$

where ω_1 is the frequency of oscillation in the first cavity, ω_{21} is the transition frequency, and $\bar{v}$ is the velocity of the molecular beam. For $\omega_1 = \omega_{21}$ the phase modulation would be zero, so providing a criterion for tuning the maser to the frequency ω_{21}. As far as literature indicates, up to now experimental difficulties have hindered this method from being verified in practice (Section 2.5).

From Eq. (6.1) it might be seen that if the inter-coil distance of the two-coil proton maser is varied by an amount $\Delta\ell$ then the corresponding expression for the phase change of the voltage across the second coil is given by

$$\Delta\psi = (\omega - \overline{\omega_o(x)}) \frac{\Delta\ell}{\bar{v}} \qquad (1)$$

where $\overline{\omega_o(x)}$ is the average value of the local LARMOR frequencies in the inter-coil space, and $\bar{v}$ is the velocity of the liquid.

The two-coil proton maser has been designed such that it can be switched over into a mode of operation where the inter-coil distance is varied sinusoidally (Section 5.5). In this mode of operation the phase modulation of the voltage across the second coil could easily be observed on the screen of the oscilloscope. Fig. 37 shows a typical oscilloscope trace as it can be observed when the first emission coil

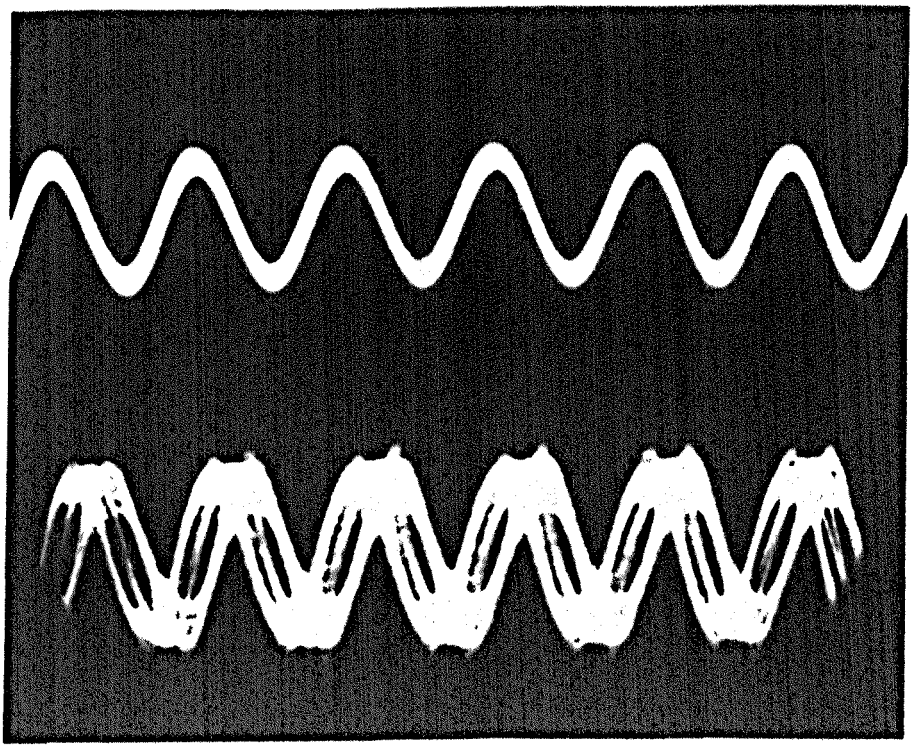

FIG. 37. Typical phase modulation of the voltage across the second coil (lower trace) as observed when the inter-coil distance is mechanically modulated. The phase modulation vanishes as the first coil is tuned exactly to the LARMOR frequency. Upper trace: voltage across the first coil.

is not precisely tuned to the average circular frequency $\overline{\omega_o(x)}$. In recording Fig. 37 the maximum variation of the inter-coil distance was 10 cm and the frequency of the mechanical modulation was about 1 Hz; the photographic exposure time was about 2 sec.

Measurements of the phase change $\Delta\psi$ have been performed for $\Delta\ell$ = 10 cm and F = 30 cm^3/sec. Fig. 38 shows how the experimental results compare with the phase change predicted by Eq. (1). The experimental values were obtained by comparing the phases of the voltage across the second coil on the oscilloscope screen; hence the error of the measurements will be about 10%. Considering that in deriving Eq. (1) the relaxation effects have been neglected, the agreement between theory and experiment appears to be reasonable.

The slope of the curve shown in Fig. 38 is about 80°/0.5 Hz. If the phase of the voltage across the second coil would be measured with an accuracy of 0.1° then the accuracy with which the proton maser could be tuned to the frequency $\overline{\nu_o(x)}$ would be 6×10^{-4} Hz. For $\overline{\nu_o(x)} \approx 2$ kHz this corresponds to a relative tuning accuracy of 3 parts in 10^7. (The magnetogyric ratio γ of protons in water is known with an accuracy of a few parts in 10^6; BENDER and DRISCOLL 1958, COHEN and DUMOND 1965.) Phase measurements with an accuracy of 0.1° can be performed using a normal digital phase meter or a phase sensitive detector (coherent amplifier). The latter device allows short-term measurements of phase changes $<0.01^\circ$.

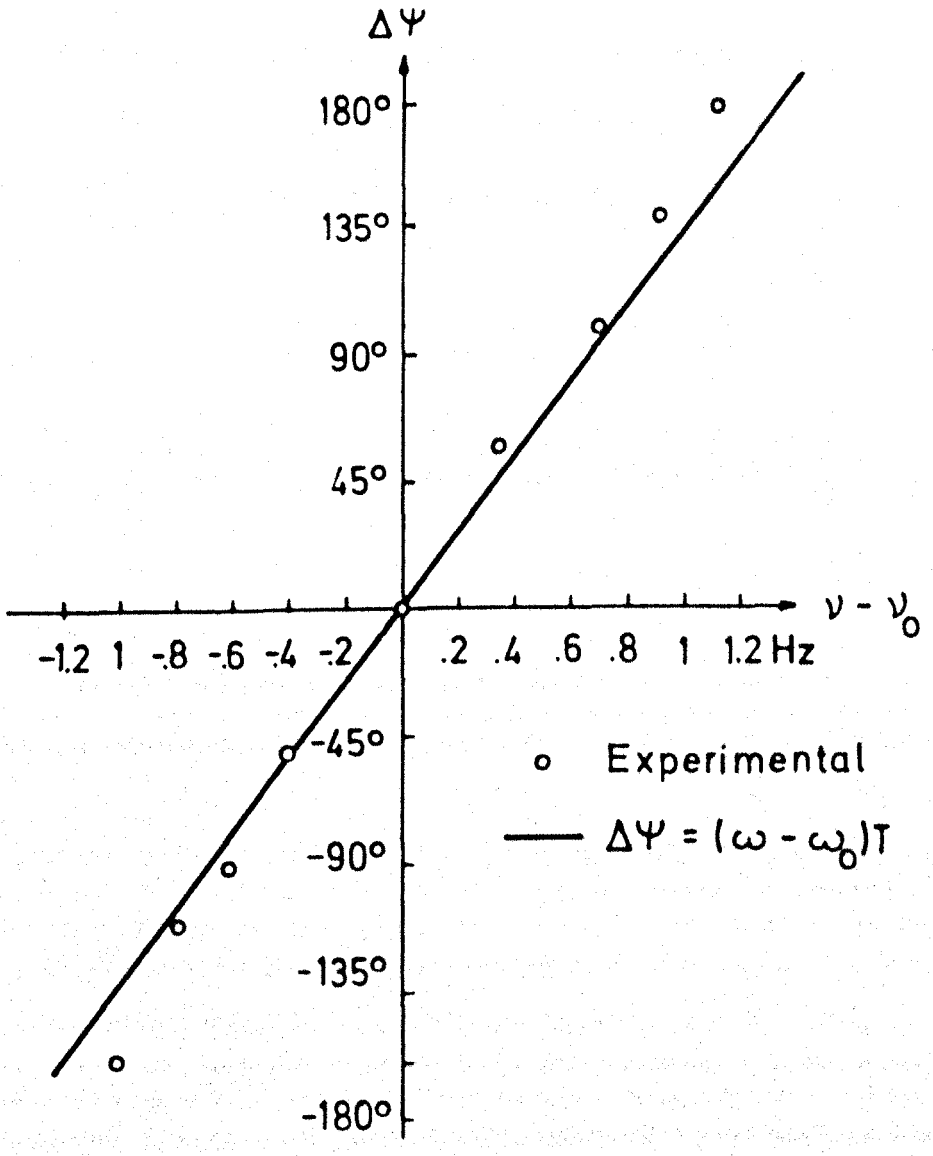

FIG. 38. Relation between the phase change $\Delta\Psi$ of the voltage across the second coil and the frequency detuning $\nu - \nu_0$ of the first coil, for a change of the inter-coil distance $\Delta l = 10$ cm ($F = 30$ cm^3/sec).

Thus apart from the double-hump detuning phenomenon which can also be used as a tuning criterion, mechanical modulation of the inter-coil distance and adjustment for zero phase modulation makes it possible to tune the maser with considerable precision to the frequency $\overline{\nu_o(x)}$. This is important in such applications as magnetometry. The conventional one-coil nuclear maser magnetometers do not offer a suitable tuning criterion (GRIVET and MALNAR 1967).

9.5 Summary

Concerning the HIGA-type of amplitude modulation which has previously been observed using two-cavity ammonia beam masers, the two-coil nuclear devised behaves in an analogous way. Apart from the normal sinusoidal beat signal, a distorted modulation signal has however been observed.

The mechanical modulation of the inter-coil distance of the two-coil maser leads in general to a phase modulation of the voltage across the second coil. The phase modulation becomes zero if the maser is tuned to the average local LARMOR precession frequency corresponding to the average local magnetic field in the inter-coil space. The dependence of the maximum phase change on the frequency detuning can be pre-calculated rather accurately using an uncomplicated formula.

CHAPTER X

GENERAL DISCUSSIONS

10.1 Introduction

In Chapter VIII and Chapter IX it was shown that the performance of a two-coil nuclear maser is in many respects analogous to that of a two-cavity ammonia beam maser. It was also shown that the double-hump detuning phenomenon can be explained using a classical analysis. However, the performance of molecular beam masers is usually discussed quantum-mechanically and it remains to show whether the experimental performance of a two-resonator maser can also be explained in terms of quantum mechanical probabilities.

In this concluding chapter the consequences of the present investigation with respect to flow masers in general shall also be discussed. Proposals for further experimental investigations will be made, and practical applications of the two-coil proton maser will be mentioned.

10.2 The Two-Cavity Maser Problem and Quantum Mechanical Probabilities

In Chapter VII it was shown that the double-hump detuning effect which had previously been observed using two-cavity ammonia beam masers can occur in a two-coil nuclear maser also. Moreover, it was seen that for the case of the nuclear maser the values of the parameters for which the oscillation in the second coil ceases can be evaluated

very accurately (Fig. 26). However, the condition for which the radiation intensity in the second cavity of a beam maser can become zero has not yet been specified.

For a molecular beam maser it can be shown (FEYNMAN, LEIGHTON and SANDS 1965) that if a molecule enters the resonator in the upper energy state $|I\rangle$ at the time $t = 0$ then the probability that the molecule will be found in this state at a time t later is given by

$$P_I(t) = \cos^2 \frac{\mu_e \varepsilon t}{\hbar} \qquad (1)$$

Here ε is one half of the amplitude of the oscillating electric field present inside the resonator, μ_e is the electric-dipole moment, and $\hbar$ is PLANCK's constant divided by 2π. This equation which can be derived using time-dependent perturbation theory is valid for $T_1 = T_2 = \infty$, and for zero detuning of the cavity. The probability that the molecule will be found in the lower state $|II\rangle$ is given by $P_{II}(t) = 1 - P_I(t)$.

From Eq. (1) it is obvious that if the molecules remain for a time τ inside the resonator and the electric field ε is made large enough, for example by increasing the number of the excited molecules, the probability of finding the molecule after the emergence from the exit of the resonator in the upper energy state is $P_I = 0$, if the condition

$$\frac{\mu_e \varepsilon}{\hbar} \tau = \frac{\pi}{2}$$

is fulfilled. In other words, if the electric field inside the first resonator is just such that

$$\varepsilon = \frac{\pi\hbar}{2\mu_e\tau} \qquad (\pi \text{ pulse}) \qquad (2)$$

then the molecules which are initially in the state $|I\rangle$ emerge from the resonator in the lower energy state $|II\rangle$. The molecular beam emerging from the first resonator will be energetically empty and no radiation field could be established in the second resonator.

Eq. 2 should be the condition for which the gap in the double-hump curve observed with ammonia beam masers occurs (Fig. 2).

In order to support this hypothesis, let us derive an expression analogous to Eq. (1) for the two-coil nuclear maser.

In Chapter VII it was shown that if the relaxation effects are neglected the equation of motion of M_z for the first emission coil is given by:

$$M_z(t) = -M_o' \cos \gamma H_1 t \qquad (3)$$

M_z changes in time because when the nuclei pass through the first emission coil some of them make a transition from the upper energy state $|m = -\frac{1}{2}\rangle$ to the lower energy state $|m = +\frac{1}{2}\rangle$, thereby delivering energy to the rotating H_1 field. It is now possible to obtain an expression for the probability $P_{-\frac{1}{2}}(t)$ that those nuclei which are initially in the state $|m = -\frac{1}{2}\rangle$ can be found there at some later time t also.

The component M_z varies from $+M_o'$ to $-M_o'$ and can be expressed by

$$M_z(t) = -M_o' P_{-\frac{1}{2}}(t) + M_o' P_{+\frac{1}{2}}(t)$$

where $P_{+\frac{1}{2}}(t)$ is the probability of being in the lower state $|m = +\frac{1}{2}>$. The probability that a nucleus will be found in one of the two energy states is given by

$$P_{-\frac{1}{2}}(t) + P_{+\frac{1}{2}}(t) = 1$$

and this leads to

$$P_{-\frac{1}{2}}(t) = \tfrac{1}{2}\left(1 - \frac{M_z(t)}{M_o'}\right)$$

Introducing Eq. (3), one finds

$$P_{-\frac{1}{2}}(t) = \cos^2 \frac{\gamma H_1 t}{2} \qquad (4)$$

which is an expression analogous to Eq. (1). The condition for zero voltage across the second emission coil is $\gamma H_1 \tau/2 = \gamma k E \tau/2 = \pi/2$, in agreement with Eq. (8.6) and the experimental observations (Chapter VIII).

One can proceed by remarking that the energy difference between parallel and antiparallel alignment of the proton spin is $\omega_o \hbar = \gamma H_o \hbar = 2\mu H_o$ from which it might be seen that $\gamma = 2\mu/\hbar$. Using this latter relation, the condition for zero voltage across the second coil (Eq. (8.6)) can also be expressed by

$$\frac{\gamma H_1 \tau}{2} = \frac{\mu H_1 \tau}{\hbar} = \frac{\pi}{2}$$

or

$$H_1 = \frac{\pi \hbar}{2\mu\tau} \qquad (5)$$

which is the condition analogous to Eq. (2).

The double-hump detuning phenomenon of two-cavity ammonia beam masers has first been observed in 1962 and, if the condition for this effect to occur is given by an expression as straightforward as Eq. (2), the question arises why this has not been seen earlier. One reason will be that using a two-cavity beam maser it is much more difficult to measure the parameters involved in absolute units than it is for a two-coil nuclear maser, and hence for the beam maser is is more difficult to compare theoretical with experimental results. A second reason could eventually be that it has not always been realized that the particles passing through the resonator of a maser oscillator can absorb part of their own radiation (Chapter VIII).

In fact one is tempted to think that the field amplitude in a flow maser (in its general sense) has reached its upper limit if the particles which enter the resonator in the upper energy state emerge from it in the lower energy state. If this would be the case, introducing Eq. (2) into Eq. (1) shows that by increasing ε to its upper limit (in practice one would expect that because of loss effect the upper limit of ε could not be adjusted) the emerging molecules have

always a finite probability of being in the upper state $|I>$, and one could not expect that by increasing ε from a small value to the value given by Eq. (2) the radiation in the second resonator could decrease to zero, and subsequently increase, as seen in Fig. 2 for $\Delta\nu = 0$. One could then conclude to the presence of second-order effects (Section 2.4) such as interference effects caused by the non-uniform velocity distribution of the molecules.

However, the results obtained by means of the two-coil proton maser indicate that the maximum field amplitude of a flow maser is not obtained in that situation where a particle being initially in the upper energy state, after passing through the resonant component, emerges at its exit in the lower energy state. On the contrary, we have to stress that

> the field amplitude (H_1 or ε) of an oscillating flow maser is maximum if the particles which enter the resonant component in the upper energy state emerge from it in the upper energy state.

Here we understand the term "flow maser" in its general sense, i.e. we include all different types of flow masers enumerated in Section 1.5.

Our statement is not a paradox. A proof can be given as follows. According to Eq. (7.5) the amplitude of the field $H_1 = kE$ of nuclear flow maser increases as the ohmic losses decrease, i.e. as the quality factor of the resonant circuit, Q, increases. If no JOULE heat is

dissipated in the circuit ($Q = \infty$) then this requires - from Eq. (7.5) - that $\cos \gamma H_1 = 1$, i.e. the maximum H_1 is given by $\gamma H_1 \tau = 2\pi$. If we introduce this latter relation into Eq. (4) we see that the probability $P_{-\frac{1}{2}}(\tau)$ of finding the nucleus at the exit of the emission coil in its original energy state $|m = -\frac{1}{2}\rangle$ is given by $P_{-\frac{1}{2}}(\tau) = 1$. Relying on the FEYNMAN theorem (Section 1.4) one has to conclude that what holds for a spin $\frac{1}{2}$ maser must also be correct for any other two-level maser.

It should be stressed that using the two-coil nuclear maser it has actually been observed that if the voltage across the second coil is increased to its upper limit the residual macroscopic magnetization of the protons emerging from the exit of the first emission coil tends to re-align itself to the position antiparallel to the field $\vec{H}_o$ (Fig. 28). This can be regarded as an experimental proof of the above statement.

The above statement could also be expressed by saying that the operation of a maser does not depend on the circumstance that the excited particles lose energy to the resonant circuit. If no JOULE heat is dissipated in the resonator ($Q = \infty$) there is no reason why the maser should not oscillate. However if no JOULE heat is dissipated the particles passing through the resonator cannot lose energy; they must emerge from the exit of the resonator in the original excited state.

On the other hand, if the particles which enter the resonator in the excited state emerge from it in the lower energy state then the JOULE heat dissipated in the resonator walls and in the load will be maximum.

To come back to the two-cavity maser problem, the coherent spontaneous rediation produced by the ringing molecules in the second resonator is maximum if the probabilities of finding the molecules in the states $|I\rangle$ and $|II\rangle$ are equal, $P_I(\tau) = P_{II}(\tau)$. (In the analogous magnetic case $\vec{M}$ is then aligned perpendicularly to the main field $\vec{H}_o$.) From Eq. (1) and $P_I(\tau) + P_{II}(\tau) = 1$, we must have for a maximum "superradiant" state

$$\cos^2 \frac{\mu_e \varepsilon \tau}{\hbar} = \sin^2 \frac{\mu_e \varepsilon \tau}{\hbar}$$

or

$$\cos \frac{2\mu_e \varepsilon \tau}{\hbar} = 0 \qquad (6)$$

On the other hand, according to our statement that in the first resonator ε must be maximum if $P_I(\tau) = 1$, from Eq. (1)

$$\varepsilon_{max} = \frac{\pi \hbar}{\mu_e \tau} \qquad (2\pi \text{ pulse}) \qquad (7)$$

If the first resonator is tuned to the centre frequency of the molecular transition and its field ε is gradually increased from 0 to ε_{max} then - from Eq. (6) and Eq. (7) - the radiation intensity in the second resonator will be maximum twice, for

$$\varepsilon = \frac{\pi \hbar}{4\mu_e \tau} \qquad (\tfrac{\pi}{2} \text{ pulse}) \qquad (8)$$

and for the larger value

$$\varepsilon = \frac{3\pi\hbar}{4\mu_e \tau} \qquad (\tfrac{3\pi}{2} \text{ pulse}) \,, \qquad (9)$$

In summary: If ε is enhanced from 0 to ε_{max} the level of oscillations in the second cavity approaches successively a maximum (Eq. (8)), falls to zero (Eq. (2)), approaches a second maximum (Eq. (9)) and decreases finally to zero (Eq. (2)). This corresponds to situation where the action of the field in the first resonator, ε, on the molecules is that of a $\pi/2$ pulse, a π pulse, $3\pi/2$ pulse and a 2π pulse, respectively.

This dependence can be seen in Fig. (2) (for $\Delta\nu = 0$, ε increases with the focusser voltage) up to that point where the radiation intensity in the second resonator increases towards the second maximum. BASOV, ORAEVSKII, STRAKHOVSKII and TATARENKOV (1964) found experimentally that the molecular beam in the second cavity absorbs strongly an external radiation if the ringing signal in the second cavity is zero ($\Delta\nu = 0$). This is also in complete agreement with our explanation since the condition for zero oscillation in the second cavity is given by Eq. (2) and combining Eq. (2) with Eq. (1) shows here that $P_I(\tau) = 0$: the emerging molecules are in the lower energy state $|II\rangle$, i.e. the absorption must be maximum in the second cavity if an external field is applied there.

Starting from Eq. (1) we have discussed the behaviour of a molecular beam maser for zero detuning of the first cavity. The corresponding behaviour of the two-coil nuclear maser was seen in Fig. 23 and Fig. 24. The off-resonance behaviour of the two-cavity molecular beam maser can also be estimated using the different conditions stated here. However, if the detuning is too large, the conditions for

maximum radiation in the second cavity (double-humps of the detuning curve) must be found through a more general analysis which takes the frequency detuning into account. Such analysis can for example be carried out using BLOCH's equations (Chapter III) for the FEYNMAN theorem (Section 1.4) is in effect a generalization of these equations to arbitrary two-level atomic systems, including such cases where an electric-dipole moment is involved.

Finally it should be stressed that the double-hump detuning phenomenon occurs twice as the field in the first resonator is increased from zero to its maximum level (Section 8.5). However, since in order to achieve the theoretical maximum oscillation level in the first resonator an infinite quality factor is necessary it is in practice impossible to observe the gap of the second double-hump curve reaching zero. In this context it is interesting that using a two-cavity ammonia beam maser experimental observations have been made (LAINE and SMITH 1966a,b) where a double-hump effect occurred at a low focusser voltage and a further one at a higher focusser voltage. The gap of the second double-hump curve did not reach zero. However, at this time the double-hump curve which was observed at the lower focusser voltage was interpreted as possibly due to a hyperfine splitting of the ammonia inversion line.

10.3 Meaning of the Experiment with Respect to Flow Masers in General

The circumstance that a two-coil nuclear maser behaves in much the same way as a two-cavity ammonia beam maser could be regarded as a further proof of the quantum-mechanical theorem which states that the motion of any two-level atomic system be equivalent to the motion of a spin $\frac{1}{2}$ in a magnetic field (FEYNMAN, VERNON and HELLWARTH 1957). The positive outcome of the experiment suggests that such phenomena as the double-hump detuning phenomenon and the self-modulation effect can also be observed using the remaining different flow masers enumerated in Section 1.5, if these masers are furnished with tandem resonators.

In practice the presence of a second resonator can only be an advantage.

The double-hump detuning effect could in any case be utilized in order to tune the maser with some precision to the centre of gravity of the atomic resonance line for only for $\Delta\nu = 0$ an enhancement of the level of oscillations in the first resonator can lead to zero radiation in the second resonator (Section 8.5).

Furthermore, zero radiation in the second resonator is a criterion for maximum energy gain from the excited particles in the first resonator.

If the residence time τ of the particles passing through the first resonator and the value of the dipole-moment are known, adjustment for zero radiation in the second resonator allows to determine accurately the absolute value of the average field amplitude (average over the

length of the resonator) existing in this particular adjustment in the first resonator. For a molecular beam maser this field amplitude is given by Eq. (2).

If a molecular beam maser is furnished with a tandem resonator it should be possible to determine the beam velocity and hence the average residence time τ by electric labelling of the particles in the first resonator and recording their arrival in the second resonator. A similar technique (magnetic labelling of nuclei) is currently used in order to measure the flow rate of liquids (ZHERNOVOI and LATHYSHEV 1965, McCORMICK and BIRKEMEIER 1969). This method could be superior to beam chopping techniques.

A further advantage of the use of separated emission fields is that experimental studies of the saturation effect which tends to decrease the polarization of the maser medium can be made by increasing the field amplitude in the first resonator and recording the signal of the second resonator. From the results of such measurements a locus of the residual-polarization vector can be reconstructed and the influence of the saturation effect can be clearly seen (Fig. 28). However, in such measurements the field in the first resonator should not be altered by varying parameters of the particle flow, e.g. by altering the focusser voltage in the case of a molecular beam maser. For instance, if the focusser voltage of a beam maser is increased, the increase of polarization due to the larger number of excited-state molecules will overshadow the decrease of polarization due to the

saturation effect. In fact here the only suitable parameter which can be altered in order to change the field amplitude in the first resonator is its quality factor. In the case of microwave masers it would be necessary to use a high Q cavity and to alter the field amplitude in the cavity by deteriorating artificially by some suitable means the natural cavity quality. Furthermore, in recording the locus of the residual-polarization vector the quality factor of the second resonator should be small so that the additional "tilting" of the polarization vector in the second cavity can be neglected.

Although in principle any flow maser can be furnished with tandem resonators, the constructive difficulties will vary from case to case. For example, since the atomic hydrogen beam maser utilizes a storage bulb from which the atoms emerge through the same orifice through which the excited beam enters, it would be necessary to arrange a second exit.

Arranging a second resonator should be particularly simple in the case of the low-frequency type of molecular beam maser (SHIMODA, TAKUMA and SHIMUZU 1960) where the excited molecules pass through a parallel-plate condenser. In this particular case it should also not be difficult to take advantage of the mode of operation using mechanical distance modulation.

The use of separated emission fields and mechanical distance modulation could be especially interesting in the case of the helium-3 diffusion nuclear maser devised by ROBINSON and MYINT (1964).

the natural transverse relaxation time of the ^{3}He nuclear orientation is some 10 seconds, and hence, if the main field is homogeneous, the distance between the two emission fields could be modulated by much larger amounts than is possible for other nuclear flow masers. Therefore it should be possible to tune this maser with a great accuracy to the centre frequency of the nuclear ZEEMAN transition.

The self-modulation effect of two resonator masers which could eventually also find practical applications can only be observed when the quality factor of the second resonant circuit is large enough. However, as was mentioned before, in investigations of the residual polarization the quality factor of the second resonator should be as low as possible, thereby ensuring that the dependence between the oscillation level and the component of polarization which excited the second resonator is a linear one.

10.4 Proposals for Further Investigation

For the two-coil nuclear maser it was found experimentally that the tilting angle of the macroscopic magnetization $\vec{M}$ in the first emission coil can be considerably larger than π (Fig. 28). As the quality factor of the first emission coil is increased and the tilting angle as observed at the exit of the first coil changes from $\theta < \pi$ to $\theta > \pi$, or vice versa, then a 180° phase change could be observed in the voltage available at the terminals of the second coil (Fig. 27).

In the case of an ammonia beam maser the existence of a corresponding "tilting" angle θ of the electric polarization vector is less obvious, and it is not immediately clear why one should look for 180° phase changes of the ringing signal induced in the second cavity. However the close analogy between the two-coil maser and the two-cavity maser suggests that the 180° phase change must also be observable in the latter case. If it can be measured, its existence could hardly be explained by interference effects which could be caused by the non-uniform velocity distribution of the molecules. In investigating this phase shift in the two-cavity beam maser it will not be necessary to alter the amplitude of the electric field in the first cavity by varying its quality factor. Since the amplitude of the field in the first cavity depends monotonically on the focussing voltage (e.g. BARNES 1959) the latter can be altered instead. However, it should be remarked that as the focusser voltage is altered the magnitude of the residual polarization in the second cavity changes also. Hence if the phases of ringing signals having equal amplitudes are compared in the manner indicated in Fig. 27, the result might be that the phase shift differs slightly from 180°. However, if two very small signals are compared the error of the phase measurement should be negligible.

Concerning the self-modulation effect of the two-coil proton maser, this phenomenon occurs only if the first coil is sufficiently detuned so that the field H_1 and the torque produced by this field are

very small, and the residual magnetization is aligned nearly anti-parallel to $\vec{H}_o$. The appearance of the self-modulation effect indicates the presence of two different macroscopic moments which precess with different angular velocities. An investigation of the tilting angles and the relative lengths of these components should bring about information on the tilting angle distribution of the residual magnetization available at the entrance of the second coil.

10.5 Practical Applications of the Two-Coil Proton Maser

The two-coil proton maser devised can be used in order to measure the absolute value of the earth's magnetic field. Since the system offers two tuning criteria the accuracy of field measurements will be higher than for the conventional one-coil maser from which the system has been derived. The influence of the leakage field of the prepolarizing magnet can be made inoperative by carefully adjusting the position of the emission coils with respect to the magnet. As was demonstrated by HENNEQUIN (1961) for a one-coil flow maser, this can be achieved in a systematic manner. In order to exploit fully the possibility of tuning the maser to the centre frequency by modulating mechanically the inter-coil distance and adjusting for zero phase modulation, it might be helpful either to control the liquid flow rate by means of a servo mechanism or to use a gravitational-flow system. The two-coil maser can also be operated successfully if tap water is used as the maser medium. However, the accuracy available in field

measurements will be considerably higher if deoxygenated water (natural T_2 = 3.1 sec) or benzene (T_2 = 13 sec) are utilized.

The modulation of the inter-coil distance offers also the possibility of using the phase error signal in order to activate a servo mechanism which retunes the first emission coil automatically when the earth's magnetic field changes. Conventional maser magnetometers which follow automatically the natural changes of the earth's magnetic field, utilize two separated one-coil masers (RÖMER 1961)

On the other hand, as the present investigation has shown, the two-coil proton maser is a magnetic analogue of the two-cavity molecular beam maser, and it offers flexible demonstrations of the principle and of the basic performance of flow masers which utilize separated emission fields.

The new instrument offers a simple method of measuring spin-spin interaction times of protons in flowing liquids.

10.6 Summary

It has been shown that the behaviour of a two-cavity ammonia beam maser can also be explained qualitatively using simplified quantum-mechanical arguments. The conditions obtained for maximum and zero oscillation in the second resonator agree qualitatively with those obtained for the two-coil nuclear maser by means of a classical analysis.

This chapter considered also some general aspects of the practical application of flow masers with separated emission fields.

In principle any flow maser can be furnished with a tandem resonator and its presence can only be an advantage, for a two-cavity maser offers criteria for the precise frequency tuning and it allows also the experimental investigation of the radiation process in the first resonator.

CONCLUSIONS

A liquid flow nuclear maser with separated emission fields has been devised and investigated, and it has been found that this apparatus behaves on the macroscopic scale analogously to a two-cavity ammonia beam maser. The analogous performances of the two different types of maser systems is quantum-mechanically well established through the FEYNMAN theorem.

The double-hump detuning phenomenon which has previously been observed using two-cavity ammonia beam masers and for which hitherto no cogent explanation had been found, has been identified as being caused by a fundamental radiation process occurring in the first resonant component.

For the nuclear maser the condition for the appearance of the double-hump detuning effect can be derived using BLOCH's phenomenological equations. In the case of a molecular beam maser a discussion of the problem in terms of quantum-mechanical probabilities leads to qualitatively the same result.

The investigation of the two-coil nuclear maser has shown that the excited particles passing through the resonant component of a maser can re-absorb a large number of the energy quanta which they emit. It is this less familiar feature of maser oscillators, which largely determines the behaviour of flow masers with separated emission fields.

Flow masers which utilize separated emission fields have numerous advantages over conventional masers. For instance, the double-hump detuning phenomenon can be used in order to tune the maser to the centre frequency of the atomic transition and simultaneously to adjust the first resonant component for maximum gain of particle energy. If the distance of the resonant components is mechanically modulated a further frequency tuning criterion can be obtained. Hence masers with separated emission fields can improve the accuracy of conventional maser clocks, spectrometers, magnetometers etc. Furthermore, by altering the distance between the resonant components the relaxation time T_2^* can be measured conveniently.

REFERENCES

ABRAGAM, A. 1961, The Principles of Nuclear Magnetism (Oxford University Press).

ABRAGAM, A., COMBRISSON, J. and SOLOMON, I. 1957, Comptes rendus 245, 157.

ANDREW, E.R. 1958, Nuclear Magnetic Resonance (Cambridge University Press).

ARNOLD, D.W. and BURCKART, L.E. 1965, J. Appl. Phys. 36, 870.

BARNES, F.S. 1959, I.R.E. 47, 2085.

BASOV, N.G. and ORAEVSKII, A.N. 1962, Soviet Phys. JETP 15, 1062.

BASOV, N.G., ORAEVSKII, A.N., STRAKHOVSKII, A.N. and TATARENKOV, V.M. 1964 (a), Sov. Phys. JETP 18, 1211;

1964 (b), Quantum Electronics III, (Paris, Dunod) p.377 (Proc. 3rd Congress Quantum Electronics, Paris 1963).

BASOV, N.G.,ORAEVSKII, A.N., STRAKHOVSKII, G.M. and USPENSKII, A.V. 1966, JETP Lett. 3, 468; (Eng. transl. 1966, 3 305).

BASOV, N.G., ORAEVSKII, A.N. and USPENSKII, A.V. 1967, Optics and Spectroscopy 23, 504.

BASOV, N.G. and PROKHOROV, A.M. 1954, Zh. Eksperim. i. Teor. Fiz. 27, 431.

BECKER, G. 1966, Z. angew. Phys. 20, 398.

BELENOV, E.M. and ORAEVSKII, A.N. 1966, Sov. Phys. Tech. Phys. 11, 413.

BENDER, P.L. and DRISCOLL, R.L. 1958, I.R.E. Trans. Instr. 1 176.

BENOIT, H. 1958, Comptes rendus 246, 2123.

BENOIT, H. 1959, Ann. Physique 4 1439.

BENOIT, H. 1960, J. Phys. Radium 21, 212.

BENOIT, H., FRANCOIS, M., POZZI, J-P., THELLIER, E. and KASTLER, A. 1967, Comptes rendus 265B, 943.

BENOIT, H. and FRIC, C. 1959, Comptes rendus 249, 537.

BLOCH, F. 1946, Phys. Rev. 70, 460.

BLOCH, F. 1954, Phys. Rev. 94, 496.

BLOCH, F., HANSEN, W.W. and PACKARD, M. 1946, Phys. Rev. 70, 474.

BLOEMBERGEN, N. 1956, Phys. Rev. 104, 324.

BLOEMBERGEN, N. and POUND, R.V. 1954, Phys. Rev. 95, 8.

BLOOM, S. 1957, J. Appl. Phys. 28, 800.

BONAMI, J., HERRMANN, J., DE PRINS, J. and KARTASCHOFF, P. 1957, Rev. Sci. Instr. 28, 879.

CARRINGTON, A. and McLACHLAN, A.D. 1967, Introduction to Magnetic Resonance (London: Harper & Row).

COHEN, E.R. and DUMOND, J.W.M. 1965, Rev. Mod. Phys. 37, 537.

COLGROVE, F.D., SCHAERER, L.D. and WALTERS, G.K. 1963, Phys. Rev. 132, 2561.

COMBRISSON, J. 1960, Quantum Electronics (New York: Columbia University Press), p.167.

COMBRISSON, J., HONIG, A. and TOWNES, C.H. 1956, Comptes rendus, 242, 2451.

DAVIDOVITS, P. 1964, Appl. Phys. Lett. 5, 15.

DEHMELT, H.G. 1968, Am. J. Phys. 36, 911.

DICKE, R.H. 1954, Phys. Rev. 93, 99.

FEYNMAN, R.P., VERNON, F.L. and HELLWARTH, R.W. 1957, J. Appl. Phys. 28, 49.

FEYNMAN, R.P., LEIGHTON, R.B. and SANDS, M. 1965, The Feynman Lectures on Physics III. (Reading: Addison-Wesley).

FRIC, C. 1960, Ann. Physique 4, 1501.

GABILLARD, R. 1955, see GRIVET, P.A. 1955.

GANSSEN, A. 1962, I.R.E. Trans. Instrum. I-11 3/4, 1966.

GERLACH, W. and STERN, O. 1924, Ann. Physik, 74, 673.

GOLDENBERG, H.M., KLEPPNER, D. and RAMSEY, N.F. 1960, Phys. Rev. Lett. 5, 361.

GORDON, J.P., ZEIGER, H.J. and TOWNES, C.H. 1955, Phys. Rev. 99, 1265.

GRASYUK, A.Z. and ORAEVSKII, A.N. 1964, Radio Eng. Electron. Phys. 9, 424.

GRIVET, P. (Ed.) 1955, La resonance paramagnetique nucleaire, Centre National de la Recherche Scientifique, Paris.

GRIVET, P. 1960, Bull. Ampere 9, 567.

GRIVET, P.A. and MALNAR, L. 1967, Adv. Electronics and Electron Physics, 23, 39 (New York: Academic Press Inc.).

GRIVET, P., SAUZADE, M. and LORY, H. 1964, IEEE Trans. Instr. Measur. IM-13, 231.

HAHN, E.L. 1950, Phys. Rev. 80, 580.

HARRIS, H.E. 1951, Electronics 24 No. 5, 130.

HENNEQUIN, J. 1961, Ann. Physique 6, 949.

HERMS, W. 1961, Ann. Physik 8, 280.

HIGA, W.H. 1957, Rev. Sci. Instr. 28, 726.

KROUPNOV, A.F., SKVORTSOV, V.A. and SINEGOUBKO, L.A. 1968, Izv. VUZ Radiofiz. (USSR) 2, 244.

KUKOLICH, S.G. 1967, Phys. Rev. 156, 83.

KURNIT, N.A., ABELLA, I.D. and HARTMANN, S.R. 1964, Phys. Rev. 13, 567.

LAINÉ, D.C. 1967, Private communication.

LAINÉ, D.C. and SMITH, A.L.S. 1966(a) IEEE J. Quantum Electronics QE-2, 399.

1966(b), Phys. Lett. 20, 374.

LAINÉ, D.C. and SRIVASTAVA, R.C. 1963, Radio Electron. Engr. 26, 173.

TIE-CHENG, Li and LI-ZHI, Fang 1964, Acta Physica Sinica 20, 753.

LÖSCHE, A. 1957, Kerninduktion (Berlin: Deutscher Verlag der Wissenschaften).

MACOMBER, J.D. 1968, Appl. Phys. Lett. 13, 5.

MARCUSE, D. 1961, Proc. I.R.E. 49, 743.

McCORMICK, W.S. and BIRKEMEIER, W.P. 1969, Rev. Sci. Instrum. 40, 346.

MUKHAMEDGALIEVA, A.F., ORAEVSKII, A.N. and STRAKHOVSKII, G.M. 1965, JETP JETP Lett. 1, 13.

MUKHAMEDGALIEVA, A.F. and STRAKHOVSKII, G.M. 1966, Radio Engng. and Electronic Physics 11, 818.

ORAEVSKII, A.N. 1964, Molekulyarnye generatory (Moscow: Nauka Press).

ORAEVSKII, A.N. 1967, Sov. Phys. USPEKHI 10, 45.

PÉPIN, H. 1968, Étude d'un maser basse-frequence. Office National d'Etudes et de Recherches Aérospatiales (France) Publ. No. 125.

POWLES, J.G. 1958, Proc. Phys. Soc. 71, 497.

POWLES, J.G. 1959, Rep. Prog. Phys. 22, 462.

POWLES, J.G. and CUTLER, D. 1957, Nature 180, 1344.

DE PRINS, J. 1961, Theses, Université de Neuchatel (Switzerland).

PURCELL, E.M. and POUND, R.V. 1951, Phys. Rev. 81, 279.

REDER, F.H. and BICKART, C.J. 1960, Rev. Sci. Instr. 31, 1164.

ROBINSON, H.G. and MYINT, Than., 1964, Appl. Phys. Lett. 5, 116.

RÖMER, G. 1962, C.R. X^{e} Colloque Ampere 1961 (Amsterdam: North-Holland), p.273.

SHERMAN, C. 1959, Rev. Sci. Instr. 30, 568.

SHIMODA, K., TAKUMA, H. and SHIMUZU, T. 1960, J. Phys. Soc. Japan 15, 2041.

SINGER, J.R. 1959, Masers (London: Wiley).

SKRIPOV, F.I. 1958, Sov. Phys. Doklady 3, No. 4, 806.

SMITH, A.L.S. and LAINÉ, D.C. 1968, Brit. J. Appl. Phys. (J. Phys. D), Ser. 2, Vol. 1, 727.

SOLOMON, I. 1961, Note C.E.A. No. 346, Centre d'Etudes Nucleaires de Saclay, France.

STRAKHOVSKII, G.M. and TATARENKOV, V.M. 1962, Sov. Phys. JETP 15, 625.

SUCHKIN, G.L. 1966, Radio Engng. and Electronics 11, 256.

SZÖKE, A. and MEIBOOM, S. 1958, Phys. Rev. 113, 585.

Texas Instruments (M. MILLER ed.) 1966, Solid-state communications, (New York: McGraw-Hill) p.138 and 296.

TOWNES, C.H. 1964 Nobel Lecture. IEEE Spectrum, August 1966, 30.

TROUP, G. 1959, Masers and Lasers (London: Methuen).

VESELAGO, V.G., ORAEVSKII, A.N., STRAKHOVSKII, G.M. and TATARENKOV, V.M. 1965, JETP Lett. 2, 49.

VLADIMIRSKY, K.V. 1957, Nuclear Instrum. 1, 329.

WELLS, W.H. 1958, J. Appl. Phys. 29, 714.

YARIV, A. 1967, Quantum Electronics (London: Wiley).

ZHERNOVOI, A.I. and LATYSHEV, G.D. 1958, Izv. Akad. Nauk. SSSR, Ser. Fiz. 22, 993.

ZHERNOVOI, A.I. and LATYSHEV, G.D. 1965, Nuclear Magnetic Resonance in a Flowing Liquid (New York: Consultants Bureau).